ICHNOLOGY, SEDIMENTOLOGY, AND STRATIGRAPHY OF THE HIBERNIA FORMATION, JEANNE D'ARC BASIN, OFFSHORE, NEWFOUNDLAND

© Elizabeth Rose Schatz

A Thesis submitted to the School of Graduate Studies

in partial fulfillment of the requirements for the degree of

Doctor of Philosophy

Department of Earth Sciences

Memorial University of Newfoundland

September 2018

St. John's Newfoundland

ABSTRACT

The Jeanne d'Arc Basin is located approximately 350 km east of St. John's, Newfoundland, Canada. The basin contains many prolific hydrocarbon reservoirs and is still actively explored and studied. The Hibernia Field, on the western edge of the basin along the Murre Fault, contains four sandstone reservoirs: the Jeanne d'Arc Formation (Late Jurassic), the Hibernia Formation (Early Cretaceous), the Catalina Formation (Early Cretaceous), and the Ben Nevis-Avalon Formation sandstones (Early Cretaceous). The Hibernia Formation, Hibernia Field, is a sandstone reservoir of fluvial deltaic origin and is estimated to contain 1644 million barrels of oil. The Hibernia Formation in the southern Jeanne d'Arc Basin displays good reservoir potential but few studies have been undertaken.

Seventeen lithofacies are identified from core analysis of seven core samples from the southern Hibernia expression: three from the Upper Hibernia Zone and four from the Lower Hibernia Zone. Six facies associations were inferred and a wave-influenced delta classification was determined. Ichnological analysis resulted in the identification of 10 distinct ichnofabrics. Core plug data was analyzed by lithofacies and ichnofabric to assess trends in permeability and porosity in the Upper Hibernia Zone. Cross bedded medium- to coarse-grained sandstones (Facies 10, interpreted as deltaic mouthbar sandstones) display the highest permeabilities up to 962 mD and porosities averaging 13%, and commonly contain *Ophiomorpha* burrows. Minipermeametry of a slabbed core section from Facies 10 showed that clay material was removed from the host sediment immediately surrounding the burrow effectively enhancing the porosity and permeability.

Cryptobioturbated and unbioturbated, parallel laminated storm beds display the same range of permeabilities and porosity; however, the cryptobioturbated storm beds display higher vertical connectivity between sandstone laminations as shown from minipermeametry analysis. Deeply eroded and amalgamated storm bed tops can result in vertical connectivity between potential reservoir-quality sandstone units. Muddy siltstone facies containing *Phycosiphon*-dominated ichnofabric are observed to have increased porosity which has the potential to serve as a conduit for hydrocarbon migration since the *Phycosiphon* burrow halo is lacking in clay material and shows increased porosity when compared to the host rock.

Analysis of facies distribution using both core logs and wireline log data allowed for the placement of a paleoshoreline (Valanginian). Stratigraphic analysis of the southern expression of the Hibernia Formation suggests that autocyclic lobe switching, longshore drift from west to east, and tectonically-driven sea level changes were the main controlling factors on facies distribution. Sandstones in the Hebron Field area displayed higher permeability and porosity characteristics than equivalent facies in the West Bonne Bay area. Further exploration is recommended for the Hebron Field, specifically in shoreface settings where storm beds are amalgamated and interbedded with deltaic mouthbars.

ACKNOWLEDGEMENTS

Thank you to my supervisor, Duncan McIlroy, for his guidance and support through the thesis writing process. Thank you to Richard Callow for his comments and editions to my writing. Thank you to Ali Aksu for his thorough review of my thesis work and for helping me to improve my writing. Thank you to Husky Energy for providing this research topic and the resources needed to see it through to completion. Thank you also to the School of Graduate Studies and Husky Energy for funding this research. Thank you to Iain Sinclair, Doug Stewart, Paula Marner, and countless others from Husky Energy who asked excellent questions and set me on new paths of discovery and thinking. I have learned and grown a great deal through this experience.

Thank you to my spouse, Lonnie Schoenthal, who was always the bright light at the end of the tunnel and who was there, no matter what, to encourage me to push through the difficult parts. Forever and always, Lonnie. Thank you to my amazing family for their undying support, endless encouragement, and patience. Thank you to my friends, near and far, who sent me their thoughts and wishes. Thank you to Lina Stolze for being an amazing friend and confidant, and for our long walks to whale watch on Signal Hill. Thank you to Florian Bulle for his friendship, encouragement, and coffee breaks. Thank you to Dario Harazim for his friendship and invaluable suggestions to improve my thesis. Thank you to all my knitting friends for always being there to listen and provide constructive, logical advice over coffee and yarn. This has been a long and winding road to completion and I thank you all for your patience and support.

TABLE OF CONTENTS

LIST OF TABLES

LIST OF FIGURES

CHAPTER 1

Introduction and Overview

1. Introduction to Research Topic

Currently available research surrounding the Hibernia Formation focuses on structural geology of the Jeanne d'Arc Basin and reservoir characteristics within the Lower Hibernia zone (e.g. Tankard and Welsink, 1987; Mackay and Tankard, 1990; Sinclair et al., 1992, 1999). A study by Brown et al. (1989) presented a petrographic and sedimentological look at the entire Hibernia Formation with descriptions of diagenetic processes. However, little information is presented in the published literature regarding the ichnology of the Hibernia Formation and rare mention is given to the effects of bioturbation on reservoir quality. This thesis presents a detailed sedimentological and ichnological record of the Hibernia Formation with the dominant focus on the Upper Hibernia zone and will further refine the present paleoenvironmental interpretation within a sequence stratigraphic context.

Biological controls on reservoir permeability and porosity are becoming more well-known and the importance of integrated ichnological-sedimentological studies is being realized (McIlroy 2004, 2008). Bioturbated rock units were initially thought to have a decreased permeability as compared to non-bioturbated units (Pemberton and Gingras, 2005). However, many studies exist emphasizing both the positive and negative effects of bioturbation on permeability and porosity in oil and gas reservoirs (e.g. Gingras et al., 2004; Pemberton and Gingras, 2005; Spila et al., 2007; Tonkin et al., 2010; Lemiski et al, 2011; Bednarz and McIlroy, 2012; La Croix et al., 2012, 2013; Leaman, 2013). These authors note that permeability can be increased when low permeability rock units contain burrows with highly permeable burrow fills. Such burrows may be interconnected forming a branching network (e.g. *Thalassinoides*, *Chondrites*;) or interconnected through crosscutting behaviours (Gingras et al., 2004; Pemberton and Gingras, 2005; Spila et al., 2007; Bednarz and McIlroy, 2012; La Croix et al., 2012). Traces with mud lining and/or sand-mud alternating burrow fill have been noted to cause a decrease in permeability (Tonkin et al., 2010; La Croix et al., 2013; Leaman, 2013).

This study provides an excellent opportunity to further develop our knowledge of biologically controlled trends in permeability and porosity within a reservoir setting. As the cores utilized for this research have not yet been publicly described, it offers a chance to advance the sedimentological and environmental interpretations through the integration of ichnological concepts. The Hibernia Formation is already of considerable interest to the petroleum industry; therefore a more accurate depositional model that will both better predict basin-wide trends in permeability and also promote more favorable oil recovery is needed.

2. Research Objectives

The primary research objectives for this thesis project are as follows:

1) to document the sedimentology and ichnology of the Hibernia Formation through core analysis

2) to assess the controls on reservoir quality in the Hibernia Formation through

a) analysis of core plug permeability and porosity data by lithofacies and well location and

b) minipermeametry analyses of slabbed core faces to determine bedding-scale changes in permeability and porosity characteristics

3) to interpret the paleoenvironment of deposition and propose a sequence stratigraphic framework of the Hibernia Formation in the southern Jeanne d'Arc Basin.

The first objective will incorporate detailed sedimentological descriptions (e.g. grain size, sorting, cementation, sedimentary structures) and facies classifications combined with ichnofabric analyses to better understand the depositional processes and environment as a whole. The second objective will assess reservoir quality through analyses of burrow wall and burrow fill permeabilities of specific trace fossil types as well as permeability of the host rock using a minipermeameter. Large scale controls on reservoir quality will be assessed within the depositional model using trends in permeability and porosity based on core plug data supplied by Canada-Newfoundland and Labrador Offshore Petroleum Board (C-NLOPB), sedimentological data collected from objective one, and also from facies-specific trends in small scale permeability throughout the depositional environment (i.e. permeability trends attributed to specific ichnofabric associations). The third objective will utilize facies interpretations to construct a depositional model, within a sequence stratigraphic framework, from the studied core samples in combination with wireline logs provided by Husky Energy Inc. This thesis has been arranged as an introductory chapter, followed by 3 stand-alone papers, and a final chapter summary of the main contributions.

3. Literature Review

3.1. Regional Geology of the Jeanne d'Arc Basin

The Jeanne d'Arc Basin is situated on the Grand Banks of Newfoundland, Canada and contains sedimentary rocks Triassic to Tertiary in age (Figure 1.1; Brown et al., 1989; Mackay and Tankard, 1990; Sinclair et al., 1999). These deposits formed as a result of three rifting episodes during the opening of the Atlantic Ocean (Tankard and Welsink, 1987; Mackay and Tankard, 1990; Sinclair et al., 1999). The first of these episodes occurred from the Late Triassic to the Early Jurassic, at which time reddish siltstones and mudstones of terrestrial origin were deposited followed by a thick evaporite salt (Figure 1.1, Eurydice and Argo Formations respectively; Brown et al., 1989; Mackay and Tankard, 1990; Sinclair et al., 1999). Basin subsidence and the formation of a broad epeiric sea resulted in the deposition of carbonaceous mudstones thereafter (Tankard and Welsink, 1987; Mackay and Tankard, 1990; Sinclair et al., 1999).

The Hibernia Formation was deposited during the second rifting episode which began in the Late Jurassic and continued into the mid-Cretaceous (Tankard and Welsink, 1987; Brown et al., 1989; Mackay and Tankard, 1990; Sinclair et al., 1999). This episode was marked by extension, then subsidence of the Grand Banks which resulted in the accumulation of thick sedimentary successions representing both fluvial processes and subsequent marine incursions (Mackay and Tankard, 1990; Sinclair et al., 1999). Uplift in

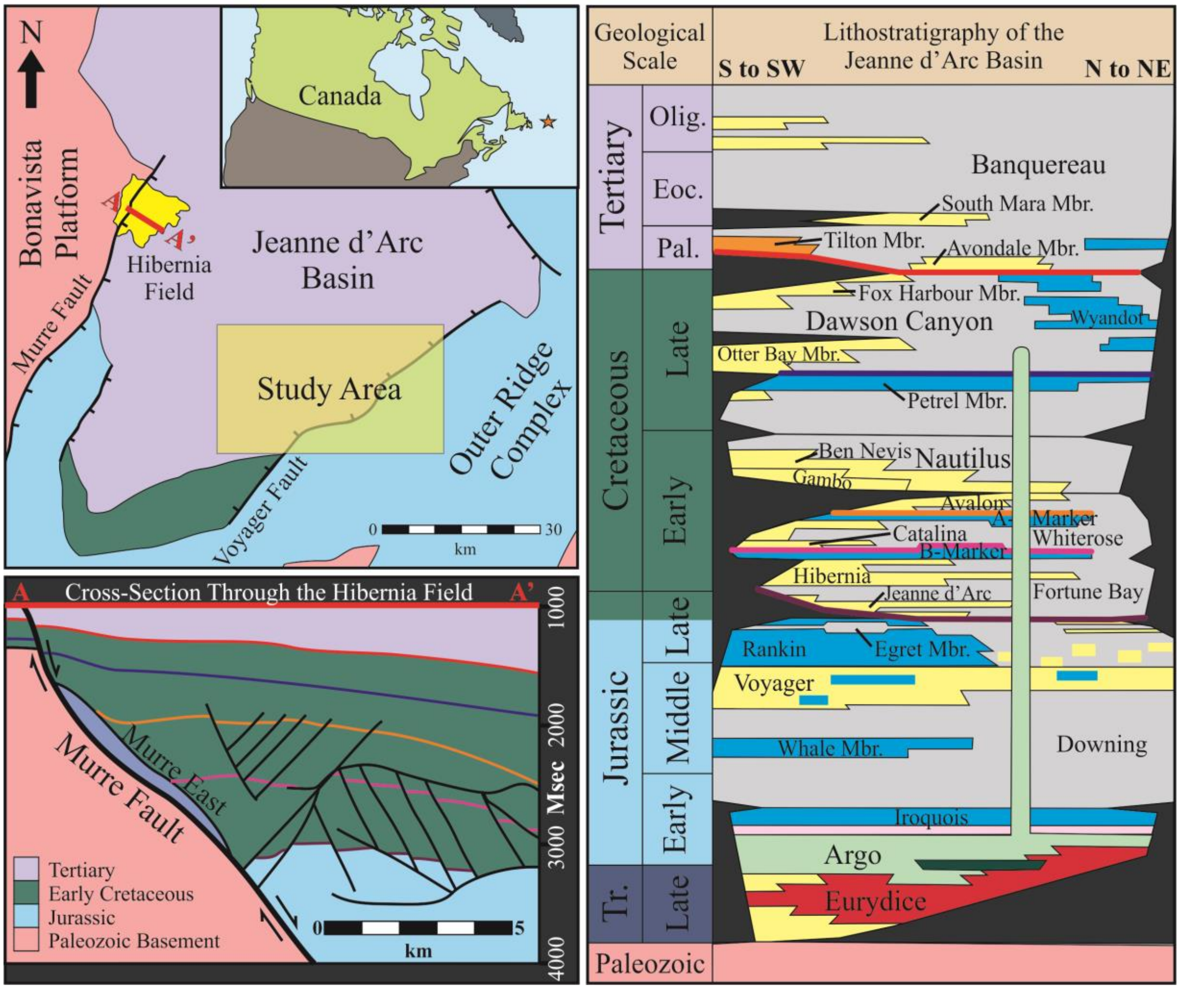

Figure 1.1. An overview map of the Jeanne d'Arc Basin with cross-sections through both the Hibernia oil field and the Jeanne d'Arc Basin. The cross-sectional view through the Hibernia Field shows major and minor faults and stratigraphic surfaces identified through 3D seismic trace (Sinclair et al., 1999). The surfaces of stratigraphic significance are coloured to match surfaces displayed in the lithostratigraphic cross-section: red (base tertiary unconformity); blue (top of the Petrel Member limestone); orange (top of the A-Marker limestone); dark pink (top of the B-Marker limestone); and burgundy (Tithonian unconformity at the base of the Jeanne d'Arc Formation). All geological periods and eras are colour coded. Abbreviations are as follows: Olig. (Oligocene), Eoc. (Eocene), Pal. (Paleocene), Mbr. (Member). Illustration modified from Sinclair et al. (1992, 1999).

the southwestern region of the Grand Banks at this time (the Avalon Uplift) contributed a considerable amount of sediment to the Jeanne d'Arc Basin (Brown et al., 1989; Mackay and Tankard, 1990; Sinclair et al., 1999). The dominant direction of sediment migration is inferred to be from the Avalon Uplift in the southwest towards the northeast area of the basin (Brown et al., 1989; Mackay and Tankard, 1990; Sinclair et al., 1999). Minor contributions from both the western craton and the Outer Ridge Complex in the east are noted in the igneous and metamorphic origin of some mineral grains in the Hibernia sandstones (Brown et al., 1989).

During the early stages of basinal extension within the Grand Banks region, a series of large graben-horst faults resulted (Tankard and Welsink, 1987; Mackay and Tankard, 1990; Sinclair et al., 1999). The Murre and Murre East faults represent the largest of these and display an approximate north-south trend along the west side of the basin margin (Figure 1.1; Tankard and Welsink, 1987; Mackay and Tankard, 1990; Sinclair et al., 1999). Movement along these faults is responsible for the fault-bound antiform morphology of the Hibernia Formation (Figure 1.1; Tankard and Welsink, 1987; Mackay and Tankard, 1990; Sinclair et al., 1999).

3.2. Discovery and Importance of the Hibernia Formation, Hibernia Field

The Hibernia Formation serves as one of the main oil reservoirs of the Hibernia Oil Field located approximately 300 km southeast of St. John's, Newfoundland, Canada in the Jeanne d'Arc Basin (Brown et al., 1989; Mackay and Tankard, 1990; Sinclair et al., 1999). Test drilling in the region began in 1966 and was followed by discovery of an organic rich source rock of Jurassic age in 1973-74 (Mackay and Tankard, 1990). It was not until 1979 that the Hibernia discovery well was drilled and oil was discovered (Mackay and Tankard, 1990). Four oil rich sandstone formations were discovered within the Jeanne d'Arc Basin at this time: the Jeanne d'Arc Formation (Late Jurassic), the Hibernia Formation (Early Cretaceous), the Catalina Formation (Early Cretaceous), and the Ben Nevis-Avalon Formations (Early Cretaceous; Mackay and Tankard, 1990; see Figure 1.1). The Egret Member (Kimmeridgian) of the Rankin Formation is the source rock (Mackay and Tankard, 1990; Sinclair et al., 1999).

There is a considerable amount of interest in the Hibernia Formation, Hibernia Field, as an oil reservoir owing to its high porosity and permeability (Brown et al., 1989; Mackay and Tankard, 1990; Sinclair et al., 1999). During early diagenesis, the sandstones of the Hibernia Formation were only partially silica-cemented (Brown et al., 1989). At a later stage, carbonate infiltration replaced some framework grains and filled pore spaces resulting in decreased porosity and permeability (Brown et al., 1989). The current, enhanced porosities and permeabilities observed in the Hibernia Formation are the result of extensive decarbonization which removed much of the carbonate cement, minor feldspar and clay minerals, and some framework grains producing oversized pore spaces (Brown et al., 1989). The Hibernia sandstones are estimated to contain as much as 71×10^6 m^3 of recoverable oil with porosities averaging 15% and permeability ranging from 10 mD to 10 D (Mackay and Tankard, 1990; Sinclair et al., 1999).

4. References

BEDNARZ, M., AND MCILROY, D. 2012. Effect of phycosiphoniform burrows on shale hydrocarbon reservoir quality. *APPG Bulletin*, v. 96, p. 1957-1980.

BROWN, D.M., MCALPINE, K.D., AND YOLE, R.W. 1989. Sedimentology and sandstone diagenesis of Hibernia Formation in Hibernia Oil Field, Grand Banks of Newfoundland. *The American Association of Petroleum Geologists Bulletin*, v. 73, p. 557-575.

GINGRAS, M.K., MENDOZA, C.A., AND PEMBERTON, S.G. 2004. Fossilized worm burrows influence the resource quality of porous media. *AAPG Bulletin*, v. 88, p. 875-883.

LA CROIX, A.D., GINGRAS, M.K., DASHTGARD, S.E., AND PEMBERTON, S.G. 2012. Computer modeling bioturbation: the creation of porous and permeable fluid-flow pathways. *AAPG Bulletin*, v. 96, p. 545-556.

LA CROIX, A.D., GINGRAS, M.K., PEMBERTON, S.G., MENDOZA, C.A., MACEACHERN, J.A., AND LEMISKI, R.T. 2013. Biogenically enhanced reservoir properties in the Medicine Hat gas field, Alberta, Canada. *Marine and Petroleum Geology*, v. 43, p. 464-477.

LEAMAN, M.K. 2013. Three-dimensional morphology of *Diplocraterion* and *Ophiomorpha* and their impact on reservoir properties. MSc. Thesis Memorial University of Newfoundland, St. John's, Newfoundland, Canada.

LEMISKI, R.T., HOVIKOSKI, J., PEMBERTON, S.G., AND GINGRAS, M.K. 2011. Sedimentological, ichnological and reservoir characteristics of the low-permeability, gas-charged Alderson Member (Hatton gas field, southwest Saskatchewan): implications for resource development. *Bulletin of Canadian Petroleum Geology*, v. 59, p. 27-53.

MACKAY, A.H., AND TANKARD, A.J. 1990. Hibernia Oil Field-Canada Jeanne d'Arc Basin, Grand Banks Offshore Newfoundland. *In*, N.H. Foster and E.A. Beaumont (Compilers), *Structural Traps: Tectonic Fold Traps*, 3, p. 145-175. American Association of Petroleum Geologists Atlas of Oil and Gas Fields.

MCILROY, D. 2004. Some ichnological concepts, methodologies, applications and frontiers. *Geological Society of London*, Special Publication, v. 228, p. 3-27.

MCILROY, D. 2008. Ichnological analysis: the common ground between ichnofacies workers and ichnofabric analysts. *Palaeogeography, Palaeoclimatology, Palaeoecology*, v. 270, p. 332-338.

PEMBERTON, S.G., AND GINGRAS, M.K. 2005. Classification and characterizations of biogenically enhanced permeability. *AAPG Bulletin*, v. 89, p. 1493-1517.

SINCLAIR, I.K., EVANS, J.E., ALBRECHTSONS, E.A., AND SYDORA, L.J. 1999. The Hibernia Oilfield: effects of episodic tectonism on structural character and reservoir compartmentalization. *In*, A.J. Fleet and S.A.R. Boldy (eds.), *Petroleum Geology of Northwest Europe: Proceedings of the 5th Conference*, p. 517-528. Geological Society of London.

SINCLAIR, I.K., MCALPINE, K.D., SHERWIN, D.F., MCMILLAN, N.J., TAYLOR, G.C., BEST, M.E., CAMPBELL, G.R., HEA, J.P., HENAO, D., AND PROCTER, R.M. 1992. Petroleum resources of the Jeanne d'Arc Basin and environs, Grand Banks, Newfoundland. *Geological Survey of Canada Paper*, v. 92, p. 8-48.

SPILA, M.V., PEMBERTON, S.G., ROSTRON, B., AND GINGRAS, M.K. 2007. Biogenic textural heterogeneity, fluid flow and hydrocarbon production: bioturbated facies Ben Nevis Formation, Hibernia Field, Offshore Newfoundland. *In*, J.A. MacEachern, K.L. Bann, M.K. Gingras, and S.G. Pemberton, *Applied Ichnology*. SEPM Short Course Notes, v. 52, p. 363-380.

TANKARD, A.J., AND WELSINK, H.J. 1987. Extensional tectonics and stratigraphy of Hibernia Oil Field, Grand Banks, Newfoundland. *AAPG Bulletin*, v. 71, p. 1210-1232.

TONKIN, N.S., MCILROY, D., MEYER, R., AND MOORE-TURPIN, A. 2010. Bioturbation influence on reservoir quality: a case study from the Cretaceous Ben Nevis Formation, Jeanne d'Arc Basin, offshore Newfoundland, Canada. *AAPG Bulletin*, v. 94, p. 1059-1078.

CHAPTER 2

Sedimentology and Ichnology of the Hibernia Formation

Elizabeth R. Schatz[1,2], Duncan McIlroy[2],

[1] Corresponding author: elizabeth.schatz@mun.ca

[2] Department of Earth Sciences. Memorial University of Newfoundland, 300 Prince Philip Drive, St. John's, NL, A1B 3X5, Canada. dmcilroy@mun.ca

1. Abstract

A total of 7 core samples were taken from 5 offshore wells that intersected the Hibernia Formation in the southern Jeanne d'Arc Basin approximately 350 km east of St. John's, Newfoundland, Canada. Detailed sedimentological analysis of the core samples resulted in the classification of 17 lithofacies ranging from offshore marine mudstones to delta distributary channel conglomerates. Facies associations 1, 2, and 3 characterize a collection of bioturbated mudstone to sandstone facies interbedded with hummocky cross-stratified sandstone facies inferred to represent offshore, offshore transition, and storm-dominated lower shoreface settings, respectively. Marine facies commonly display trace fossil assemblages containing *Phycosiphon*, *Asterosoma*, *Chondrites*, *Teichichnus*, *Ophiomorpha*, *Palaeophycus*, and *Planolites*. Facies association 4 represents a progradational wave-influenced delta front characterized by moderately bioturbated

sandstones abruptly overlain by coarse-grained, delta front mouthbar sandstones transitioning upwards to wave-reworked sandstones. A gradual, upward transition from delta mouthbar sandstones to sandstones displaying dominantly wave-induced sedimentary structures, characterizes facies association 5. This facies association is interpreted as delta lobe abandonment as the association is only noted from the West Bonne Bay F-12 core. Facies association 6 is characterized by poorly sorted pebble conglomerates and coarse-grained, cross-bedded sandstones representing distributary channel fill and delta front mouthbar facies. Facies analysis resulted in the classification of wave-influenced delta which contrasts from the fluvial-dominated deltaic setting of the Hibernia Formation, Hibernia Field.

2. Introduction

The sedimentary basins of offshore Newfoundland are of significant interest to the petroleum industry. Many significant oil discoveries have been made there over the last 40 years (Arthur et al., 1982; MacKay and Tankard, 1990; Sinclair et al., 1992; Canada-Newfoundland and Labrador Offshore Petroleum Board (C-NLOPB) Annual Report 2015-16). Most notably the Hibernia Field, Jeanne d'Arc Basin, was developed after the Chevron et al. Hibernia P-15 discovery well intersected four sandstone intervals (Ben Nevis-Avalon, Catalina, Hibernia, and Jeanne d'Arc Formations) with an estimated production capacity of 20,000 barrels of oil per day (Figure 2.1; Arthur et al., 1982; MacKay and Tankard, 1990). Current petroleum reserve estimates for the Hibernia Field are 1644 million barrels of oil with 963 million barrels having been produced to date (C-NLOPB Annual Report 2015-16).

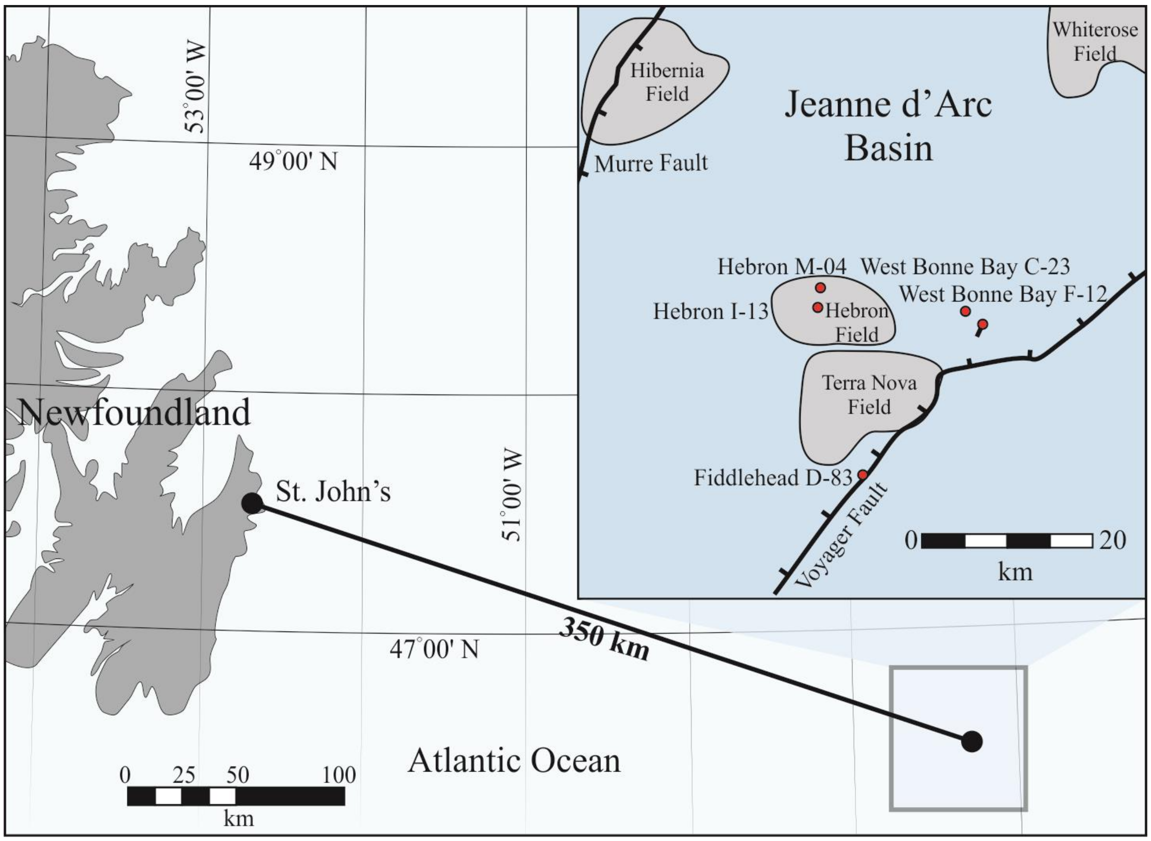

Figure 2.1. Map of Jeanne d'Arc Basin showing the location of the studied wells and surrounding oil fields: Hibernia, Hebron, Terra Nova, and Whiterose Fields. Major faults are shown with tick marks indicating downthrown sides.

The Hibernia Formation in the Hibernia Field region of the Jeanne d'Arc Basin has high quality reservoir sandstones in the lowermost intervals (Brown et al., 1989; Sinclair et al., 2005). The formation becomes progressively finer grained towards the top and is not well developed as a reservoir (Brown et al., 1989; Sinclair et al., 2005); however, the upper Hibernia interval becomes coarser-grained towards the southern portion of the basin (Sinclair et al., 2005). There has been greater interest in the reservoir potential of the upper Hibernia Formation since the drilling of the Husky Oil et al. West Bonne Bay F-12 discovery well in 2006 in the southern Jeanne d'Arc Basin (Figure 2.1; Sheppard et al., 2006). A significant gas column was discovered in the upper most portion of the Hibernia Formation in West Bonne Bay F-12, but no oil was present (Sheppard et al., 2006). A sidetrack well, West Bonne Bay F-12Z, was drilled down-dip in the same fault block where of gas and oil columns were discovered (Sheppard et al., 2006).

While the discovery of oil in the West Bonne Bay region did spark interest in the upper Hibernia sandstones, very little research has been conducted on the Hibernia Formation in the southern Jeanne d'Arc Basin. This paper aims to: a) present a sedimentological description of core from the Hibernia Formation in the southern Jeanne d'Arc Basin; and b) determine their paleodepositional setting.

3. Study location and geological setting

The Jeanne d'Arc Basin is situated on the Grand Banks, offshore Newfoundland, approximately 350 km east of St. John's. The study area includes two wells from the West Bonne Bay area, two wells from the Hebron Field, and one well from approximately

5 km south of the Terra Nova Field (Figure 2.1). The wells are spread over an area of approximately 250 km^2.

The Jeanne d'Arc Basin formed as a result of three stages of rifting beginning in the Late Triassic and continuing into the Tertiary (Enachescu, 1987; Tankard and Welsink, 1987; Sinclair, 1988; MacKay and Tankard, 1990; Sinclair et al., 1992; Sinclair et al., 1999). The first stage of rifting took place from the Late Triassic to the Early Jurassic (Sinclair, 1988; Sinclair et al., 1999). The Hibernia Formation was deposited near the end of the second stage of rifting, which ran from the Late Jurassic to Early Cretaceous (Sinclair et al., 1999). The Hibernia Formation is overlain by a basin-wide carbonate deposit that formed following a flooding event during a period of thermal subsidence (see Sinclair, 1988; Sinclair et al., 1999). The third rifting stage began in the late Early Cretaceous with minor faulting continuing into the Tertiary (Tankard and Welsink, 1987; Sinclair, 1988; Sinclair et al., 1999).

The Hibernia Formation is separated into the Upper Hibernia and Lower Hibernia Zones following the unofficial oilfield nomenclature presented by Sinclair et al. (2005; see Figure 2.2). The Upper Zone is divided into the Hebron and Cape Island Members. The stratigraphy of the Lower Zone is quite complex and is composed of several sandstone and shale sequences. The basal Hibernia sandstone (Layer 3) is found near the bottom of these sequences above the Fortune Bay Formation.

4. Methods

The core materials for this study are housed at Canada-Newfoundland Offshore Petroleum Board (C-NLOPB) core facility in St. John's, Newfoundland. Three cores from

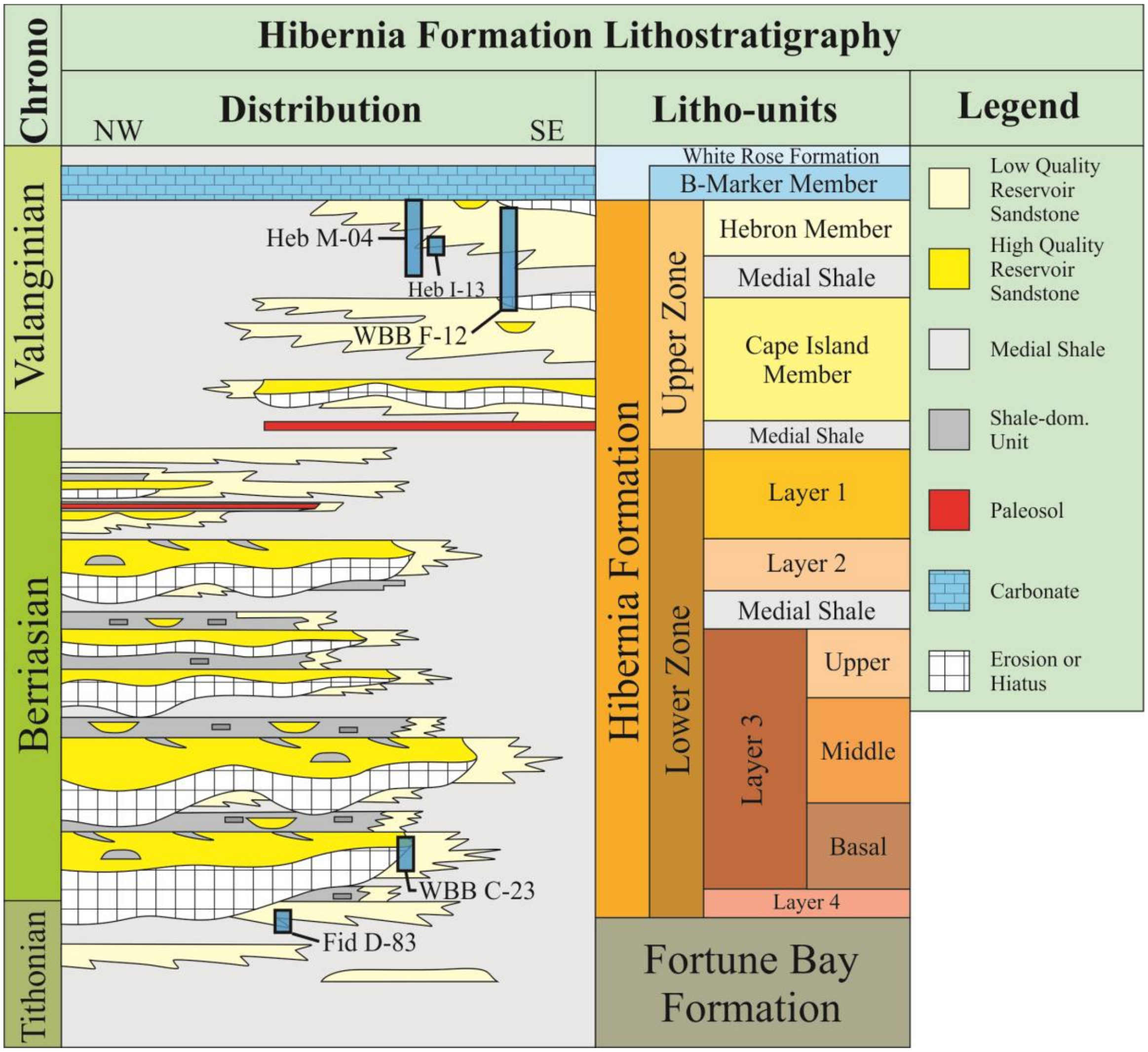

Figure 2.2. Lithostratigraphy and distribution of the Hibernia Formation, Jeanne d'Arc Basin (modified from Sinclair et al., 2005). Approximate core locations are identified: Hebron M-04 (Heb M-04), Hebron I-13 (Heb I-13), West Bonne Bay F-12 (WBB F-12), Fiddlehead D-83 (Fid D-83), and West Bonne Bay C-23 (WBB C-23).

the Hebron Member, Upper Hibernia Zone were investigated: 1) Mobil et al. Hebron I-13, core 4 (2944-2962 m; 17.48 m recovered of 18 m); 2) Chevron et al. Hebron M-04, core 3 (2984-3094 m; 110 m complete recovery); and 3) Husky Oil et al. West Bonne Bay F-12, core 1 (3923-4033 m; 110 m complete recovery; deviated approximately 40° from vertical). Four cores from the basal unit of Layer 3, Lower Hibernia Zone were studied: 1) Statoil Canada Ltd. Fiddlehead D-83, core 1 (1412-1417.1 m; 5.1 m complete recovery) and core 2 (1418.5-1442.43 m; 23.93 m complete recovery); and 2) Amoco et al. West Bonne Bay C-23, core 1 (3788-3789.2 m; 1.2 m complete recovery) and core 2 (3798-3816.6 m; 18.6 m complete recovery). The Fiddlehead D-83 penetrated into the underlying Fortune Bay Formation (Figure 2.2). As a result of the shallow burial depth in the Fiddlehead D-83 well, much of the sandstone that was not calcite cemented remains weakly consolidated. All given depths are measured depths from the core samples.

All sedimentological data were documented through direct observation of the core samples at the C-NLOPB core laboratory. Lithofacies descriptions were produced from the core log data and used as the basis for facies analysis. Petrographic thin sections were produced to compliment sedimentological descriptions of core material, and to further investigate morphological characteristics of the studied trace fossils. Thin sections were blue-dye impregnated to assess porosity of the sediments and to evaluate effects of burrowing behaviour on porosity (e.g. removal of clay-sized particles from the surrounding host sediment by the burrowing organism). Alizarin Red stain was used to differentiate between calcite and dolomite grains and cements under transmitted light microscopy. Additional porosity and permeability data were provided by C-NLOPB from core plug analyses of core materials.

The bioturbation index (BI) was assessed as a percentage of the bioturbated primary sedimentary rock fabric (see Taylor and Goldring, 1993). Trace fossils were classified only to the level of ichnogenus owing to uncertainties in species level identification from cross sections (cf. McIlroy 2008). A description of the observed ichnofabrics and tiering patterns is included with facies analysis.

5. Facies Analysis of the Hibernia Formation

Facies 1: Clay-Rich Mudstone

Description: This mudstone facies is composed predominantly of water-sensitive, swelling clays with minor silt grains (Figures 2.3a and b). The mudstone is massive in texture with faint mottling and rare siltstone laminae, but no discrete burrows could be seen. Rare disarticulated bivalves approximately 1 mm in size are observed. These clay-rich mudstones range in thickness from 10 cm to 2.5 m. Porosity values from core plug analyses average 6.4% with an average permeability of 0.44 mD; however, the high porosity is likely the result of destabilization of the core related to the swelling clays (Figure 2.3a).

Ichnofabric: Only post-depositional *Thalassinoides* and *Chondrites* filled with light-colored sediment from the overlying bed were observed.

Interpretation: Facies 1 is rarely interbedded with wave-generated siltstone deposits and is commonly overlain by sharp-based parallel-laminated sandstone beds (respectively Facies 3 and 6). The massive texture of the mudstone is likely the result of thorough reworking by infaunal organisms though no discrete burrows could be observed due to a lack of burrow fill of contrasting colour (Bromley, 1996). Comparable offshore

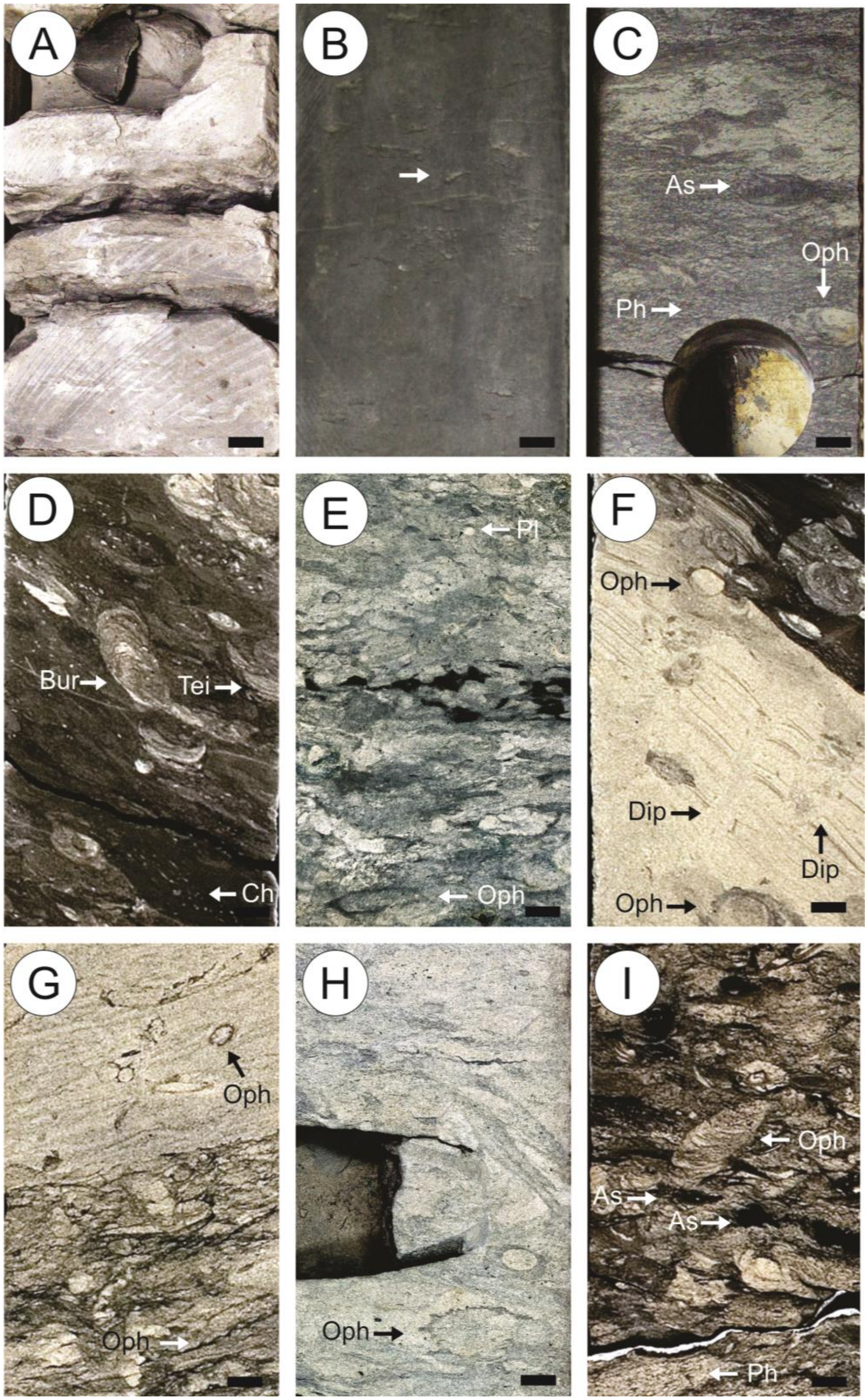
A
B
C
As
Oph
Ph
D
Bur
Tei
Ch
E
Pl
Oph
F
Oph
Dip
Dip
Oph
G
Oph
Oph
H
Oph
I
Oph
As
As
Ph

Figure 2.3. Sedimentary facies of the Hibernia Formation. A-B, Facies 1 unstratified clay-rich mudstone containing abundant swelling clay (A) and containing patchy swelling clay (B, arrow). Photos from 3052 m (A) and 3017.3 m (B) of Hebron M-04. C-D, Facies 2 bioturbated muddy siltstone. C, *Phycosiphon* (Ph) dominated ichnofabric with *Asterosoma* (As) and overprinted by *Ophiomorpha* (Oph) burrows from a higher stratigraphic interval. D, Completely bioturbated ichnofabric displaying *Teichichnus* (Tei), *Chondrites* (Ch), and a large, actively filled burrow (Bur). Photos from 3068.5 m in Hebron M-04 (C) and 3024 m in WBB F-12 (D). E, Facies 2 with abundant carbonaceous material displaying mottling by *Planolites* (Pl) with *Ophiomorpha* burrows (Oph). Photo from Fiddlehead D-83, 1428 m. F-G, Facies 3 laminated very fine-grained sandstone. F, wave-ripple lamination visible at the top of the photo with *Ophiomorpha* (Oph) and *Diplocraterion* (Dip) burrows below (photo from WBB F-12, 3024 m). G, erosive contact between Facies 3 (above) and Facies 4 (below) with *Ophiomorpha* (Oph) present in both (photo from WBB F-12, 3985 m). H-I, Facies 4 bioturbated very fine sandstone: H, an *Ophiomorpha* (Oph) dominated ichnofabric in Fiddlehead D-83 core 2, 1426 m; I, ichnofabric containing *Ophiomorpha* (Oph), *Asterosoma* (As), and *Phycosiphon* (Ph) from WBB F-12, 4023 m. Scale bars are 1 cm.

facies are described from the Cretaceous Western Interior Seaway of North America (MacEachern and Pemberton, 1992; Pemberton et al., 2001; Hovikoski et al., 2008). This facies is inferred to represent suspension fall-out processes in a lower offshore depositional setting above storm wave base.

Distribution: This facies is only observed in the Hebron M-04 core sample.

Facies 2: Bioturbated Muddy Siltstone

Description: This facies is characterized by highly bioturbated muddy siltstone (Figures 2.3c-e). Grains range in size from lower very fine sand to fine silt and are composed of subangular to angular quartz with minor feldspar. Amorphous organic material, fine particulate carbonaceous debris, and opaque minerals are moderately abundant. Pore spaces are filled with calcite cement or mica and swelling clays. Moderately well sorted, laminated, sharp-based, thin siltstone beds with ripple cross-lamination are present throughout. This facies is commonly found as bedsets ranging from 4 cm to 5 m in thickness. Bioturbation is moderate to high (BI 3-6). Porosity from core plug analyses average 7.6 % with an average permeability of 0.07 mD.

Ichnofabric: Two distinct ichnofabrics were noted in this facies: one dominated by *Phycosiphon* and *Asterosoma*, and a second which includes *Ophiomorpha*, *Thalassinoides*, *Phycosiphon*, *Chondrites*, *Asterosoma*, *Teichichnus*, *Palaeophycus*, *Planolites*, and ?*Scolicia*. The first ichnofabric rarely contains *Teichichnus* and *Palaeophycus* but these are commonly reworked by *Phycosiphon* (Figure 2.3c). The second ichnofabric has equal abundance of *Teichichnus*, *Palaeophycus*, and *Asterosoma* with less abundant *Phycosiphon* burrows clustered in thin, sub-horizontal bands.

Ophiomorpha and *Thalassinoides* burrows are present in the fabric in low abundance. *Chondrites* burrows are noted in the muddy *Asterosoma* burrows and rarely in the muddy wall linings of *Ophiomorpha* (Figure 2.3d).

Interpretation: The fine-grained nature of this facies suggests deposition under low energy conditions. The high degree of bioturbation and diversity of deposit-feeding structures is indicative of favorable feeding conditions and sufficient time to colonize the substrate (Bromley, 1996; Pemberton et al., 2001). Thin siltstone beds and lenses are interpreted as wave oscillation deposits from low intensity storm events, which is additionally evinced by the common inter-bedding with Facies 6, likely resulted from storm events (Plint, 2010). The increased frequency and thickness of interbeds suggests a shallower bathymetric position than is inferred for Facies 1, though both Facies 1 and 2 were deposited below fair-weather wave base. This facies has been inferred to represent fair weather deposition in an upper offshore setting.

Distribution: Thick deposits of Facies 2 are commonly observed in the Hebron M-04 well. This facies is much less common in the West Bonne Bay F-12 and Hebron I-13 wells, where it is present in beds less than 1 m thick. Facies 2 is also observed in the Fiddlehead D-83 core 2, Lower Hibernia Zone (Figure 2.3e).

Facies 3: Laminated Very Fine-Grained Sandstone with Wave Ripple Tops

Description: This facies is characterized by sharp-based, moderately well sorted, very fine-grained quartzose sandstone beds 5 to 30 cm in thickness, with symmetrical ripples and mud-drapes at bed tops (Figures 2.3f and g). Grains are sub-rounded, and range from upper fine-grained sand to coarse silt. Bed tops are moderately bioturbated, and contain both mud and sand-filled burrows (BI 2-3; Figure 2.3f). Foraminifera were observed within this facies. Porosity from core plug analyses average 13.7% with an average permeability of 24.8 mD.

Ichnofabric: This facies is moderately bioturbated by trace fossils conventionally inferred to be suspension/dwelling structures (e.g. *Skolithos*, *Diplocraterion*, *Thalassinoides*, and *Ophiomorpha*; Figure 2.3f; Bromley, 1996). Mud-filled *Asterosoma*, observed locally in bed tops, originated from overlaying bioturbated mudstone (Facies 2). Rarely, *Chondrites* are observed to have reworked muddy *Ophiomorpha* linings and *Asterosoma* burrows and, as such, likely originate from a higher stratigraphic level.

Interpretation: This facies is commonly interbedded with Facies 2 and is inferred to have been deposited in an offshore setting under conditions where initial erosion was followed by deposition under the influence of oscillatory wave conditions (Coe, 2003; Plint, 2010). Sand-filled burrows within the underlying mudstone indicate that deposition was abrupt, filling shallower-tier open burrows (Frey, 1990; MacEachern and Pemberton, 1992; Pemberton et al., 2001; MacEachern et al., 2005). The low degree of bioturbation and rarity of deposit feeding structures in these thin deposits may be the result of a lack of labile organic matter (Pemberton et al., 2001; MacEachern et al., 2005).

Distribution: This facies is observed in the West Bonne Bay F-12, Hebron I-13, and Hebron M-04 wells.

Facies 4: Bioturbated Very Fine-Grained Sandstone

Description: This facies is characterized by highly bioturbated very fine-grained sandstone with variable mud content (Figures 2.3g-i). Grain sizes range from lower fine sand to coarse silt composed predominantly of quartz with minor feldspar and mica. Grains are subangular to subrounded and moderately sorted, and clay minerals are locally present either in pore spaces or concentrated in thin laminae. Bedding boundaries and primary sedimentary structures are mostly obscured by bioturbation. This facies may range from 10 cm to 3 m thick, and contains rare carbonaceous debris surrounded by oxidized burrow halo. Calcite and dolomite cement are common, though appear to be mutually exclusive in this facies. Foraminifera are observed in low abundance through this facies. Thin section analysis demonstrates low porosity values, and pore spaces are rarely interconnected unless enhanced by fossil burrows (e.g. *Phycosiphon* isp.; cf. Tonkin et al., 2010). However, average porosity from core plug analysis is 11% with and average permeability of 4.2 mD. A bioturbation index (BI) of 4 to 6 is noted for this facies.

Ichnofabric: Common trace fossils observed in this facies are *Chondrites*, *Ophiomorpha*, *Teichichnus*, *Asterosoma*, *Planolites*, ?*Palaeophycus*, and ?*Scolicia*. As this facies transitions to Facies 2, *Phycosiphon* and *Thalassinoides* are observed locally. Rarely, *Phoebichnus* is observed in the Hebron M-04 core. The overall ichnofabric observed in this facies similar to the diverse ichnofabric observed in Facies 2 though *Ophiomorpha* burrows are more common.

Interpretation: Reworking by infaunal organisms likely kept pace with sedimentation rates resulting in a highly bioturbated sedimentary fabric. This facies is commonly interbedded with storm-generated deposits and is inferred to have been deposited during fair weather conditions within the lower shoreface to offshore transition (MacEachern and Pemberton, 1992; Pemberton et al., 2001; MacEachern et al., 2005;

Plint, 2010). The diversity of the trace fossil assemblage and high degree of bioturbation suggest normal marine conditions were present (cf. MacEachern et al., 2005; MacEachern and Gingras, 2007), though storm frequency may have been stress factor.

Distribution: Facies 4 is observed in all three studied wells from the Upper Hibernia Zone and in both cores from the Fiddlehead D-83 well of the Lower Hibernia Zone. The facies has a higher abundance of clay minerals and the maximum grainsize is restricted to very fine-grained sandstone in the Hebron M-04 well. The Hebron M-04 well also has enhanced porosity in this facies where *Phycosiphon* burrows are present.

Facies 5: Bioturbated Fine-Grained Sandstone

Description: This facies is characterized by highly bioturbated fine-grained sandstone with little to no mud content (Figures 2.4a-d). Grain sizes range from coarse silt to upper medium sand, but deposits are commonly moderately to well sorted. Grains are subangular and composed of mainly quartz with minor feldspar and bioclastic debris from bivalves and serpulid worm tubes is common. Locally, lithic clasts of sedimentary origin are observed. Bedding boundaries are mostly obscured by burrows, though sharp basal contacts are locally observed. Rarely, faint horizontal laminae may be seen within beds where bioturbation activity is decreased. Beds with low mud content may appear massive. Deposits range in thickness from 10 cm to 2 m. Bioturbation index is 4-6. Porosity measured from core plugs of the Upper Hibernia Zone wells averages 10.7% with an average permeability of 2.9 mD. Core plugs taken from the West Bonne Bay C-23 core samples, Lower Hibernia Zone, display coarser grain sizes with average porosities and permeabilities of 13.4% and 13 mD.

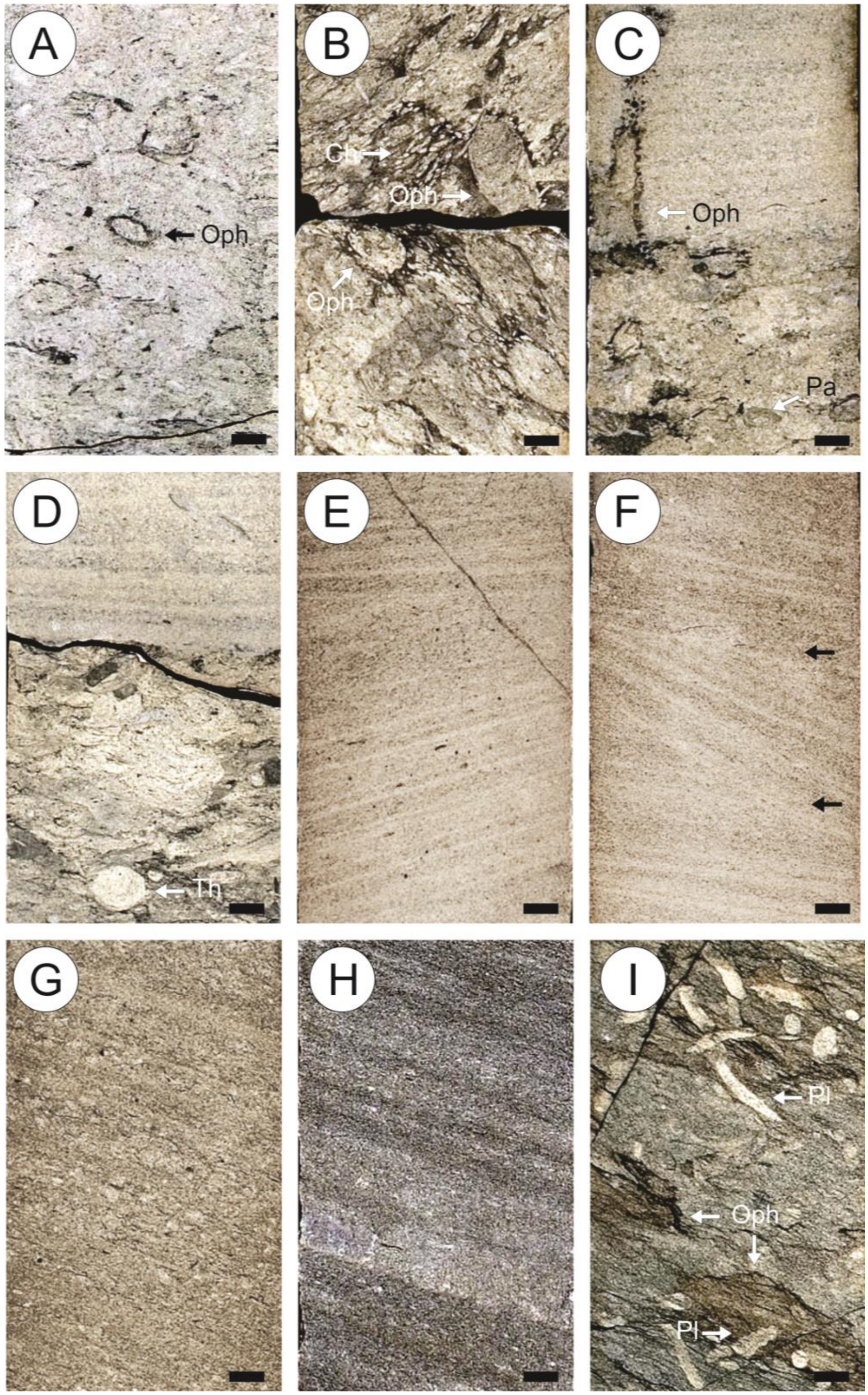
A
Oph
B
Ch
Oph
Oph
C
Oph
Pa
D
Th
E
F
G
H
I
Pl
Oph
Pl

Figure 2.4. Sedimentary facies of the Hibernia Formation. A-B, Facies 5 bioturbated fine-grained sandstone displaying abundant *Ophiomorpha* (Oph) burrows and *Chondrites* (Ch). Photos take from 3814 m in WBB C-23 core 2 (A) and 3992 m in WBB F-12 (B). C-D, eroded Facies 5 overlain by Facies 6 showing *Ophiomorpha* (Oph) crossing both facies (C) and *Thalassinoides* (Th) in-filled by sandstone above (D). *Palaeophycus* (Pa) visible at the bottom of image C, taken from 4026 m of WBB F-12. D, Photo from WBB F-12, 3987 m. E-F, Facies 6 parallel laminated sandstone displaying low angle truncations (E) and more frequent changes in angle interpreted as swaley cross-stratification (F). Photos from WBB F-12, 3965 m (E) and 3957 m (F). G-H, Facies 7 laminated sandstone with abundant shell material. Facies 7 may contain abundant fine particulate carbonaceous debris (H). Photos from WBB F-12, 3925 m (G) and 3952 m (H). I, Facies 8 fine-grained sandstone with *Ophiomorpha* (Oph) and overprinting *Planolites* (Pl) taken from WBB F-12, 3938 m. Scale bars are 1 cm.

Ichnofabric: This facies is highly bioturbated with discrete trace fossils of *Ophiomorpha*, *Palaeophycus*, *Planolites*, *Chondrites*, *Teichichnus*, and *Asterosoma*. Rarely, vertical burrows resembling *Skolithos* and *Arenicolites* are observed. Four ichnofabrics were identified:

1) An ichnofabric containing *Ophiomorpha*, *Chondrites*, *Planolites*, *Palaeophycus*, *Asterosoma*, and *Teichichnus*. *Ophiomorpha* is the most abundant form and commonly has an alternating sand-mud burrow fill suggestive of deposit feeding behaviour. *Chondrites* is observed reworking the *Asterosoma* burrows and muddy *Ophiomorpha* wall linings (Figure 2.4b).

2) This facies is commonly interbedded with laminated sandstones and thinly bedded sandstones. When these thin sandstones are more abundant, the diversity of the assemblage decreases and an ichnofabric dominated by *Ophiomorpha*, *Planolites*, and *Palaeophycus* is observed. This is the most common ichnofabric observed in Facies 5 (Figures 2.4a and c).

3) A monospecific *Planolites* assemblage may signify a short-lived hiatus between events (i.e. colonization window; cf. Pollard et al., 1993; Taylor et al., 2003). However, when observed associated with deltaic deposits, the *Planolites* assemblage may be a response to salinity changes and/or the introduction of xylic organic matter that is not as suitable a food source for other trace makers (Bromley, 1996; MacEachern et al., 2005; MacEachern and Gingras, 2007).

4) The final ichnofabric contains *Ophiomorpha* with rare *Skolithos* and *Arenicolites*. *Skolithos* and *Arenicolites* are found in sandier sections of this facies with decreased mud content. Horizontal galleries of *Ophiomorpha* commonly cross-cut the

vertical burrows and likely originate from a higher stratigraphic level or may represent a shallower tier (Bromley, 1996).

Interpretation: Scoured basal contacts and faint horizontal laminae are sometimes observed in this facies indicating that the sandstones were deposited following hydrodynamic events (Plint, 2010). The sandstones were likely colonized by opportunistic infaunal organisms resulting in ichnofabrics 1, 2 and 4 listed above. The high degree of bioturbation suggests that the time available for colonization was sufficient to completely rework the deposit (Pollard et al., 1993; MacEachern et al., 2005). The *Skolithos* and *Arenicolites* ichnofabric likely reflects the presence of a suspension feeding community that colonized the substrate shortly after deposition during waning energy conditions (MacEachern et al., 2005). The subsequent horizontal trace fossils are inferred to be deposit-feeding structures representing the activity of a fair-weather community. This facies is inferred to have been deposited in a shoreface setting above fair-weather wave base (MacEachern and Pemberton, 1992; MacEachern et al., 2005).

Distribution: This facies is most common in the West Bonne Bay F-12 core 1 and was observed in lower abundance in the Hebron I-13 and M-04 wells. It is also present in both cores of the West Bonne Bay C-23 well.

Facies 6: Parallel Laminated Fine-Grained Sandstone

Description: This facies is characterized by parallel to subparallel laminated fine-grained sandstone with low angle truncations (Figures 2.4c-f). Grain sizes range from very fine- to fine-grained sand, and are composed of quartz with minor feldspar. Sandstone laminae range in thickness from 1-12 mm and may be separated by very thin laminae of muddy sediment. Locally, sandstone laminae have very subtle, concave up curvature. Erosional basal contacts are observed containing bioclastic debris and rounded mud rip-up clasts. Some beds show cryptobioturbation of the sand and mud laminae, which results in local homogenization of the sandstone fabric. This facies commonly exhibits fining upward trends to bioturbated very fine-grained sandstone (Facies 4). The degree of bioturbation within the bed is BI 0-1 and increases to a BI 3 at bed tops. Fragmented serpulid worm tubes and bivalve shells are observed throughout this facies. Beds are commonly calcite cemented though some beds contain abundant dolomite within pore spaces. Beds commonly range from 30 cm to 1 m in thickness, though amalgamated deposits may be as thick as 7 m. Porosity values from core plug analyses average 10.3% with an average permeability of 17.8 mD.

Ichnofabric: This facies commonly contains *Ophiomorpha*, *Planolites*, and *Palaeophycus* in low abundance (BI 1). At the top of sandstone beds, *Teichichnus*, *Planolites*, *Asterosoma*, *Palaeophycus*, *Ophiomorpha*, and *Chondrites* are observed where this facies transitions into Facies 4 or 5 (BI 1-3). Some beds have cryptobioturbation (Figures 2.4e and f) or locally may have a fabric that resembles that of *Macaronichnus* (cf. Clifton and Thompson, 1978).

Interpretation: The parallel laminated sandstones with low angle truncations are inferred to represent hummocky cross-stratification (HCS) expressed in core sample (cf. MacEachern and Pemberton, 1992; MacEachern et al., 1998; Hiscott et al., 2008; MacEachern et al., 2005). This facies is commonly interbedded with bioturbated sandstone of Facies 4 and 5 which were interpreted as shoreface to offshore transition. Thick, successions of amalgamated sandstone beds are indicative of a shoreface setting with frequent of storm deposition (Frey, 1990; MacEachern et al., 1998; MacEachern et al., 2005). Erosional truncation in amalgamated sections gives the impression of swaley cross-stratification (SCS; Frey, 1990; MacEachern and Pemberton, 1992).

Distribution: This facies is observed in all the studied wells.

Facies 7: Laminated Fine to Medium Grained Sandstone with Shell Debris

Description: This facies is characterized by laminated fine to medium grained sandstone composed of sub-angular quartz and minor feldspar, with abundant fine shell debris contained within the laminae (Figure 2.4g). Variable mud content and fine particulate carbonaceous debris result in a dirty appearance of some sand layers (Figure 2.4h). The calcite cemented sediment filling the shell cavities has a slightly different colour than the surrounding sediment; however, all grains are tightly carbonate cemented within this facies. Beds are 10-30 cm in thickness and have a higher concentration of bioclastic debris at the base. Bioturbation is low to absent (BI 1-0).

Ichnofabric: Only rare *Ophiomorpha* burrows are observed in this facies.

Interpretation: The shell fragments in Facies 7 display a uniform size range, less than 1 cm in length. It is inferred that this facies was influenced by constant wave action with a consistent energy level (Plint, 2010). The dissolution of shell material which then cemented the surrounding sand grains appears to be different from the overall calcite cement indicating the potential for two stages of cementation. This facies is observed in a fining-upward succession of sandstones ranging from distributary channel conglomerates to shoreface sandstones.

Distribution: This facies is only observed in the West Bonne Bay F-12 core 1.

Facies 8: Fine-Grained Sandstone With *Planolites* Burrows

Description: This facies is characterized by fine-grained sandstone with abundant carbonaceous material and *Planolites* burrows (Figure 2.4i). Grain sizes range from coarse silt to fine-grained sandstone though rare, coarse sand grains are present. Deposits are commonly poorly to moderately sorted and composed of quartz with minor feldspars and micas. Grains are subangular and tightly calcite cemented. Fine particulate carbonaceous material within the sandstone gives the appearance of horizontal bedding. The grain size and mineralogy of the burrow fill is identical to the host rock but lacks carbonaceous material and much of the calcite cementation. Beds are 10-40 cm thick and closely associated with Facies 10. Locally, faint *Ophiomorpha* burrows are observed to be overprinted by the *?Planolites* burrows (BI 2-3).

Ichnofabric: Two stages of colonization are indicated by the trace fossil assemblage. *Ophiomorpha* burrows are found in low abundance and represent the initial colonization of the sediment after the depositional event. These burrows have a slightly squashed appearance suggesting that compaction took place sometime afterwards, likely as a result of further burial (Bromley, 1996). The sharp-walled nature of the overprinting *?Planolites* burrows suggests that the sediment was of a firmground consistency during the second stage of colonization (sensu Ekdale, 1985). Erosional exhumation of the firmground sediment would have been required to bring the substrate back to a shallower stratigraphic level to allow colonization by *?Planolites* (Bromley, 1996). The fill of *?Planolites* burrows appears cleaner than the surrounding rock and does not match the overlaying sandstones suggesting that one or more depositional units are missing from the depositional record.

Interpretation: The two stages of colonization inferred from trace fossil evidence suggest that this facies represents a complex depositional history. This facies is commonly interbedded with coarse-grained sandstones (Facies 10 and 11) interpreted as mouthbar facies and the high abundance of carbonaceous fragments implies fluvial influence. Monospecific *?Planolites* assemblages are often attributed to stressful hydrological conditions such as differential salinity (Pemberton et al., 2001;MacEachern et al., 2005; MacEachern and Gingras, 2007). Considering the predominance of wave-influenced sedimentary structures observed in the studied core samples, a wave-influenced environment is likely. Following the wave-influenced deltaic model presented by Bhattacharya and Giosan (2003), a sheltered lagoon landward of a barrier island could provide the conditions required to produce this sedimentary facies (i.e. rapid changes in sedimentation rate and type, differential salinity, erosion).

Distribution: This facies is only observed in the West Bonne Bay F-12 core.

Facies 9: Massive Fine- To Medium-Grained Sandstone

Description: This facies is composed of massively bedded, quartz-rich, fine- to medium-grained sandstone (Figure 2.5a). The basal contact is commonly erosive with abundant bivalve and serpulid worm tube fragments (Figure 2.5b). Medium-grained sandstone is observed at the base grading into fine-grained sandstone. Sandstone beds are poorly to moderately sorted ranging in grain size from coarse silt to medium sand. Locally, beds have a coarsening upward trend with bioclastic material at the top. Beds are

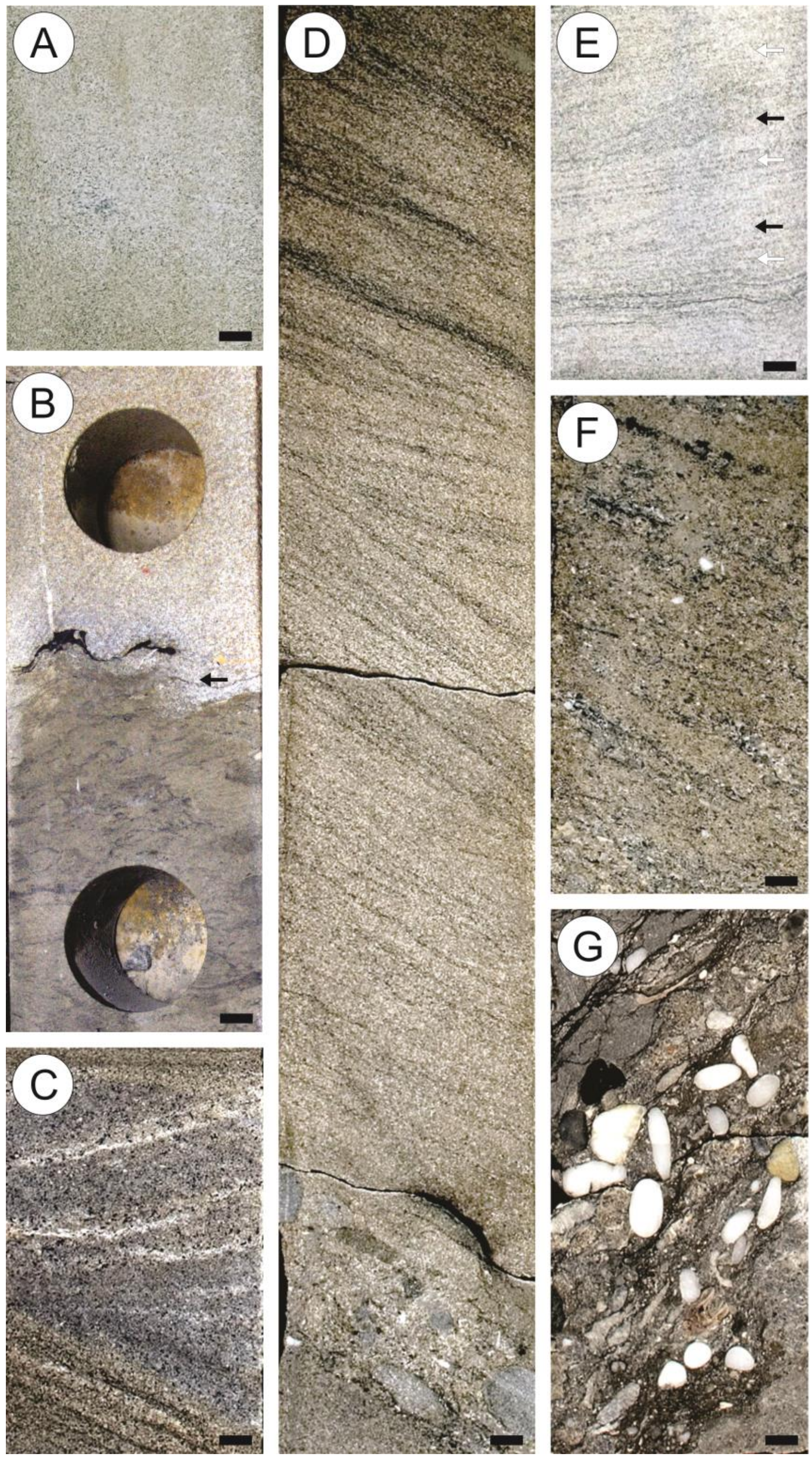
A
B
C
D
E
F
G

Figure 2.5. Sedimentary facies of the Hibernia Formation. A, Facies 9 massive fine- to medium-grained sandstone from WBB C-23, 3804.5 m. B, Facies 9 overlaying Facies 4 is interpreted as a candidate sequence boundary with compactional deformation (arrow). Photo from Hebron M-04, 3036 m. C-E, Facies 10 cross-bedded sandstone. Photo taken from WBB F-12, 3937 m (C) and 3998 m (showing erosional basal contact and pebble lag, D). E, photo taken from WBB C-23, 3807 m, showing stacked unidirectional ripples (cross-laminations marked by black arrows, topsets by white arrows). F, Facies 11 parallel bedded medium- to coarse-grained sandstones from WBB F-12, 4011m. G, Facies 12 conglomerate bed containing large, white quart pebbles from WBB F-12, 3945 m. Scale bars are 1 cm.

commonly 20-60 cm thick with a blocky profile. Grains may be either silicate cemented with minor calcite or tightly calcite cemented. Discrete burrows are not visible though the massive texture of the sandstone may be the result of extensive burrowing activity and a lack of clay and silt grade sediment. Core plug analyses from the Upper Hibernia Zone core samples show average porosities of 10.8% with average permeabilities 32.2 mD. Lower Hibernia Zone core plug analysis averages 15.4 % porosity and 352.1 mD permeability.

Ichnofabric: Locally, West Bonne Bay C-23 core samples display a *Macaronichnus*-like appearance.

Interpretation: The massive texture of the sandstone may be the result of either *Macaronichnus*-like bioturbation or a lack of fine-grained material of contrasting colour or a combination of the two. Above fair weather wave base, fine-grained material is kept in suspension by high energy wave processes (Coe, 2003). This facies is commonly poorly to moderately sorted with coarse-grained or bioclastic lags preserved at the base. This would suggest high energy conditions that decreased rapidly (Coe, 2003). Similar "structureless" sandstone facies are described from the Dunvegan Formation, northwestern Alberta, in association with fluvial-dominated delta front sandstones (Facies 4F, Bhattacharya and Walker, 1991). Massive sandstones are also described by Walker (1986) from the Cardium Formation of the Cretaceous Western Interior Seaway. Walker (1986) associated these massive sandstones with upper flow regime conditions comparable to basal turbidite sandstone deposits (i.e. Bouma division a; Bouma, 1962). In this study, this facies is commonly associated with sandstones representing delta front processes.

Distribution: The facies is observed most commonly in core samples from the Hebron I-13 and M-04 wells as well as both core samples from the West Bonne Bay C-23 well. It is rarely seen in the West Bonne Bay F-12 core.

Facies 10: Cross-Bedded Medium- To Coarse-Grained Sandstone

Description: This facies is characterized by medium- to coarse-grained, low-angle cross-bedded sandstone with abundant bioclastic and carbonaceous debris (Figures 2.5c-e). Coarse-grained sandstone to pebbles are locally observed at the base of normally graded beds (Figure 2.5d). Grain sizes range from very fine- to very coarse-grained sand. Grains are subrounded and poorly sorted composed predominantly of quartz with minor feldspar, quartzite lithic clasts, and rare amphibole. Beds are observed as low angle cross-bedding transitioning to more horizontally-oriented beds. Locally, cross beds display a concave-up curvature. Carbonate cement is common, especially where bioclastic debris is most concentrated, occupying approximately 50% of the mineral composition. Bioclastic debris is composed of fragmented coral, shell debris, and serpulid tubes. All bioclastic debris has some degree of rounding though coral fragments are typically spherical. Bedsets are 10-40 cm forming successions up to 2 m thick. Cross-beds are draped with fine particulate carbonaceous material and muddy sediment. Basal contacts are commonly erosional and bed profiles may be blocky or have a slight fining upward trend. Porosity values from core plug analyses average 13% with permeabilities ranging from less than 1 mD to 900 mD.

Ichnofabric: Discrete *Ophiomorpha* burrows are rare. Locally, cryptobioturbation is observed within medium-grained beds (BI 2).

Interpretation: The low angle cross-bedding with bed curvatures transitioning to horizontal bedding may represent trough cross-bedding expressed in core sample (Bhattacharya and Walker, 1991; Pemberton et al., 2001; Bhattacharya, 2006). Trough cross-bedding is commonly the result of migration of large scale bedforms (Coe, 2003). The poorly sorted but normally graded beds are indicative of waning flow conditions (Nichols, 1999; Coe, 2003). The erosional basal contact observed in this facies indicates that erosional exhumation following a high-energy event likely preceded sandstone deposition. Taking the high abundance of carbonaceous material into account, it is inferred that this facies is the result of high fluvial discharge in a shoreface setting. Facies 10 is interpreted as delta front mouthbar sandstones.

Distribution: This facies is observed in the West Bonne Bay F-12 core 1 and West Bonne Bay C-23 core 2.

Facies 11: Parallel Bedded Medium- To Coarse-Grained Sandstone

Description: This facies is characterized by parallel bedded medium- to coarse-grained sandstone fining upward to parallel laminated or thinly bedded fine-grained sandstone (Figure 2.5f). Very coarse-grained sandstone to granules are common at the base of normally graded thin beds. Grain sizes range from very fine- to very coarse-grained sand. Grains are subrounded and poorly sorted composed predominantly of quartz with minor feldspar and quartzite lithic clasts. Beds are carbonate cemented and contain fragmented bivalve and serpulid tubes. Carbonaceous debris composed of fine particulate material or larger wood fragments and stringers is common forming layers parallel to bedding. Rarely, low-angle, unidirectional cross-lamination is observed between horizontal beds. Beds are 5-40 cm thick and have erosional basal contacts. Bioturbation is low to absent (BI 0-1).

Ichnofabric: This facies contains only rare occurrences of *Ophiomorpha* burrows.

Interpretation: Parallel bedding and coarse grain sizes are suggestive of high energy hydrodynamic conditions; however, those conditions likely waned resulting in the finning upward bed transition (Dalrymple, 2010). Rare cross-lamination indicates that energy conditions decreased enough to allow ripple formation (Dalrymple, 2010). These beds commonly grade into parallel laminated sandstones with abundant carbonaceous material. It is inferred that this facies represents high energy discharge, possibly originating from a fluvial source.

Distribution: This facies is observed in the West Bonne Bay F-12, Hebron M-04, and Hebron I-13 wells.

Facies 12: Erosively Based Conglomerate Beds

Description: This facies contains erosively based, normally graded, granule to pebble conglomerate beds fining upward to cross-bedded or planar laminated sandstones (Figure 2.5g). Locally, cobble sized clasts have been observed within coarse to very coarse sand. This facies is commonly matrix-supported, composed variably of fine- to very coarse-grained sand, and are very poorly sorted. Clasts are rounded to ovoid and composed of pure quartz, chert, or metasedimentary lithic material. Bioclastic and carbonaceous debris are common. Locally, large, laminated mud rip-up clasts and concentrically layered mud balls are present within overlying units which may be reworked examples of the trace fossil Rosselia. Bed successions range from 10-50 cm in thickness. Bioturbation is absent within the coarser-grained beds, though *Ophiomorpha*, *Planolites*, and *Teichichnus* burrows (BI 2-3) are observed in the finer-grained facies overlying the basal conglomerate.

Ichnofabric: No bioturbation is observed in the conglomerate facies.

Interpretation: This facies represents high energy processes that deeply eroded the underlying shoreface sandstones. The rounded clasts may have eroded from a higher stratigraphic level or been carried by high energy flows to fill the excavated channel (Coe, 2003; Dalrymple, 2010). The facies fines upwards to cross-bedded and planar laminated sandstones which likely represent bedform migration within the channel (Bhattacharya, 2006). This facies is interpreted as a distributary channel fill.

Distribution: This facies is only observed within the West Bonne Bay F-12 core 1.

Facies 13: Erosively Based Shell Beds

Description: This facies is characterized by 10-60 cm thick erosively-based beds composed of bioclastic debris with little to no clastic material (Figure 2.6a). Beds are commonly highly calcite cemented. Occasionally, the bioclastic material is observed to transition upwards to more clastic, finer-grained facies. Thin carbonaceous stringers are locally observed within the beds. Fragmented bivalve, gastropod, and serpulid shells are commonly observed as well as coral and crinoid fragments. Shell fragments form rounded blades while coral material is commonly spherical or ovoid. Bioturbation is rare to absent (BI 0-1). Horizontal *Ophiomorpha* burrows filled with bioclastic debris have been observed at the base or directly below these beds. Porosity values from core plug analyses average 3.5% with an average permeability of 0.08 mD.

Ichnofabric: Only rare *Ophiomorpha* burrows are observed in this facies.

Interpretation: The bioclastic material contained within these beds is highly fragmented, likely as a result of high energy wave processes (Pemberton et al., 2001; Plint, 2010). The lack of clastic material in the shell beds may be a result of strong currents keeping the finer-grained clastic material in suspension while the heavier shell debris is reworked on the ocean floor. The fining upward character of some of these beds suggests waning energy. This facies is inferred to represent sand-winnowed shelly storm deposits.

Distribution: This facies is observed in the West Bonne Bay F-12, Hebron I-13, and Hebron M-04 wells.

Facies 14: Laminated Sandstone With Coal Fragments And Carbonaceous Debris

Description: This facies is composed of moderately to well-sorted thin beds of laminated sandstone with abundant carbonaceous material in the form of fine particulate matter or coal debris (Figure 2.6b). Grain sizes range from coarse silt to coarse sand. Grains are angular to subrounded and composed of quartz and lithic clasts with minor feldspar, mica, and pyroxene. Laminae are dominantly parallel and draped with fine particulate carbonaceous material. Concentrated bands of carbonaceous material are observed to form layers 1-2 cm thick. Bed thickness ranges from 15-40 cm, though locally range up to 1.5 m in medium- to coarse-grained beds. Beds are variably calcite cemented and fine bioclastic debris is common. Foraminifera were observed within this facies. Rare occurrences of *Ophiomorpha* and *Planolites* were observed for this facies (BI 0-1). Porosity measurements from core plug analyses average 3.2% with an average

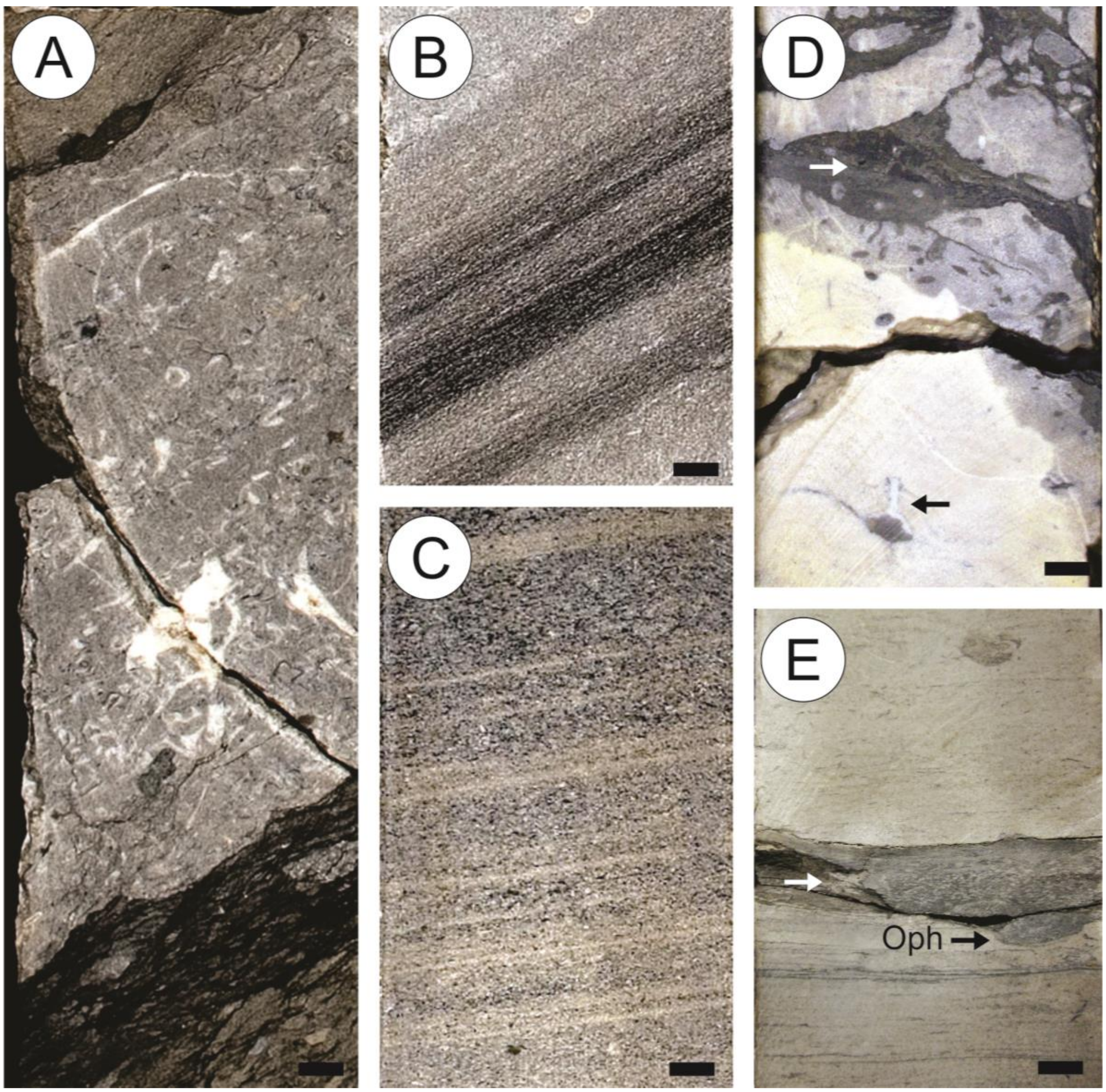
A
B
C
D
E
Oph

Figure 2.6. Sedimentary facies of the Hibernia Formation. A, Facies 13 erosively based shell beds from WBB F-12, 3974 m. B, Facies 14 laminated sandstone with coal fragments and carbonaceous debris from WBB F-12, 3949 m. C, Facies 15 thinly bedded fine sandstone from WBB F-12, 3996 m. D, Facies 16 coral debris in laminated mudstone (white arrow) showing borings and healing scars (black arrow) from Hebron M-04, 3049 m. E, Facies 17 fluid muds (white arrow) with cross-cutting *Ophiomorpha* (Oph) burrow. The fluid mud appears to be bioturbated by *Phycosiphon* (Hebron M-04, 3028 m). Scale bars are 1 cm.

permeability of 0.02 mD in fine-grained sandstones, though coarser-grained sandstone beds average 14% and 135.8 mD.

Ichnofabric: Only rare *Ophiomorpha* and *Planolites* were observed.

Interpretation: This sandstone shows both textural and mineralogical immaturity compared to other sandstone facies in this study. The abundant carbonaceous material present in the sandstone implies that proximity to a fluvial source is likely (Coe, 2003). However, the parallel laminated structure and moderately good sorting suggest that wave processes may have also influenced the formation of this facies (Pemberton et al., 2001). A shoreface-foreshore environment commonly exhibits high wave energy and parallel laminated, well sorted sandstones (MacEachern and Pemberton, 1992; Pemberton et al., 2001; Clifton, 2006; Plint, 2010). The lack of bioturbation, however, suggests that differential salinity in proximity to a fluvial source may have been a stress factor inhibiting colonization (Pemberton et al., 2001; MacEachern and Gingras, 2007). This facies likely represents wave-reworking of distributary mouthbar sandstones in shoreface-foreshore setting.

Distribution: This facies is observed in West Bonne Bay F-12 core 1, in both cores from the Fiddlehead D-83 well, and in West Bonne Bay C-23 core 2.

Facies 15: Thinly Bedded Fine-Grained Sandstones

Description: This facies is characterized by thinly bedded, normally graded sandstones (Figure 2.6c). Grain sizes range from very fine- to medium-grained sand composed of quartz, feldspar, and rare amphibole. Some lithic clasts and mica flakes are observed in these poorly to moderately sorted beds. Bioclastic and carbonaceous debris are common. Individual beds are 1 to 2 cm forming bedsets up to 20 cm thick. Bedsets commonly have a fining upward trend and may contain wavy laminae towards the top. This facies is often associated with parallel bedded coarse sandstones of Facies 11 and parallel laminated sandstones of Facies 6. Bioturbation is rare to low (BI 0-1). Porosity measured from core plug analysis averages 9% with an average permeability of 5 mD.

Ichnofabric: *Ophiomorpha* burrows are observed in this facies.

Interpretation: The immature nature of the sandstone suggests that it did not travel far from its original source. The thin, graded beds imply short pulses of high energy, waning flows (Nichols, 1999; Bhattacharya, 2006). Bioturbation is mostly absent, which may suggest stressful salinity conditions, high sedimentation rates, and/or a lack of edible organic material (MacEachern et al., 2005; MacEachern and Gingras, 2007).

Distribution: In the West Bonne Bay F-12 core, coarse-grained, parallel bedded sandstones are often observed to fine upwards into these thinly bedded finer-grained sandstone beds. The storm-generated parallel laminated sandstones are also closely observed with Facies 15, though these may either overlie or precede the thinly bedded sandstones. In the Hebron M-04 core 3 sample, Facies 15 is typically observed to be interbedded with bioturbated marine mudstones and storm beds. This facies was not observed in the Hebron I-13 core 4 sample.

Facies 16: Coral Debris In Mudstone

Description: This highly calcite cemented facies is composed of abundant calcareous debris with minor clay-rich cavity fills between coral fragments and shelly material (Figure 2.6d). The muddy component of this facies consists of amorphous organic material, micas, and clastic grains ranging in size from fine to coarse silt. Locally, mud exhibits laminated texture that conforms to the curvature of the underlying debris. Isolated beds may range from 5-15 cm, while thicker successions are 1-1.5 m thick. Mud-filled bivalve shells and fragmented coral branches commonly form the base of the layer and are overlain by larger pieces of coral and massively calcite cemented fragments. The outer surfaces of coral branches, coral domes, and some bivalve shells contain borings of variable diameter. Locally, Scleractinia coral was identified by examining septa in thin section. Porosity measurements from core plug analyses average 5% with an average permeability of 0.1 mD.

Ichnofabric: Borings with a rage of diameters are observed in this facies. Some coral fragments have healing scars suggesting that the borings occurred when the colony was still living (Figure 2.6d). No cross-cutting was observed suggesting that the borings occurred before the corals were concentrated into beds.

Interpretation: This facies likely represents the downslope debris of a coral reef community. The reef likely acted as a baffle for coarser grained sediments allowing only clay and silt to accumulate with the debris; however, the laminated appearance of some mud layers may indicate flow conditions. Due to poor well control in the study area, no reef source was identified though an oolitic limestone was described from drill cuttings in the Hebron I-13 well in the same interval.

Distribution: This facies is only observed in the Hebron M-04 well.

Facies 17: Laminated Clay-Rich Mudstone

Description: This facies is characterized by very thinly laminated mudstone composed of swelling clay (Figure 2.6e). Basal contacts are commonly sharp though are occasionally irregular or distorted by what appears to be burrowing activity. Beds are 1-2 cm thick and are overlain or interbedded with coarse grained sandstones. Rarely, beds contain discrete burrow structures but are more commonly cross-cut by burrows originating from adjacent sandstone beds.

Ichnofabric: Beds may contain *Chondrites*, *Palaeophycus*, *Phycosiphon*, or small horizontal *Ophiomorpha* and may be cross-cut by *Skolithos*-like vertical burrows or large *Ophiomorpha* originating from a different stratigraphic level (Figure 2.6e).

Interpretation: The laminated mudstone facies is interbedded with coarse-grained sandstones representing high energy depositional events or processes. The thin mudstones likely represent fluid mud deposition that occurred during the same event (see Bhattacharya and MacEachern, 2009; Zavala et al., 2011; Harazim and McIlroy, 2015). As the bedding boundaries are quite sharp, it is unlikely that these muds represent fairweather conditions between events. Due to the swelling nature of the clay material, no thin sections could be collected to determine if small-scale sedimentary structures were present (cf. Harazim and McIlroy, 2015). The burrows present within the mudstones and cross-cutting through them likely represent post-depositional colonization of the event beds (Hovikoski et al., 2008).

Distribution: This facies is observed in the Hebron M-04 core.

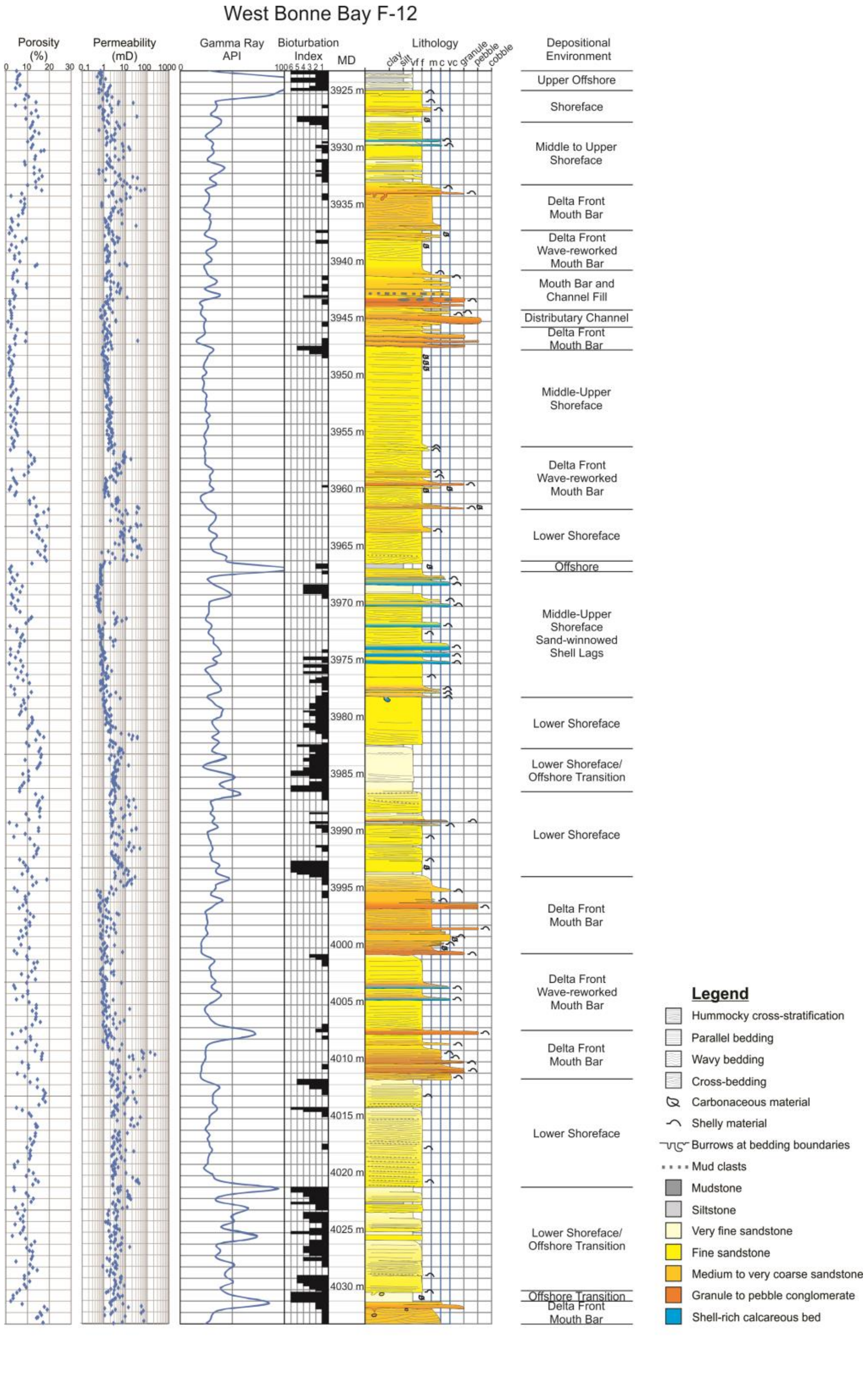
West Bonne Bay F-12
Porosity (%)
Permeability (mD)
Gamma Ray API
Bioturbation Index
MD
Lithology
clay
silt
vf
f
m
c
vc
granule
pebble
cobble
Depositional Environment
Upper Offshore
Shoreface
Middle to Upper Shoreface
Delta Front Mouth Bar
Delta Front Wave-reworked Mouth Bar
Mouth Bar and Channel Fill
Distributary Channel
Delta Front Mouth Bar
Middle-Upper Shoreface
Delta Front Wave-reworked Mouth Bar
Lower Shoreface
Offshore
Middle-Upper Shoreface Sand-winnowed Shell Lags
Lower Shoreface
Lower Shoreface/ Offshore Transition
Lower Shoreface
Delta Front Mouth Bar
Delta Front Wave-reworked Mouth Bar
Delta Front Mouth Bar
Lower Shoreface
Lower Shoreface/ Offshore Transition
Offshore Transition
Delta Front Mouth Bar
Legend
Hummocky cross-stratification
Parallel bedding
Wavy bedding
Cross-bedding
Carbonaceous material
Shelly material
Burrows at bedding boundaries
Mud clasts
Mudstone
Siltstone
Very fine sandstone
Fine sandstone
Medium to very coarse sandstone
Granule to pebble conglomerate
Shell-rich calcareous bed

Figure 2.7. Summary core diagram of the West Bonne Bay F-12 core 1.

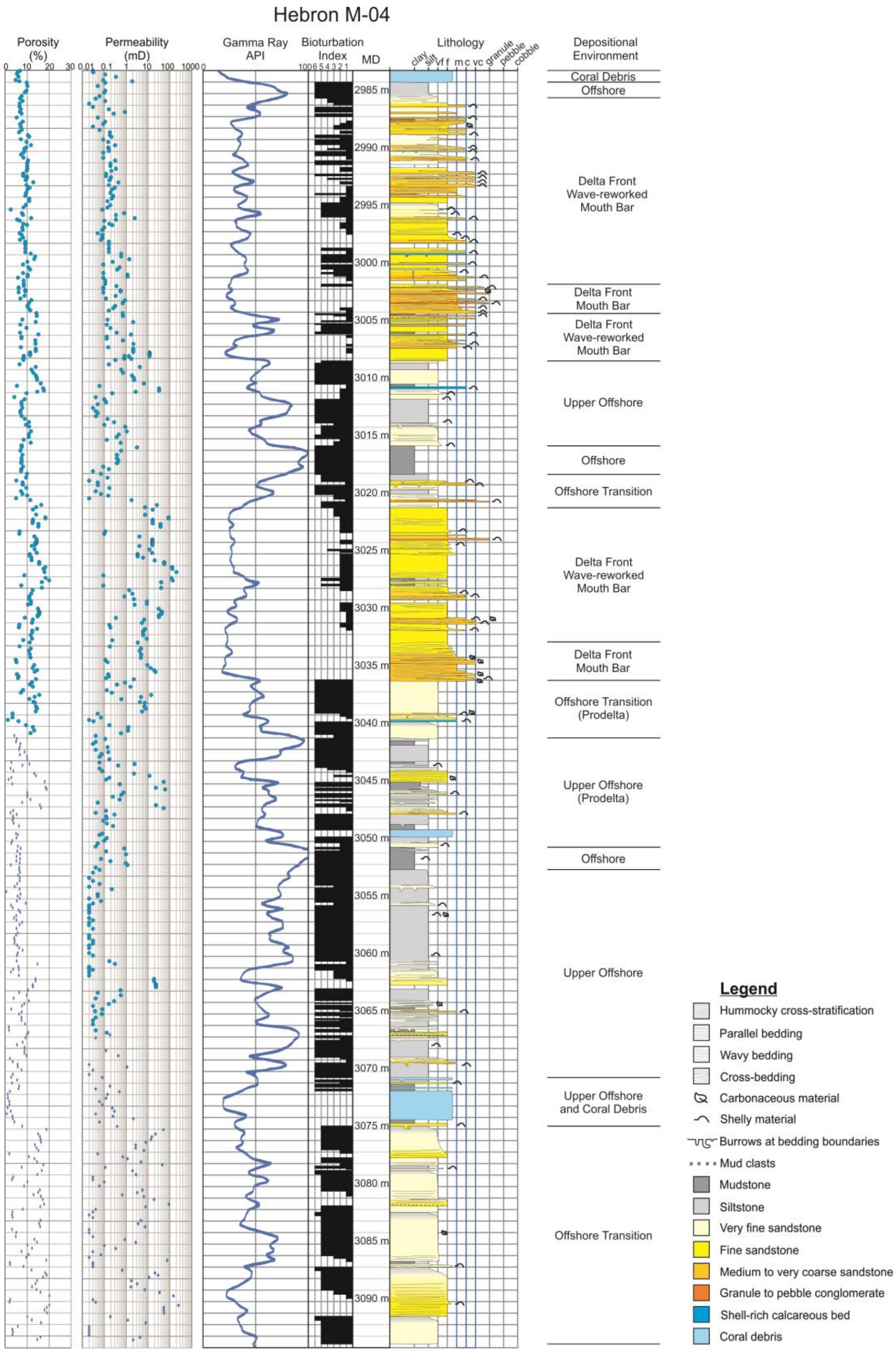
Hebron M-04
Porosity (%)
0 10 20 30
Permeability (mD)
0.01 0.1 1 10 100 1000
Gamma Ray API
0 100
Bioturbation Index
6 5 4 3 2 1
MD
Lithology
clay silt vf f m c vc granule pebble cobble
Depositional Environment
2985 m
2990 m
2995 m
3000 m
3005 m
3010 m
3015 m
3020 m
3025 m
3030 m
3035 m
3040 m
3045 m
3050 m
3055 m
3060 m
3065 m
3070 m
3075 m
3080 m
3085 m
3090 m
Coral Debris
Offshore
Delta Front Wave-reworked Mouth Bar
Delta Front Mouth Bar
Delta Front Wave-reworked Mouth Bar
Upper Offshore
Offshore
Offshore Transition
Delta Front Wave-reworked Mouth Bar
Delta Front Mouth Bar
Offshore Transition (Prodelta)
Upper Offshore (Prodelta)
Offshore
Upper Offshore
Upper Offshore and Coral Debris
Offshore Transition
Legend
Hummocky cross-stratification
Parallel bedding
Wavy bedding
Cross-bedding
Carbonaceous material
Shelly material
Burrows at bedding boundaries
Mud clasts
Mudstone
Siltstone
Very fine sandstone
Fine sandstone
Medium to very coarse sandstone
Granule to pebble conglomerate
Shell-rich calcareous bed
Coral debris

Figure 2.8. Summary core diagram of the Hebron M-04 core 3.

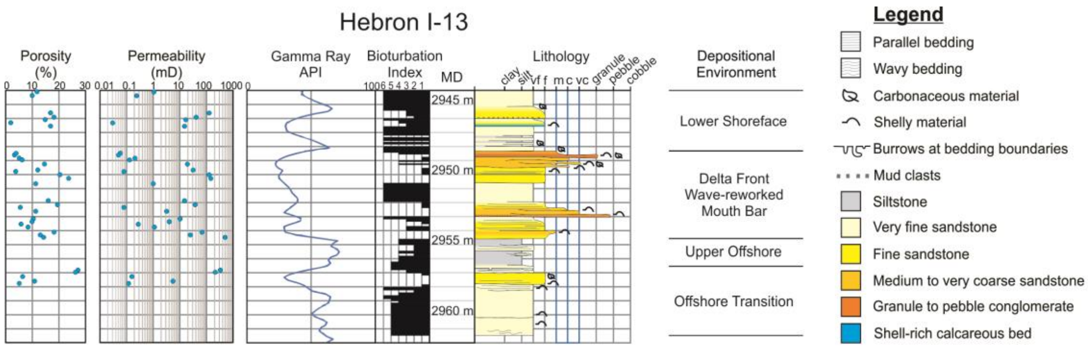
Hebron I-13
Porosity (%)
Permeability (mD)
Gamma Ray API
Bioturbation Index
MD
Lithology
clay silt vf f m c vc granule pebble cobble
Depositional Environment
2945 m
2950 m
2955 m
2960 m
Lower Shoreface
Delta Front Wave-reworked Mouth Bar
Upper Offshore
Offshore Transition
Legend
Parallel bedding
Wavy bedding
Carbonaceous material
Shelly material
Burrows at bedding boundaries
Mud clasts
Siltstone
Very fine sandstone
Fine sandstone
Medium to very coarse sandstone
Granule to pebble conglomerate
Shell-rich calcareous bed

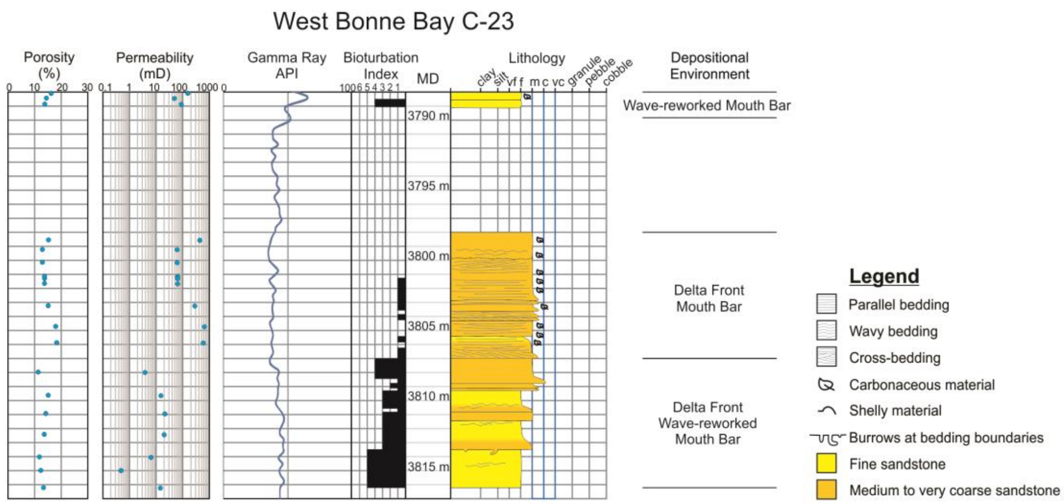
West Bonne Bay C-23
Porosity (%)
Permeability (mD)
Gamma Ray API
Bioturbation Index
MD
Lithology
clay silt vf f m c vc granule pebble cobble
Depositional Environment
3790 m
3795 m
3800 m
3805 m
3810 m
3815 m
Wave-reworked Mouth Bar
Delta Front Mouth Bar
Delta Front Wave-reworked Mouth Bar
Legend
Parallel bedding
Wavy bedding
Cross-bedding
Carbonaceous material
Shelly material
Burrows at bedding boundaries
Fine sandstone
Medium to very coarse sandstone

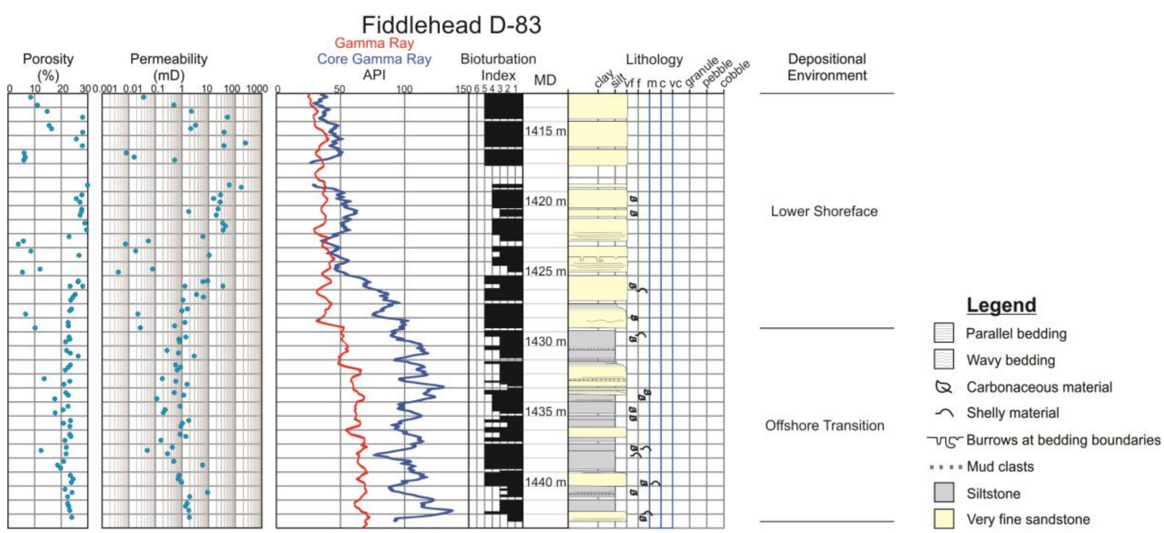
Fiddlehead D-83
Porosity (%)
Permeability (mD)
Gamma Ray
Core Gamma Ray
API
Bioturbation Index
MD
Lithology
clay silt vf f m c vc granule pebble cobble
Depositional Environment
1415 m
1420 m
1425 m
1430 m
1435 m
1440 m
Lower Shoreface
Offshore Transition
Legend
Parallel bedding
Wavy bedding
Carbonaceous material
Shelly material
Burrows at bedding boundaries
Mud clasts
Siltstone
Very fine sandstone

Figure 2.9. Summary core diagram of the Hebron I-13 core, West Bonne Bay C-23 cores 1 and 2, and Fiddlehead D-83 cores 1 and 2.

6. Facies Associations of the Hibernia Formation

Six facies associations were described from facies analyses of core materials. These associations are arranged from distal shallow marine to more proximal coastal settings. Summary core diagrams are presented in Figures 2.7-2.9 with the depositional setting interpretations listed on the right.

Facies association 1: Offshore

The offshore association contains thick beds of fine-grained, muddy facies with rare storm sandstone beds. Highly bioturbated, clay-rich mudstones (Facies 1) are present in the most distal areas and bioturbated muddy siltstones (Facies 2), interbedded with laminated storm sandstones (Facies 3), in the more proximal, upper offshore. Rarely, thick beds of parallel laminated sandstones (HCS, Facies 6) are observed deeply eroding the finer-grained beds. Locally, rounded mud rip-up clasts from eroded firmground fair-weather lithologies are observed within the basal contacts of storm beds.

Commonly, this facies association has a shallowing-upward trend to lower shoreface and delta front facies. This is consistent with delta progradation. In the lower half of the Hebron M-04 core 3, the association has a much more transgressive character. There is a distinct deepening upward trend associated with a decreased frequency of storm beds (Facies 3 and 6) that culminates in a 2m thick bed of dark, clay-rich mudstone (Facies 1). Coral debris beds (Facies 16) are commonly observed with these transgressive facies successions, though only in the upper offshore setting.

This facies association contains trace fossil assemblages characteristic of fully marine settings. The fair-weather facies are highly reworked by a diverse ichnofauna with a bioturbation index ranging from 4 to 6. Common trace fossils include *Phycosiphon*, *Chondrites*, *Asterosoma*, *Teichichnus*, *Palaeophycus*, and *Planolites*. Sandstones deposited from storms have more vertical forms such as *Skolithos* and *Diplocraterion* in addition to *Ophiomorpha* and *Thalassinoides*. Rarely, *Scolicia*-like burrows are observed.

Facies association 2: Offshore transition

Thick beds of highly bioturbated very fine-grained sandstone (Facies 4) interbedded with parallel laminated sandstones (HCS, Facies 6) is inferred to represent a transitional zone between the offshore and the lower shoreface. The presence of interbedded storm sandstones is much higher than in the offshore facies association. Quieter periods show deposition of muddy siltstones (Facies 2) interbedded with laminated very fine-grained sandstones (Facies 3). A coarsening upward trend is common in this association. The occurrence of parallel laminated sandstones (Facies 6) increases upward and become amalgamated as they transitioning to Facies Association 3 (storm-dominated lower shoreface).

The trace fossil assemblages observed in the offshore transition are similar to those described from the offshore association, though slightly more diverse. The ichnofabric is inferred to represent fully marine conditions. Bioturbation index is commonly 5-6 in fair-weather beds and 0-3 in storm beds.

Facies association 3: Storm-dominated lower shoreface

This facies association has an abundance of parallel laminated sandstones interpreted as hummocky cross-stratification (Facies 6) interbedded with very fine- to fine-grained bioturbated sandstones (Facies 4 and 5). Bed successions thicken upwards as the storm beds become more amalgamated. Locally, curved, erosional truncations are observed between beds giving the appearance of swaley cross-stratification.

Bed tops are readily colonized by infaunal organisms and deposit-feeders (Facies 5). Based on ichnofabric analysis, high energy and sedimentation rate are the main factors controlling the trace fossil assemblage. Fair-weather deposits and storm bed tops are colonized (BI 3-6) by *Ophiomorpha*, *Asterosoma*, *Chondrites*, *Teichichnus*, *Palaeophycus*, and *Planolites*. Storm beds (BI 0-3) have rare, deep burrowing, *Ophiomorpha* and vertical burrows such as *Skolithos*.

Facies association 4: Wave-influenced delta front

The wave-influenced delta front association contains a wide range of facies exhibiting both marine and deltaic characteristics. Poorly sorted, coarse-grained sandstone beds abruptly overlie bioturbated siltstones or sandstones of Facies Associations 2 and 3. These coarse-grained facies typically contain an abundance of carbonaceous material and shell debris, and are expressed as either massive (Facies 9) or parallel- to cross-bedded sandstones (Facies 11 and 10). They exhibit coarsening upward successions and the base is commonly composed of sandstones interbedded with laminated fluid-mud deposits (Facies 17). The coarse-grained beds are commonly overlain by more thinly bedded sandstones (Facies 15) and parallel laminated sandstones (HCS, Facies 6). The presence of Facies 6 suggests that wave action returns as the dominant process following deltaic discharge, as evidenced by the presence of fluid mud deposits at the base of the sedimentary cycles.

Facies successions commonly consist of net upward coarsening of stacked, fining upward beds. Each set may range from 1-3 m resulting in a succession 7-15 m thick. Bioturbation is commonly absent in the coarser gained facies but may range from BI 0-3 as sets display more wave-dominated conditions.

Bioturbation in this facies association is dominated by *Ophiomorpha*. At the top of progradational successions of this facies association, a *Ophiomorpha-Palaeophycus-Planolites* ichnofabric is observed. If parallel laminated sandstones (HCS, Facies 6) transition to more intensely bioturbated facies (Facies 5), then a more diverse ichnological assemblage is observed (BI 3-6).

This facies association is interpreted as a wave-influenced delta front following the process-based delta classification presented by Bhattacharya and Giosan (2003). The facies succession includes evidence for both deltaic and wave processes and lacks the typical heterolithic prodelta of river-dominated deltas (Bhattacharya and Walker, 1991; Bhattacharya, 2006). During periods of high river discharge, mouthbar deposits are produced with little to no wave reworking. As river output wanes, wave processes become dominant, and mouthbars are reworked into hummocky cross-stratified sandstone beds (Bhattacharya and Giosan, 2003). Much of the mud discharged from the river is likely to have stayed in suspension since it is commonly lacking from the deltaic facies. The mud are carried farther offshore or during peak flow conditions, deposited as fluid muds (Bhattacharya and Giosan, 2003; Bhattacharya and MacEachern, 2009; Harazim and McIlroy, 2015).

Facies association 5: Delta front lobe abandonment

This facies association is differentiated from the wave-influenced delta front association due to the presence of shoreface parallel laminated sands (Facies 7 and 14). The succession begins with alternating beds of parallel-bedded sandstones (Facies 11 and 15) and parallel laminated sandstones (HCS, Facies 6) similar to those observed in Facies Association 4. The hummocky cross-stratified sandstones pass upwards into more swaley-type bedding and then to parallel laminated shoreface facies. It thus has the appearance of a prograding shoreface with deltaic mouthbars limited to the base of the succession (cf. figure 28; Bhattacharya, 2006). Carbonaceous material is abundant in many of the sandstone facies suggesting that a fluvial input is present. However, the change from a deltaic facies association to facies displaying exclusively wave-dominated processes implies a change to the hydrologic regime (Bhattacharya and Giosan, 2003; Bhattacharya, 2006).

This facies association is interpreted to represent delta-lobe abandonment, most likely due to autocyclic lobe switching and subsidence (Bhattacharya and Giosan, 2003; Bhattacharya, 2006). The lowermost mouthbar deposits are reworked by wave and storm action as the distributaries are abandoned. The facies succession may also be interpreted as the downdrift migration of the distributary mouth in response to wave action and longshore drift (Figure 2.10a; cf. figure 11, Bhattacharya and Giosan, 2003). Bioturbation is mostly absent in this facies association (BI 0-1) with the exception of rare *Ophiomorpha* and *Planolites* burrows. This facies association is only observed in the West Bonne Bay F-12 core 1.

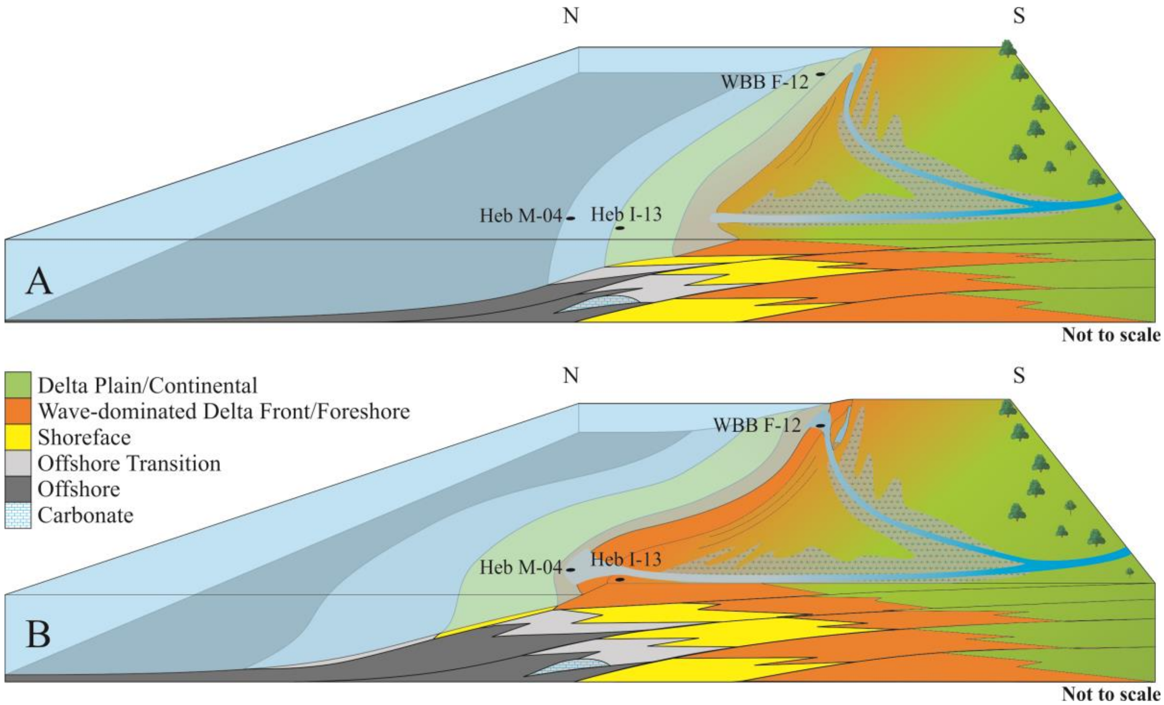

Figure 2.10. Illustrated paleoenvironmental interpretation of the Upper Hibernia Zone facies architecture showing well locations for Upper Hibernia Zone core samples. A, Delta front progradation in the Hebron area following a transgressive stage. The West Bonne Bay wells displays shoreface facies which are inferred to represent delta lobe abandonment or asymmetric migration of the distributary towards the east (pictured above). B, Delta front progradation and relative sea level drop. Suggested formation of a spit and lagoon environment in the West Bonne Bay area. Illustration not to scale.

Facies association 6: Distributary channel fill and back barrier

This facies association is only observed in the West Bonne Bay F-12 core 1 where it consists of a series of fining upward packages of granule to pebble conglomerates and parallel laminated sandstones (Facies 12 and 14). The underlying facies are deeply eroded and overlain by a pebble conglomerate with white quartz clasts up to 3 cm in diameter (Facies 12). The lowermost conglomerates are interpreted as channel lags that are overlain by the fill of a larger distributary channel. This facies succession overlies the lobe abandonment surface of Facies Association 5 and is inferred to represent the local reestablishment of delta channel and mouthbar formation.

The distributary fill consists of parallel bedded sandstones with abundant bioclastic debris and concentric mud balls. These are inferred to represent material flushed from a back barrier location, potentially a lagoon or eroded from coastal tidal flats during local coastline retreat. Overlying this are granule conglomerates with large laminated mudstone clasts that may also have been eroded from an adjacent tidal flat. The facies then transitions back to parallel bedded sandstones typical of Facies 11 and 15, which are reworked by wave action (Facies 14).

Facies 8 has *Planolites* overprinting *Ophiomorpha* in carbonaceous fine-grained sandstones interbedded with coarse-grained, cross-bedded sandstones (Facies 10 and 11). This succession overlies the channel fill and mouthbar facies. Interpreting this section is problematic; however, this facies succession could be envisioned in small lagoonal areas on the downdrift side of the distributary channel that are protected by the presence of a spit (Figure 2.10b; see Bhattacharya and Giosan, 2003).

7. Discussion

The Upper Hibernia Zone exhibits both marine and deltaic characteristics in the southern Jeanne d'Arc Basin. Facies analysis suggests that wave processes are a dominant factor controlling deposition. Interactions between both waves and fluvial processes are apparent in the reworking of deltaic mouthbar deposits into hummocky cross-stratified beds. These observations suggest that a wave-influenced delta classification is fitting (see Bhattacharya and Giosan, 2003). Figure 2.10 provides a paleoenvironmental summary of the inferred Upper Hibernia Zone facies architecture. A minimum of two distributary channels are inferred for the study area (Figure 2.10).

In the Hebron field, core samples have a greater range of facies changes from offshore mudstones to proximal mouthbar deposits (Figure 2.10a). In the Hebron M-04 well, the lower half of the examined core is dominantly composed of marine facies with high ichnodiversity. This section is composed of bioturbated mudstones and muddy sandstones interbedded with hummocky cross-stratified sandstones. Rarely, medium- to fine-grained, fining upward beds with abundant carbonaceous debris and shell fragments are observed. These are interpreted as distal gravity flow deposits originating from the delta front possibly in response to high fluvial discharge or high energy wave-reworking of gravity flow deposits. These facies commonly transition to parallel laminated sandstones before returning to fair-weather mudstones and sandstones. Abruptly overlying these marine facies are coarse-grained to granule, parallel bedded to low-angle cross-bedded facies (see Figure 2.10b). The beds form 2-5 m successions with abundant wood fragments and shell debris. The basal contact is erosive and convolute. This surface is thought to represent a candidate sequence boundary formed due to relative sea level fall.

The 20 m section immediately underlying the candidate sequence boundary in the Hebron M-04 core is correlated to the entire Hebron I-13 core 4 through comparison of wireline log data. The Hebron I-13 core samples have similar facies transitions to the M-04 but slightly coarser grained and exhibiting more proximal shoreline features (Figure 2.10). The upper section of the Hebron I-13 contains a greater mix of deltaic and wave-generated facies. The coarse-grained facies correlate across both wells and are likely part of the same event. The ichnodiversity in the upper section of the Hebron I-13 core is notably less than the ichnodiversity in the equivalent facies in the Hebron M-04 core. This may indicate greater physical and chemical stress factors associated with a more proximal deltaic setting (MacEachern and Gingras, 2007).

The West Bonne Bay F-12 core contains facies interpreted as lower shoreface to delta front and distributary channels (Figure 2.10). The lower shoreface trace fossil assemblage displays characteristics typical of fully marine settings (i.e. *Ophiomorpha* with large burrow size, presence of *Chondrites*, *Asterosoma*, and *Phycosiphon*; MacEachern and Gingras, 2007), though not as diverse as that observed in the Hebron area. The deltaic facies have a very limited to absent assemblage commonly dominated by *Ophiomorpha* or *Planolites* burrows. The distributary channel facies observed in the upper portion of the core are eventually overlain by shoreface deposits and finally by offshore mudstones with interbedded silty storm beds. The base of the distributary channel facies in the West Bonne Bay F-12 core is thought to represent the same relative sea level fall, and thus sequence boundary, inferred from the Hebron M-04 core (see Figure 2.10b).

The Lower Hibernia Zone cores (Fiddlehead D-83 and West Bonne Bay C-23) display similar characteristics suggestive of wave and deltaic processes. The offshore facies association, as represented in the Fiddlehead D-83 cores, contains abundant carbonaceous material and high clay content. The facies are thinly bedded and heterolithic, giving the impression of prodelta-like conditions which contrast with the Upper Hibernia Zone (Bhattacharya, 2006). However, the Fiddlehead core samples are short and the facies do not repeat within the cored section to make any clear determination. These facies transition upwards in core section to lower shoreface sandstones that are similar to those observed in the West Bonne Bay F-12 core.

In the West Bonne Bay C-23 cores, parallel laminated sandstones (Facies 6), highly bioturbated sandstones (Facies 5), and massively bedded sandstones (Facies 9) make up the majority of the core. Only occasionally are unidirectional ripple laminate observed. These are more common in the upper portion of the core as carbonaceous material increases. There is also a distinct decrease in bioturbation intensity towards the top of the core. When compared to the Upper Hibernia Zone facies, the West Bonne Bay C-23 cores lack mouthbar facies associated with high river discharge. It is plausible that much of the sediment was reworked by wave energy and transported by longshore currents (see Bhattacharya and Walker, 1991; Bhattacharya and Giosan, 2003; Anthony, 2015). However, more data is needed to determine the facies distribution for the Lower Hibernia Zone in the southern Jeanne d'Arc Basin.

8. Conclusions

The Hibernia Formation is of great interest to the petroleum industry but little research has been conducted on the Hibernia Formation in the southern Jeanne d'Arc Basin. This study examined three cores from the Upper Hibernia Zone and four cores from the Lower Hibernia Zone (see core locations in Figure 2.2). Both zones contained facies exhibiting both marine and deltaic characteristics. These resulted in the interpretation of a wave-influenced deltaic setting (Bhattacharya and Giosan, 2003; Bhattacharya, 2006).

Detailed facies analysis resulted in the classification of 17 lithofacies. These facies range from offshore mudstones and bioturbated sandstones interbedded with very fine- to fine-grained hummocky cross-stratified sandstones to delta mouthbar sandstones and distributary channel fill conglomerates. From these facies, 6 facies associations were determined: offshore, offshore transition, storm-dominated lower shoreface, wave-influenced delta front, delta front lobe abandonment, and distributary channel fill and back barrier. Observations from the Upper Hibernia Zone core samples suggest that longshore drift and autocyclic lobe switching may control facies architecture.

The purpose of this study was to provide a detailed look at the sedimentology and ichnology of the Hibernia Formation in the southern Jeanne d'Arc Basin. A discussion of the depositional setting was given based on facies observations. However, a greater frequency of cored wells through the Upper and Lower Hibernia Zones is needed to make a more detailed interpretation. At present, the cores utilized in this study are the only cores taken from the Hebron Member of the southern Jeanne d'Arc Basin.

9. Acknowledgments

Thank you to Doug Stewart, Iain Sinclair, Paula Marner, and Dennis MacDonald of Husky Energy for their mentorship, helpful discussions, and for supplying supplementary data. Thank you to Husky Energy and the School of Graduate Studies, Memorial University of Newfoundland, for providing funding for this research. Thank you to David Mills and Jason Newell from the C-NLOPB core facility in St. John's, Newfoundland. Thank you to Chris Boyd, Katie Power, and Jillian Evans for their assistance with core photography.

10. References

ANTHONY, E.J. 2015. Wave influence in the construction, shaping and destruction of river deltas: a review. *Marine Geology*, v. 361, p. 53-78.

ARTHUR, K.R., COLE, D.R., HENDERSON, G.G.L., and KUSHNIR, D.W. 1982. Geology of the Hibernia discovery. *In*: The Deliberate Search for the Subtle Trap, M.T. Halbouty (ed.). *American Association of Petroleum Geologists*, Memoir 32, p. 181-195.

BHATTACHARYA, J. 2006. Deltas. *In*: Facies Models Revisited, H.W. Posamentier and R.G. Walker (eds.). *SEPM Special Publication* 84, p. 237-292.

BHATTACHARYA, J. and GIOSAN, L. 2003. Wave-influenced deltas: geomorphological implications for facies reconstruction. *Sedimentology*, v. 50, p. 187-210.

BHATTACHARYA, J. and MACEACHERN, J.A. 2009. Hyperpycnal rivers and prodelta shelves in the Cretaceous seaway of North America. *Journal of Sedimentary Research*, v. 79, p. 184-209.

BHATTACHARYA, J. and WALKER, R.G. 1991. River- and wave-dominated depositional systems of the Upper Cretaceous Dunvegan Formation, northwestern Alberta. *Bulletin of Canadian Petroleum Geology*, v. 39, p. 165-191.

BOUMA, A. H. 1962. Sedimentology of some flysch deposits: a graphic approach to facies interpretation. Amsterdam, Elsevier, 168 p.

BROMLEY, R.G. 1996. Trace Fossils: biology, taphonomy and applications. London, Chapman and Hall, 361 p.

BROWN, D.M., MCALPINE, K.D. and YOLE, R.W. 1989. Sedimentology and sandstone diagenesis of Hibernia Formation in Hibernia Oil Field, Grand Banks, Newfoundland. *The American Association of Petroleum Geologists Bulletin*, v. 73, p. 557-575.

CANADA-NEWFOUNDLAND OFFSHORE PETROLEUM BOARD ANNUAL REPORT 2015-16. June 29, 2016. Submitted by Scott Tessier, Chair and Chief Executive Officer.

CLIFTON, H.E. 2006. A reexamination of facies models for clastic shorelines. *Society for Sedimentary Geology*, Special Publication 84, p. 293-337.

CLIFTON, H.E. and THOMPSON, J.K. 1978. Macaronichnus segregatis: a feeding structure of shallow marine polychaetes. *Journal of Sedimentary Petrology*, v. 48, p. 1293-1302.

COE, A.L. 2003. The Sedimentary Record of Sea-Level Change. Cambridge University Press, Cambridge. 279 p.

DALRYMPLE, R.W. 2010. Introduction to siliciclastic facies models. *In*: Facies Models 4, N.P. James and R.W. Dalrymple (eds.). Geological Association of Canada, p. 59-72.

EKDALE, A.A. 1985. Paleoecology of the marine endobenthos. *Palaeogeography, Palaeoclimatology, Palaeoecology*, v. 50, p. 63-81.

ENACHESCU, M.E. 1987. Tectonic and structural framework of the northeast Newfoundland continental margin. *In*: Sedimentary Basins and Basin-forming Mechanisms, C. Beaumont and A.J. Tankard (eds.). *Canadian Society of Petroleum Geologists Memoir* 12, p. 117-146.

FREY, R.W. 1990. Trace fossils and hummocky cross-stratification, Upper Cretaceous of Utah. *Palaios*, v. 5, p. 203-218.

HARAZIM, D. and MCILROY, D. 2015. Mud-rich density-driven flows along an Early Ordovician storm-dominated shoreline: implications for shallow-marine facies models. *Journal of Sedimentary Research*, v. 85, p. 509-528.

HISCOTT, R.N., MARSAGLIA, K.M., WILSON, R.C.L., ROBERTSON, A.H.F., KARNER, G.D., TUCHOLKE, B.E., PLETSCH, T., and PETSCHICK, R. 2008. Detrital sources and sediment delivery to the early post-rift (Albian-Cenomanian) Newfoundland Basin east of the Grand Banks: results from ODP Leg 210. *Bulletin of Canadian Petroleum Geology*, v. 56, p. 69-92.

HOVIKOSKI, J., LEMISKI, R., GINGRAS, M., PEMBERTON, G., MACEACHERN, J.A. 2008. Ichnology and sedimentology of a mud-dominated deltaic coast: Upper

Cretaceous Alderson Member (Lea Park Fm), western Canada. *Journal of Sedimentary Research*, v. 78, p. 803-824.

MACEACHERN, J.A. and GINGRAS, M.K. 2007. Recognition of brackish-water trace-fossil suites in the Cretaceous Western Interior Seaway of Alberta, Canada. *Society for Sedimentary Geology*, Special Publication 88, p. 149-193.

MACEACHERN, J.A. and PEMBERTON, S.G. 1992. Ichnological aspects of Cretaceous shoreface successions and shoreface variability in the Western Interior Seaway of North America. *In*: Applications of Ichnology to Petroleum Exploration: A Core Workshop, S.G. Pemberton (ed.). *Society for Sedimentary Geology*, Core Workshop 17, p. 57-84.

MACEACHERN, J.A., BANN, K.L., BHATTACHARYA, J.P., and HOWELL, C.D. 2005. Ichnology of deltas: organism responses to the dynamic interplay of rivers, waves, storms, and tides. *Society for Sedimentary Geology*, Special Publication 83, p. 49-85.

MACEACHERN, J.A., ZAITLIN, B.A., and PEMBERTON, S.G. 1998. High-resolution sequence stratigraphy of early transgressive deposits, Viking Formation, Joffre Field, Alberta, Canada. *American Association of Petroleum Geologists Bulletin*, v. 82, p. 729-256.

MACKAY, A.H. and TANKARD, A.J. 1990. Hibernia Oil Field-Canada Jeanne d'Arc Basin, Grand Banks Offshore Newfoundland. *In*: N.H. Foster and E.A. Beaumont (compilers), Structural traps: tectonic fold traps 3. *The American Association of Petroleum Geologists*, p. 145-175.

MCILROY, D. 2008. Ichnological analysis: the common ground between ichnofacies workers and ichnofabric analysts. *Palaeogeography, Palaeoclimatology, Palaeoecology*, v. 270, p. 332-338.

NICHOLS, G. 1999. Sedimentology and Stratigraphy. Blackwell Science Ltd., London. 355 p.

PEMBERTON, S.G., SPILA, M., PULHAM, A.J., SAUNDERS, T., MACEACHERN, J.A., ROBBINS, D., and SINCLAIR, I.K. 2001. Ichnology and sedimentology of shallow to marginal marine systems. Geological Association of Canada, Short Course Notes v. 15. 343 p.

PLINT, A.G. 2010. Wave- and storm-dominated shoreline and shallow-marine systems. *In*: Facies Models 4, N.P. James and R.W. Dalrymple (eds.). Geological Association of Canada, p. 167-200.

POLLARD, J.E., GOLDRING, R., and BUCK, S.G. 1993. Ichnofabrics containing *Ophiomorpha*: significance in shallow-water facies interpretation. *Journal of the Geological Society London*, v. 150, p. 149-164.

SHEPPARD, D., MAC PHERSON, C., MACINNIS, D. 2006. Geological Report on Husky Oil et al West Bonne Bay F-12 East Coast Canada. Husky Oil Operations Limited. pp 258.

SINCLAIR, I.K. 1988. Evolution of Mesozoic-Cenozoic sedimentary basins in the Grand Banks area of Newfouldland and comparison with Falvey`s (1974) rift model. Bulletin of Canadian Petroleum Geology, vol. 36, p. 255-273.

SINCLAIR, I.K., EVANS, J.E., ALBRECHTSONS, E.A. and SYDORA, L.J. 1999. The Hibernia Oilfield-effects of episodic tectonism on structural character and reservoir compartmentalization. *In*: A.J. Fleet and S.A.R. Boldy (eds.), Petroleum Geology of Northern Europe: Proceedings of the 5th Conference. London, Geological Society, p. 517-528.

SINCLAIR, I.K., FLINT, S., STOKES, R., and BIDGOOD, M. 2005. Hibernia Formation (Cretaceous) sequences and Breathitt Group (Pennsylvanian) analogue: implications for reservoir compartmentalization and modeling, offshore Newfoundland. *In*: R.N. Hiscott and A.J. Pulham (eds.), Petroleum Resources and reservoirs of the Grand Banks, eastern Canadian margin. *Geological Association of Canada*, Special Paper 43, p. 143-167.

SINCLAIR, I.K., MCALPINE, K.D., SHERWIN, D.F., and MCMILLAN, N.J. 1992. Part 1: Geological framework. In: Petroleum resources of the Jeanne d'Arc Basin and environs, Grand Banks, Newfoundland. Minister of Supply and Services Canada, p. 1-38.

TANKARD, A.J. and WELSINK, H.J. 1987. Extensional tectonics and stratigraphy of Hibernia Oil Field, Grand Banks, Newfoundland. *The American Association of Petroleum Geologists Bulletin*, v. 71, p. 1210-1232.

TAYLOR, A. and GOLDRING, R. 1993. Description and analysis of bioturbation and ichnofabric. *Journal of the Geological Society*, London, v. 150, p. 141-148.

TAYLOR, A., GOLDRING, R. and GOWLAND, S. 2003. Analysis and application of ichnofabrics. *Earth-Science Reviews*, v. 60, p. 227-259.

TONKIN, N.S., MCILROY, D., MEYER, R., and MOORE-TURPIN, A. 2010. Bioturbation influence on reservoir quality: a case study from the Cretaceous Ben

Nevis Formation, Jeanne d'Arc Basin, offshore Newfoundland, Canada. *AAPG Bulletin*, v. 94, p. 1059-1078.

WALKER, R.G. 1986. Cardium Formation 4. Review of facies and depositional processes in the southern foothills and plains, Alberta, Canada. *In*: Shelf Sands and Sandstone Reservoirs, R.W. Tillman, D.J.P. Swift, and R.G. Walker (eds.). *Society of Economic Paleontologists and Mineralogists*, Short Course Notes 13, p. 353-402.

ZAVALA, C., ARCURI, M., DI MEGLIO, M., GAMERO DIAZ, H., and CONTRERAS, C. 2011. A genetic facies tract for the analysis of sustained hyperpycnal flow deposits. *In*: Sediment transfer from shelf to deep water—Revisiting the delivery system, R.M. Slatt and C. Zavala (eds.). *American Association of Petroleum Geologists*, Studies in Geology 61, p.31-51.

CHAPTER 3

Porosity and permeability characteristics of the Hebron Member, Hibernia Formation in the southern Jeanne d'Arc Basin, offshore Newfoundland, Canada

Elizabeth R. Schatz[1, 2], Duncan McIlroy[2],

[1] Corresponding author: elizabeth.schatz@mun.ca

[2] Department of Earth Sciences. Memorial University of Newfoundland, 300 Prince Philip Drive, St. John's, NL, A1B 3X5, Canada. dmcilroy@mun.ca

1. Abstract

Sedimentary core samples were utilized from the Hebron Member, Upper Hibernia Zone, southern Jeanne d'Arc Basin, to assess facies-specific trends in permeability and porosity. Facies analysis resulted in the classification of 17 lithofacies and 10 ichnofabrics. Minipermeametry analyses of cross-bedded medium- to coarse-grained sandstone showed a difference of 300 mD between mud-lined burrows and surrounding clean sandstones within the same 19 cm long core section. Comparisons between parallel laminated sandstones and cryptobioturbated equivalents display similar permeability and porosity ranges; however, cryptobioturbated laminated sandstones displayed higher vertical connectivity. Core plug data indicates that parallel laminated

storm-generated sandstone beds display higher permeability and porosity values than bioturbated fair-weather facies. Coarse-grained, cross-bedded sandstones with rare *Ophiomorpha* in the Hibernia Formation display the greatest permeability values (up to 900 mD), but bioturbated mudstones and very fine-grained sandstones containing *Phycosiphon* are demonstrated, by petrography and core plug analyses, to have increased porosity and permeability.

2. Introduction

It has become evident over the past twenty years that burrowing activity alters the way in which hydrocarbons flow through reservoir rocks (e.g. Gingras et al., 2004a, 2004b, 2009; Pemberton and Gingras, 2005; Tonkin et al., 2010; Bednarz and McIlroy, 2012; La Croix et al., 2012, 2013; Baniak et al., 2014). Factoring in the effects of bioturbation to well planning has been shown to reduce net loss (Pemberton and Gingras, 2005). However, permeability associated with the complex morphology of trace fossils is not easily predicted, which is why it is important to continue these types of studies aimed at understanding how these small-scale structures might affect reservoir-scale fluid flow and improve the efficiency of hydrocarbon recovery.

The purpose of this paper is to examine the permeability and porosity characteristics of facies in the Hibernia Formation and to determine the effects of bioturbation on the reservoir quality of these facies. This is accomplished through comparative minipermeametry of bioturbated and unbioturbated equivalents of the same facies, incorporating the use of core plug permeability and porosity data. This study attempts to understand variations in porosity and permeability characteristics and make predictions as to how these differences effect reservoir quality.

3. Geological setting

The Jeanne d'Arc Basin is located approximately 350 km east of St. John's, Newfoundland and is one of several sedimentary basins situated in the Grand Banks (see Figure 2.1). The Hebron Member is the youngest member of the Upper Hibernia Zone of the Hibernia Formation (following the Hibernia stratigraphy of Sinclair et al., 2005). This Early Cretaceous sandstone-rich unit is interpreted as a wave-influenced delta by this author (see Chapter 2). Facies analysis shows that there is regional variability from offshore marine dominated facies in the Hebron Field, to more proximal shoreface and deltaic facies in the West Bonne Bay Field. The presence of hydrocarbon shows in the Hibernia Formation (Sheppard et al., 2006) make this formation of great interest to the petroleum industry, though very little research has been conducted on the upper Hibernia Formation in the southern Jeanne d'Arc Basin.

4. Methods

The core samples utilized in this study are housed at the Canada-Newfoundland and Labrador Offshore Petroleum Board (C-NLOPB) core facility in St. John's, Newfoundland, Canada. Detailed sedimentological descriptions of the slabbed core samples were completed and all sections were photographed. Samples were taken from all three cores to produce petrographic thin section, and to assess porosity characteristics for all facies.

Core plug data from all three studied cores was provided by Husky Energy Inc. for use in this study. Using detailed sedimentological core descriptions, core plug locations were assigned lithofacies and ichnofabric classifications. Core-plug data were grouped by lithofacies or ichnofabric and graphed as porosity versus permeability, and the plotted points were further identified by well name.

Core from the West Bonne Bay F-12 well was cut parallel to the core face for use in minipermeametry analyses, producing five slabs 1cm-thick. The surfaces of these sections were blown clean with a laboratory air nozzle, wetted, and photographed. A 1cm by 1cm grid was drawn on the samples leaving a boundary no less than 1cm around the outer edge of the core sample. A Temco Inc. MP-401 minipermeameter was used to inject nitrogen gas into the rock at the center of each grid square. Each grid point was tested a minimum of three times, and an average permeability was taken to be the final value.

A minipermeameter fitted with a 9.525/3.175 mm (outer diameter/inner diameter) probe tip can be used for a minimum sample size of 16 mm diameter and 8 mm thick. The flow rate and injection pressure are measured and the SmartPermTM software package calculates the permeability using a modified Darcy equation:

$$K_a = \frac{2\mu Q_b P_b T_{act}}{a G_o (P_1^2 - P_2^2) T_{ref}} \times 1000$$

Where:

K_a = air or gas permeability (mD)

μ = viscosity of gas (cp) at its average flowing temperature and pressure in core

Q_b = volumetric flow rate (scc/min)

P_b = standard reference pressure for mass flow meters (psia)

T_{act} = actual flowing temperature of gas (K)

a = internal radius of probe tip seal (cm)

G_o = geometrical shape factor based on outer and inner diameter of probe tip and the dimensions of the core sample

P_1 = upstream pressure at probe tip (psia)

P_2 = downstream pressure (psia)

T_{ref} = reference temperature of mass flow meter (K)

(Temco Inc., Instruction manual for mini-permeameter model MP-401)

5. Lithofacies

Seventeen lithofacies were described from the Hebron Member, Upper Hibernia Zone (see Figure 2.2). These facies are summarized in Table 3.1. A complete description of these facies and the depositional setting can be found in Chapter 2.

Table 3.1. Summary of lithofacies and their associated ichnofabric(s).

Facies	Lithofacies Nomenclature	Description	Depositional Environment	Ichnofabric
1	Homogeneous clay-rich mudstone	A massively-bedded mudstone composed of swelling clays and minor silt grains. Beds range in thickness from 10 cm up to 2.5 m.	Sediment accretion in a low energy setting below storm wave-base.	1
2	Bioturbated muddy siltstone	Thoroughly bioturbated siltstone with variable clay content and fine particulate carbonaceous debris. Beds are 4 cm to 5 m thick and moderately calcite cemented.	Sediment accretion in a low energy setting at or just below storm wave-base	2, 3
3	Laminated very fine-grained sandstone	Laminated beds composed of moderately sorted coarse silt to fine sandstone with mudstone drapes. Beds are 5-30 cm thick with sharp basal contacts and bioturbated tops.	Storm deposition in an offshore setting	4
4	Bioturbated very fine-grained sandstone	Thoroughly bioturbated sandstone composed of moderately sorted coarse silt to lower fine-grained sandstone with variable clay and carbonaceous content. Beds range from 10 cm to 3 m thick.	Bioturbated sandstone from lower shoreface to offshore transition	3
5	Bioturbated fine-grained sandstone	Thoroughly bioturbated sandstone composed of moderately to well-sorted very fine to fine sandstone with low clay content. Bivalve fragments and serpulid worm tubes are common. Beds range from 10 cm to 2 m.	Variable energy deposition with wave influence in a shoreface setting	4, 5, 6, 7
6	Parallel laminated fine-grained sandstone	Parallel to sub-parallel laminated sandstone with low angle truncations composed of very fine to fine sandstone with muddy laminae. Beds are 30 cm to 1 m thick with sharp basal contacts. Amalgamated beds may be up to 7 m thick.	High energy storm deposition in a shallow marine setting (Hummocky cross-stratified sandstone, shoreface to offshore transition)	6, 8

7	Laminated fine-grained sandstone with shell debris	Laminated sandstone composed of very fine to medium sandstone and abundant bivalve shell fragments. Beds are 10-30 cm thickness and tightly carbonate cemented.	High energy swash zone	10
8	Fine-grained sandstone with Planolites burrows	Laminated very fine- to fine-grained sandstone with abundant carbonaceous material. Beds are 10-40 cm thick and tightly carbonate cemented. Faint *Ophiomorpha* burrows are observed overprinted by *Planolites* burrows filled with clean sand.	Delta front setting	9
9	Massive fine- to medium-grained sandstone	Massively-bedded fine- to medium-grained sandstone with abundant bivalve shell fragments and serpulid worm tubes concentrated at sharp basal contacts. Beds are 50-60 cm thick with variable calcite cementation.	High energy delta front mouthbar	none
10	Cross-bedded medium- to coarse-grained sandstone	Medium- to coarse-grained sandstone displaying low-angle cross-bedding. Beds are commonly normally graded with pebbles at the base. Beds are 10-40 cm thick forming successions up to 2 m.	Proximal mouthbar and terminal distributary channels	10
11	Parallel bedded medium- to coarse-grained sandstone	Normally graded thin beds composed of medium to coarse sandstone with very coarse sand to granules at the base. Beds are commonly carbonate cemented and may contain shell debris. Beds are 5-40 cm thick with sharp basal contacts.	Delta mouthbar	10
12	Erosively-based conglomerate	Matrix-supported, normally graded conglomerate with clasts ranging in size from granules to cobbles. The matrix is composed of fine to very coarse sand. Bed successions range from 10-50 cm	Distributary channel fill	none

13	Erosively-based shell beds	Fragmented bivalve and gastropod shells, serpulid worm tubes, crinoid fragments, and rounded coral material tightly calcite cemented with little to no clastic material. Beds are 10-60 cm thick and sharply erosional at the base.	Sand-winnowed shelly storm bed, shoreface setting	10
14	Laminated fine-grained sandstone with carbonaceous material	Parallel laminated fine- to medium-grained sandstone with abundant carbonaceous debris. Beds are 15-40 cm with abundant carbonaceous material commonly concentrated into 1-2 cm thick layers.	Wave-reworked mouthbar, upper shoreface	10
15	Thinly bedded fine-grained sandstone	Thin, normally graded beds composed of very fine to medium sand. Beds are 1-2 cm forming bedsets up to 20 cm thick. Bedsets display a fining upward trend and may display wavy laminae at bed tops.	Delta mouthbar	10
16	Coral debris in mudstone	Large calcareous fragments, bivalve shells, and coral fragments forming clast-supported debris beds. The matrix is composed of muddy sediment and swelling clay which locally displays a laminated texture. Fragments and matrix are dominantly horizontally-oriented. Beds range in size from 5 cm to 1.5 m.	Gravity flow	none
17	Laminated clay-rich mudstone	Very thinly laminated mudstone composed of swelling clay forming beds 1-2 cm thick with sharp boundaries.	Fluid mud deposition in shallow marine setting	none

6. Ichnofabric

The sediment texture imparted by bioturbation and bioerosion is known as ichnofabric (Ekdale and Bromley, 1983; Bromley and Ekdale, 1986). Ichnofabrics produced by the burrowing activity of two of more endobenthic communities at different times are referred to as composite ichnofabric (Bromley and Ekdale, 1986). Composite ichnofabrics are the most commonly observed ichnofabric and often the most complicated to interpret (Bromley and Ekdale, 1986; Bromley, 1996; McIlroy, 2004, 2008).

Tiering refers to the vertical arrangement of traces within the substrate as a result of food availability and the type of behaviour of the producing organism (Bromley, 1996). The tiering structure of an endobenthic community is composed of shallow to deeply penetrating burrows, which may extend well below the sediment-water interface. The work of a single biologic community will result in a simple ichnofabric (Bromley and Ekdale, 1986; Bromley, 1996). However, more than one community is likely to occupy the substrate over geological time and thus, a composite ichnofabric is produced in two ways: 1) through sediment accumulation, or hiatuses on the seafloor over time; and 2) through a change in the physical conditions of the environment (Bromley and Ekdale, 1986; Bromley, 1996). These circumstances allow for the superposition of the burrows from one seafloor community over that of another.

Ten distinct ichnofabrics were observed from the studied core samples. Each was described by ichnotaxa on the ichnogenera level, bioturbation index (following Taylor and Goldring, 1993; Taylor et al., 2003), and tiering structure (cf. McIlroy, 2004, 2008).

Ichnofabric 1: This ichnofabric is characterized by indistinct mottling with rare *Thalassinoides* and *Chondrites* burrows. The *Thalassinoides* and *Chondrites* burrows are commonly filled with sediment of contrasting colour to the host rock and display sharp burrow boundaries with little compaction (Figure 3.1a). It is inferred that these burrows originate from a higher stratigraphic level and were produced at a later stage in the depositional history than the background mottling. Upper bedding contacts are commonly erosional and, locally, the overlying sediment has filled the *Thalassinoides* burrows suggesting that they were open prior to erosional exhumation and deposition.

The background mottling is indistinct though textural variations on the surface of the core sample are notable. This ichnofabric is observed only in the clay-rich mudstone facies (Facies 1), which contains high amounts of swelling clay. This water-sensitive material makes observation of discrete structures difficult especial without sediment fill of contrasting colour to accentuate the mottling. This composite ichnofabric has a bioturbation index (BI) of 5 to 6.

Ichnofabric 2: This ichnofabric is dominated by *Phycosiphon* and *Asterosoma* with rare occurrences of *Teichichnus* and *Palaeophycus* (Figure 3.1b). *Phycosiphon* and *Asterosoma* crosscut one another suggesting that the producers had competing feeding strategies and may have occupied the same tier. Rarely, *Teichichnus* and *Palaeophycus* burrows are partially overprinted and likely represent an earlier emplaced, shallower tier suite. The high bioturbation index (BI 6) and thick beds suggest that total reworking of the sediment took place with steady sediment accretion in an environment where the

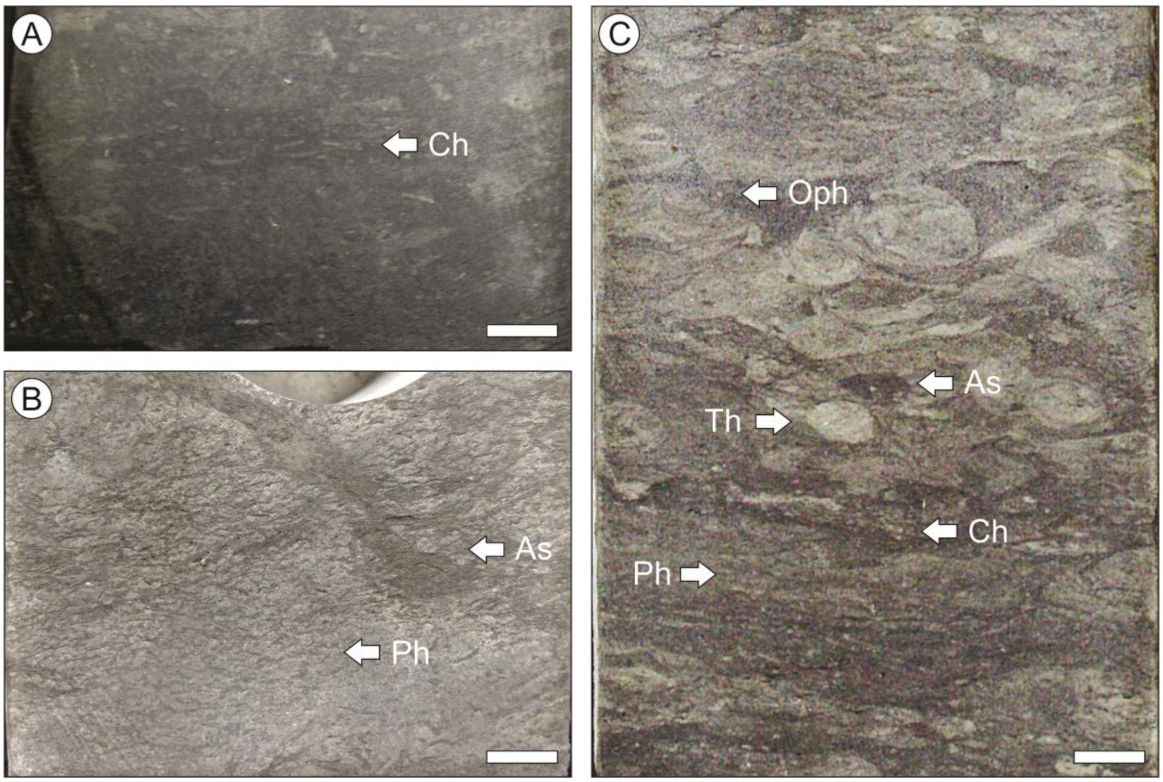

Figure 3.1. Core photographs of Ichnofabrics 1-3. A, Core photograph of clay-rich mudstone facies displaying *Chondrites* burrows (Ch) of Ichnofabric 1. B, Muddy siltstone facies with abundant *Phycosiphon* (Ph) burrows and *Asterosoma* (As) of Ichnofabric 2. C, Ichnofabric 3 displaying large *Ophiomorpha* (Oph), small *Asterosoma* (As), *Thalassinoides* (Th), *Chondrites* (Ch) reworking *Asterosoma* burrows, and *Phycosiphon* (Ph). Scale bars are 1 cm.

physical conditions remained fairly consistent for long periods of time. This ichnofabric is present in the muddy siltstone facies (Facies 2).

Ichnofabric 3: This ichnofabric is characterized by *Teichichnus*, *Palaeophycus*, and *Asterosoma* with rare *Phycosiphon* clustered in horizontal bands (Figure 3.1c). *Planolites*, *Ophiomorpha*, and *Thalassinoides* are also present in low abundance though *Ophiomorpha* burrows were observed to increase in abundance with sand to mud ratio of the host rock. *Phoebichnus* and vertical burrows (e.g. *Skolithos* and *Arenicolites*) may also be present in this ichnofabric. *Chondrites* reworked muddy *Asterosoma* burrows and the burrow linings of *Ophiomorpha*.

This ichnofabric is present in muddy siltstone and very fine-grained sandstone facies (Facies 2 and 4) with a bioturbation index of 4-6. The rare, vertical burrows were likely produced following storm deposition and were subsequently overprinted by trace fossils produced by the fair-weather endobenthic community (*Teichichnus*, *Palaeophycus*, *Asterosoma*, etc.). The dominance of fair-weather colonization suggests that storm events were infrequent. The transition to more abundant *Ophiomorpha* and sandier facies may suggest an increase in hydrodynamic energy, and potentially an increase in the frequency of storm events related to a shallower bathymetric position.

Ichnofabric 4: This ichnofabric is dominated by vertically-orientated burrows such as *Skolithos*, *Diplocraterion*, and *Arenicolites* (Figure 3.2a). *Ophiomorpha* and *Thalassinoides* are also observed in this ichnofabric, along with rare *Asterosoma* and *Chondrites* (Figure 3.2b). This ichnofabric is found in predominantly sandy facies (Facies

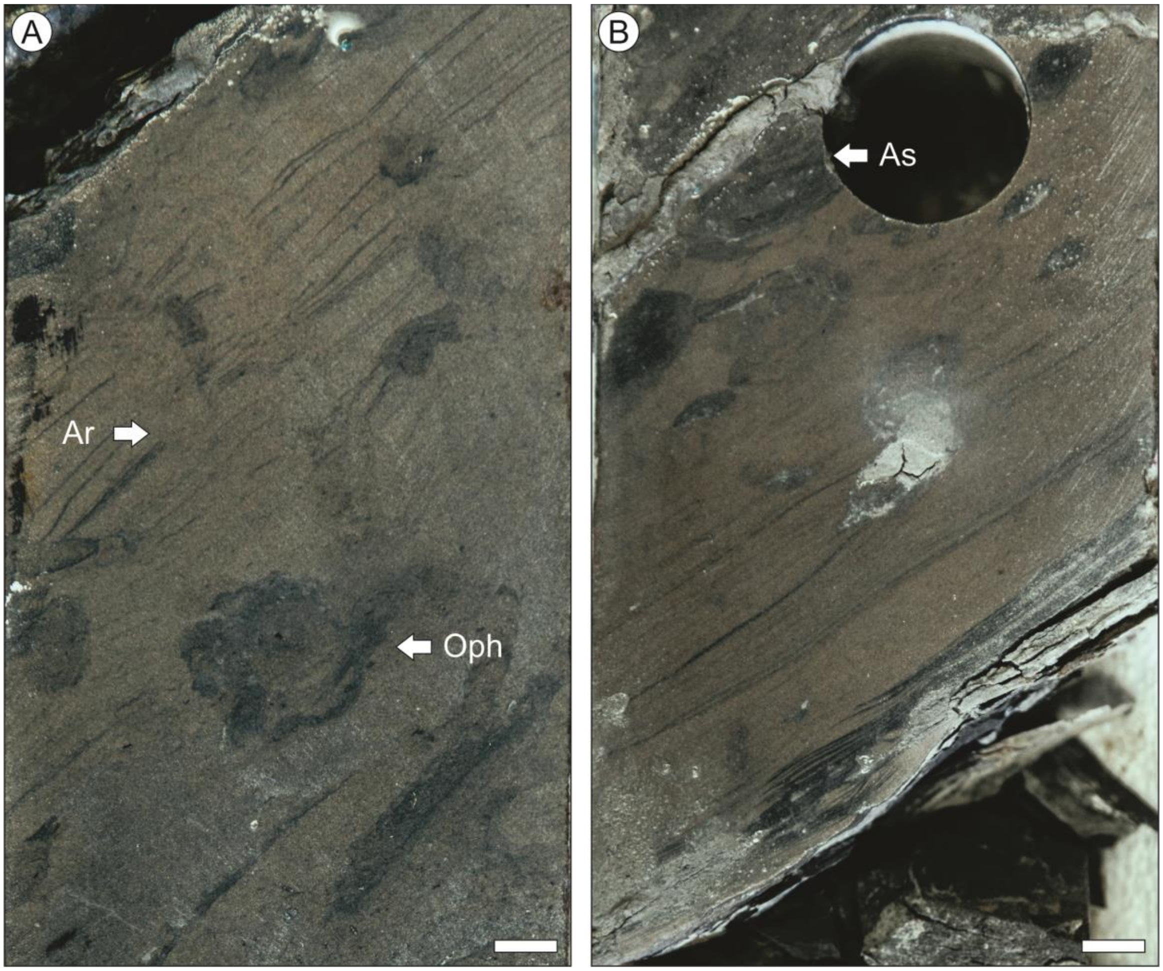

Figure 3.2. Core photographs of Ichnofabric 4 observed in very fine-grained laminated sandstone facies. A, *Arenicolites* (Ar) faintly visible by the break in laminae with associated horizontal *Ophiomorpha* (Oph) burrows. B, Mud-rich *Asterosoma* (As) near the top of the sandstone bed. Scale bars are 1 cm.

3 and 5), which are commonly interbedded with muddy fair-weather facies (Facies 2 and 4). Bioturbation indices in this ichnofabric range from 2 to 6.

The sandstone laminae commonly dip downwards towards the lateral margins of *Skolithos*, *Diplocraterion*, and *Arenicolites* burrows, suggesting that the sediment consistency was soft at the time of colonization (Figure 3.2a). The *Ophiomorpha* and *Thalassinoides* burrows displace the sediment laminae very little to not at all suggesting that these are a later stage of colonization after the sediment became firmer through compaction and dewatering. These burrows likely originated from a higher stratigraphic level as deeper tier structures.

Ichnofabric 5: This ichnofabric is dominated by *Ophiomorpha* with *Planolites*, *Palaeophycus*, and *Asterosoma* in moderate abundance. *Teichichnus* is present in low abundance and *Phoebichnus* burrows are rarely observed. Locally, *Chondrites* burrows rework *Asterosoma* burrows and muddy *Ophiomorpha* burrow linings. This ichnofabric is observed in the bioturbated sandstone facies (Facies 5) with a bioturbation index of 4-6 (Figure 3.3a, b).

Planolites burrows are commonly observed near the bed tops and decrease in abundance toward the center of the bed. These burrows often display an oblong burrow cross-section. *Chondrites* burrows are typically sharp-walled and circular suggesting that they were produced in firmer substrate. They also commonly rework other burrows suggesting that *Chondrites* is the burrow of a deeper tier trace-maker

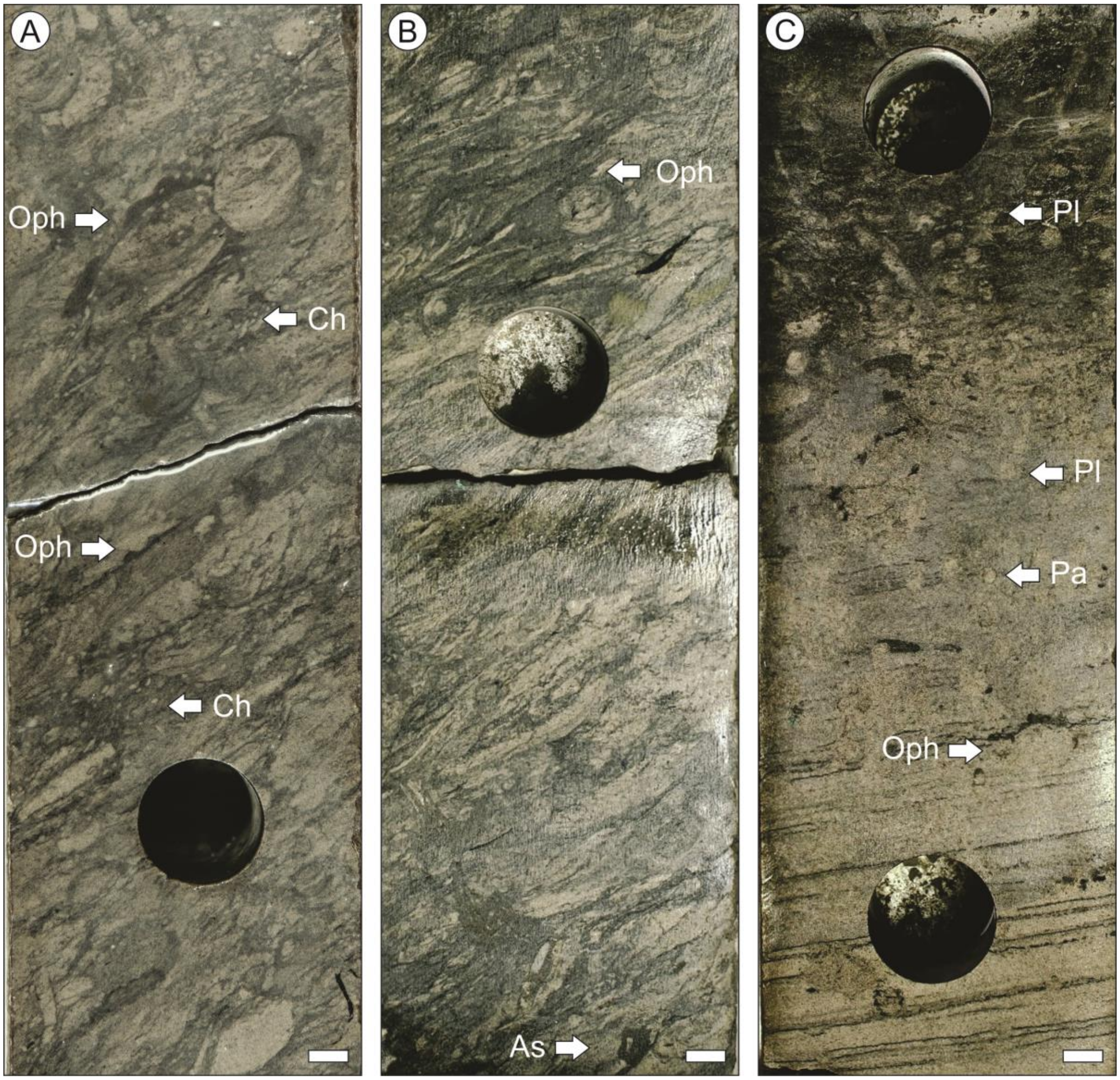

Figure 3.3. Core photographs of Ichnofabrics 5 and 6. A, Highly bioturbated Ichnofabric 5 displaying abundant *Ophiomorpha* with *Chondrites*-reworked abandoned burrows. B, Intensely bioturbated Ichnofabric 5 where discrete burrows are difficult to identify. Small *Ophiomorpha* (Oph) and *Asterosoma* (As) are indicated by the arrows. C, Core photograph of a parallel laminated sandstone bed with abundant *Planolites* (Pl) burrows at the top of the bed and less abundant *Palaeophycus* (Pa) and *Ophiomorpha* (Oph) mid-bed. Scale bars are 1 cm.

Ichnofabric 6: This ichnofabric is similar to Ichnofabric 5, but is dominated by *Ophiomorpha* with only *Planolites* and *Palaeophycus* burrows present in moderate to low abundance. This ichnofabric is commonly observed in the tops of storm beds (Facies 6). *Planolites* and *Palaeophycus* burrows are present in the bed tops with *Ophiomorpha* burrows extending downward into the laminated sandstone bed (Figure 3.3c). Bioturbation index is commonly 1-4 but may locally be BI 4-5 (Facies 5).

Ichnofabric 7: This ichnofabric contains only *Planolites* burrows, and is commonly found in the bioturbated sandstone facies (Facies 5) in association with abundant fine particulate carbonaceous debris (Figure 3.4a). Bioturbation index is commonly 4-5 and the ichnofabric is restricted to thin beds. The *Planolites* burrows may thus represent opportunistic, short-term colonization of an otherwise unfavourable setting.

Ichnofabric 8: Many of the parallel laminated sandstones observed in the Hebron Member appear fuzzy and contain broken or irregular laminae (Figure 3.4b). This texture is most likely the result of cryptobioturbation produced by meiofaunal organisms (Bromley, 1996). Locally, the texture has the appearance of Macaronichnus-like burrows. This ichnofabric is mainly documented from storm bed facies (Facies 6) near the bottom or middle of the bed.

Ichnofabric 9: This ichnofabric is characterized by diffuse *Ophiomorpha* overprinted by sharp-walled *Planolites*-like burrows (Figure 3.4c). This ichnofabric is observed in fine-grained sandstone with abundant carbonaceous debris (Facies 8) and is

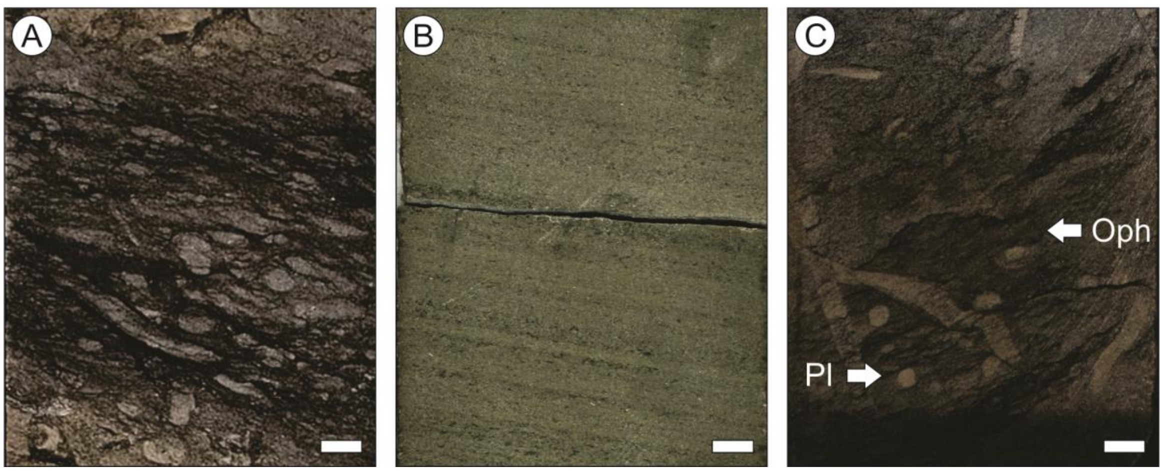

Figure 3.4. Core photographs of Ichnofabrics 7-9. A, *Planolites* burrows in carbonaceous rich sandstone. B, Cryptobioturbated fine-grained sandstone. C, Core photograph of carbonaceous rich fine-grained sandstone displaying sharp-walled *Planolites* (Pl) over printing diffuse *Ophiomorpha* (Oph) burrows. Scale bars are 1 cm.

typified by bioturbation indices of 2-3. The *Ophiomorpha* burrows are compacted and filled with muddy sandstone, and may be cross-cut by sharp-walled, *Planolites*-like burrows with circular cross sections that have clean sediment fills of contrasting colour to the host rock. The overlying deposit contains much coarser grained sandstone than the burrow fill of the *Planolites*-like burrows, which would suggest that they were not passively infilled by the overlying sediment. The filling sediment may have originated from a bed that was erosionally removed from the sedimentary record or the burrows are the product of deep tier producers burrowing down from a higher stratigraphic level (cf. Wanless' tubular tempestite model; Wanless et al., 1988; Gingras & Zonneveld 2015). The sharp burrow walls suggest that the *Planolites*-like burrows were produced at a later stage of sediment colonization, when the sediment consistency was quite firm. The *Ophiomorpha* burrows in contrast probably represent an early stage of colonization of the post-storm seafloor.

Ichnofabric 10: This ichnofabric is dominated exclusively by *Ophiomorpha* burrows and is found in association with sand-rich facies with variable, but low, clay content (Figure 3.5). This ichnofabric is observed to have a bioturbation index of 1-2.

7. Core plug analysis

The highest porosity and permeability values derived from core plug-based reservoir studies correspond to facies that display moderate to well sorting of sediment grains (Figure 3.6). The cross-bedded sandstones of Facies 10 have the highest overall

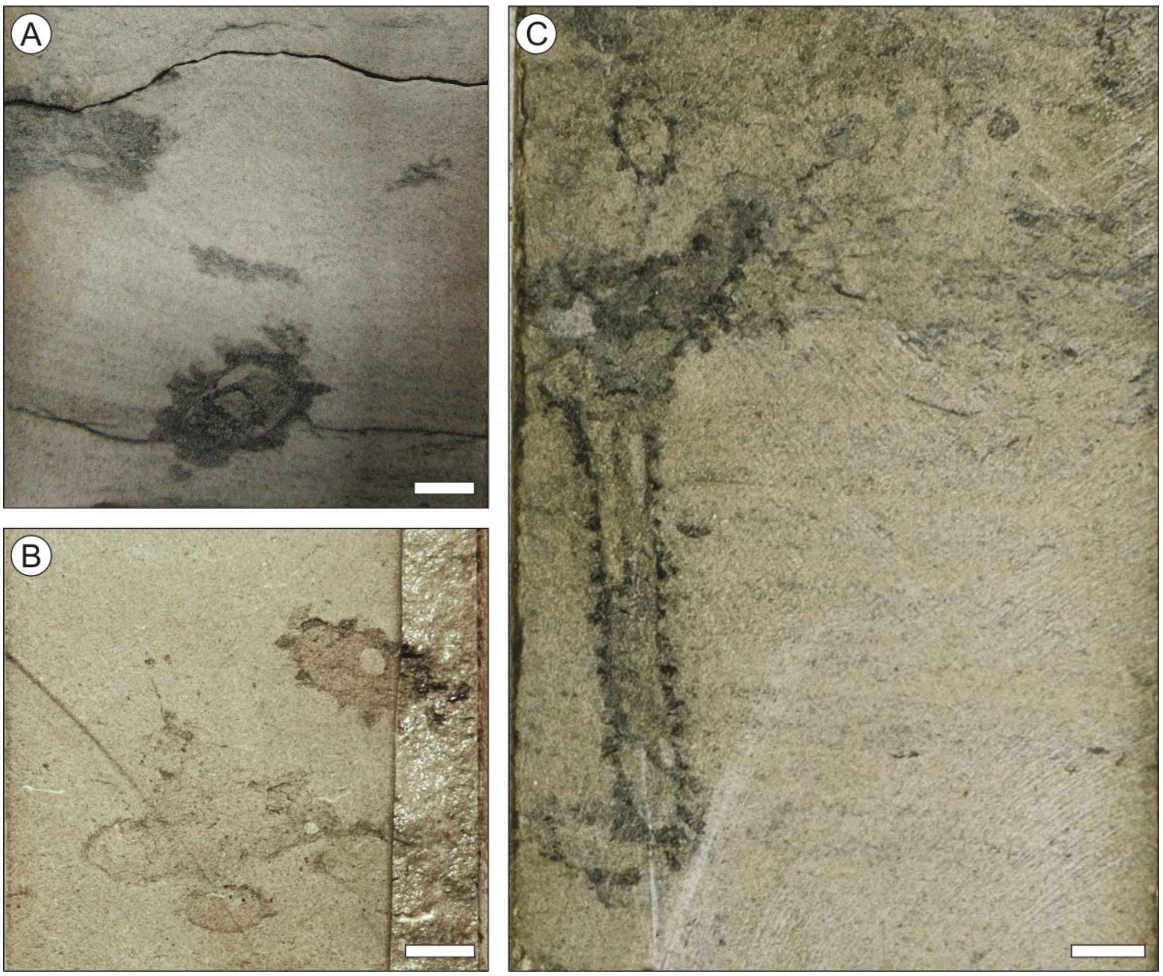

Figure 3.5. Core photographs of the *Ophiomorpha* dominated Ichnofabric 10.

permeability values up to 962.000 mD. The most notable feature is the cluster of data points corresponding to the parallel laminated sandstones (cf. Figure 3.6). Interestingly, the bioturbated sandstones of Facies 4 and 5 display a wide range of porosity values but tend to sit just below Facies 6 in permeability range.

The massively bedded and cross-bedded medium- to coarse-grained sandstone facies (Facies 9 and 10, respectively) are largely unbioturbated with the exception of rare *Ophiomorpha* in cross-bedded sandstones. Grain sorting and the low clay content are likely the controlling factors on porosity and permeability in these facies. In comparison, the parallel-bedded sandstones of Facies 11 are medium- to coarse-grained, but characteristically have poor grain sorting and variable carbonate cementation, which results in a wide (Figure 3.6).

The parallel laminated sandstones of Facies 6 commonly exhibit cryptobioturbation and bioturbated bed tops. Core plug samples taken from unbioturbated and cryptobioturbated parallel laminated sandstones display porosities ranging from 4.0% to 20.1%, and permeabilities between 0.070 and 250.000 mD (Figure 3.7). Bioturbated samples have lower overall permeability than unbioturbated and cryptobioturbated samples, though the data comes from relatively few core plug samples (cf. Ichnofabric 6, Figure 3.7). Tightly carbonate cemented samples correspond to some of the lowest porosity and permeability values in the Hebron Member (Figure 3.7).

Of all the bioturbated facies, Facies 4 and 5 displayed the highest porosity and permeability values (Figures 3.8 and 3.9). These facies are composed predominantly of sandstone with variable clay content. Facies 4 contains only Ichnofabric 3, while Facies 5 includes Ichnofabrics 4-7. Despite the differences in trace fossil assemblages between

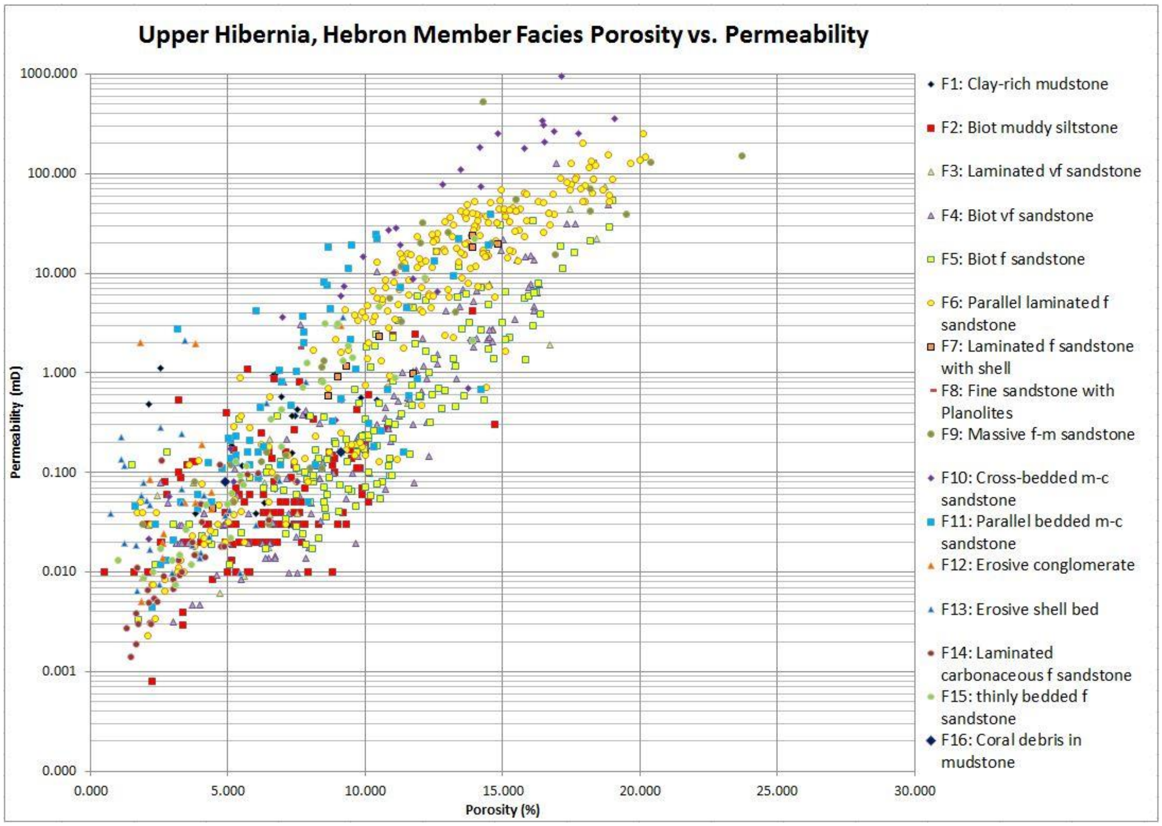

Figure 3.6. Graphic analysis of core plug porosity and permeability measurements from the Upper Hibernia, Hebron Member. Data is separated by facies classification. Note that no core plugs were taken from Facies 17.

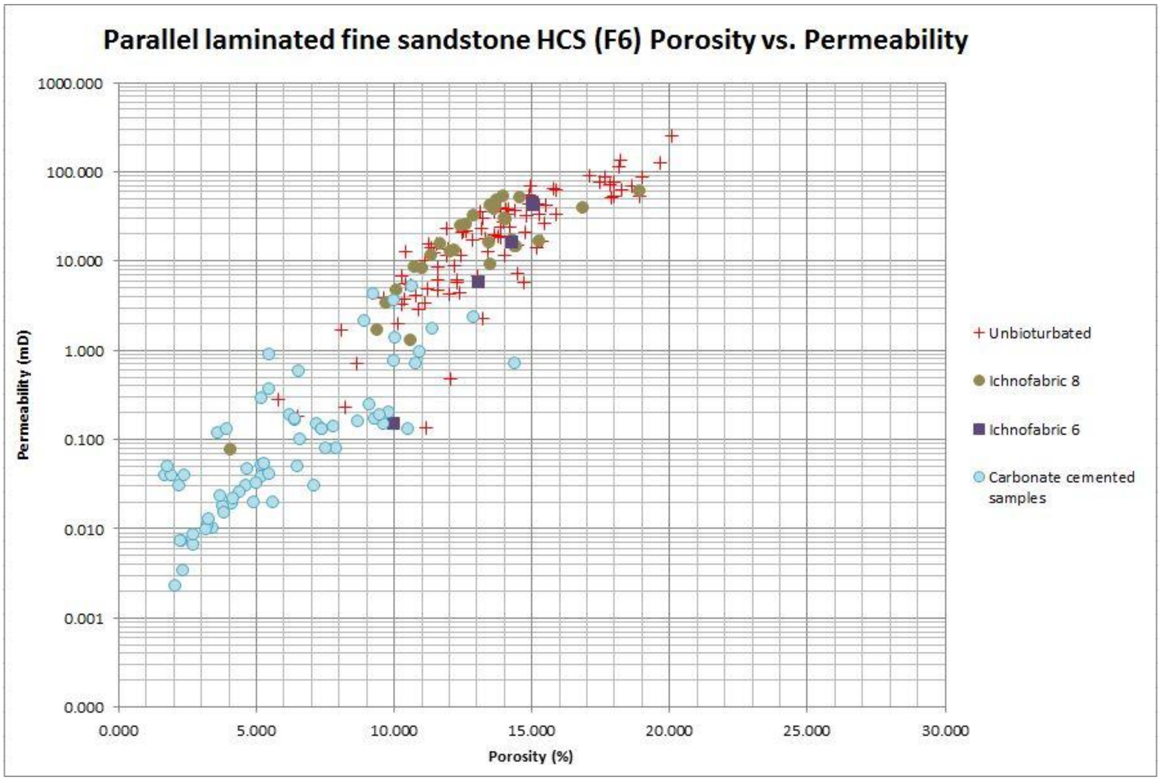

Figure 3.7. Graph of core plug porosity vs permeability for the parallel laminated fine sandstones of Facies 6.

Ichnofabrics 3 to 7, Facies 4 and 5 appear to have similar reservoir characteristics. On closer examination of the core plug sample locations, the higher overall porosity-permeability values correspond to higher sand-mud ratio. It was also noted that samples from the Hebron M-04 core were consistently higher in value than samples taken from the West Bonne Bay F-12 core (Figure 3.8). This may be due to the higher abundance of carbonate cement in the West Bonne Bay F-12 well.

Since most of the observed ichnofabrics are facies specific, no clear comparisons could be drawn between ichnofabrics that were not already evident from facies observations. In cases where more than one ichnofabric was present in a facies classification, the overall trend of porosity-permeability data was quite similar for each ichnofabric (Figure 3.9). However, in Facies 5, Ichnofabric 5 shows a slightly lower permeability range compared to Ichnofabric 6 in the same facies (Figure 3.9). This may reflect the higher overall degree of bioturbation observed in association with Ichnofabric 5, which has results in a more poorly sorted sedimentary fabric.

The muddy siltstone facies displays a wide range of porosity and permeability values despite the high clay content of the sediment (Facies 2, Figure 3.6). This facies corresponds to Ichnofabric 2, which is dominated by *Phycosiphon* and *Asterosoma* burrows (Figure 3.1b). On close examination of petrographic thin sections, it is observed that *Phycosiphon* burrows have increased porosity of 10-30 % in the sandy halo surrounding their muddy burrow core relative to the surrounding host rock (Figure 3.10).

The *Phycosiphon* producer selectively removes clay material from the adjacent sediment forming a clean, sand-rich halo. The clay material is presumably digested and redeposited as a fecal string in the burrow core (see Goldring et al., 1991; Wetzel and

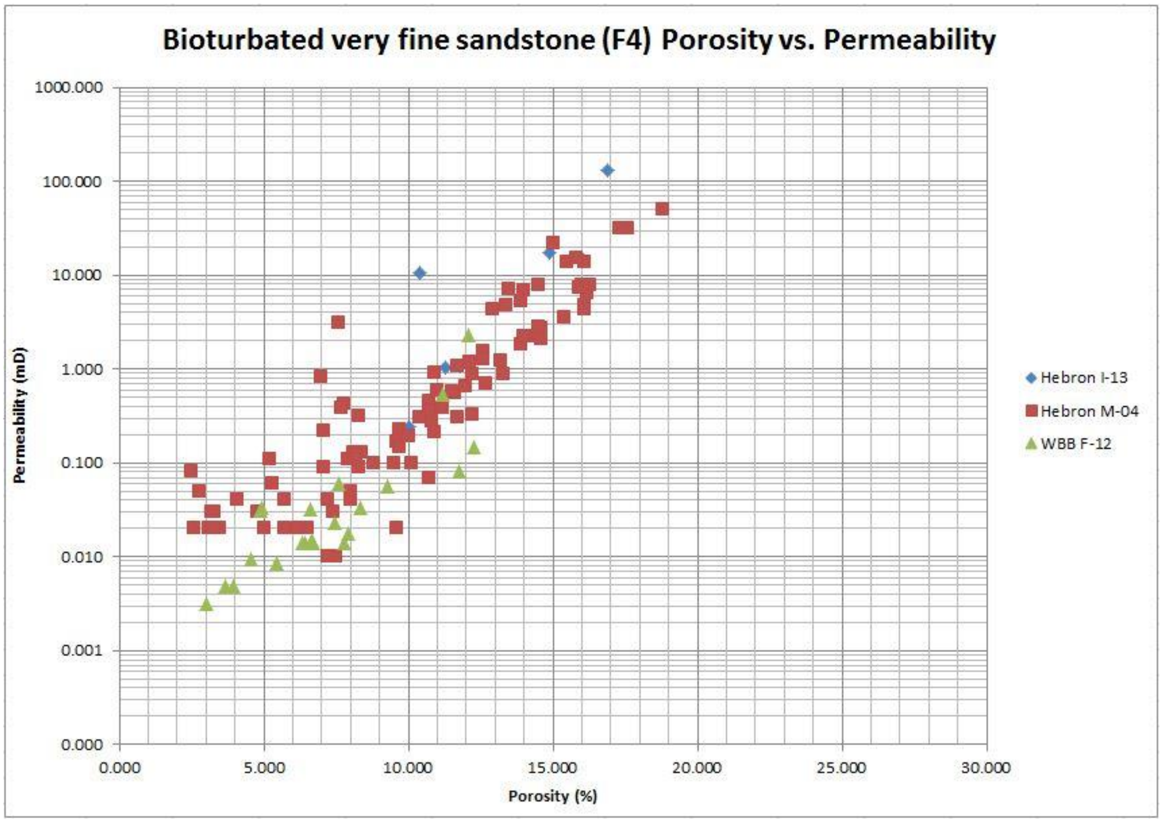

Figure 3.8. Plot of porosity versus permeability for data from core plugs of the bioturbated very fine sandstone (Facies 4), and coded for the well from which they came. This facies contains only Ichnofabric 3.

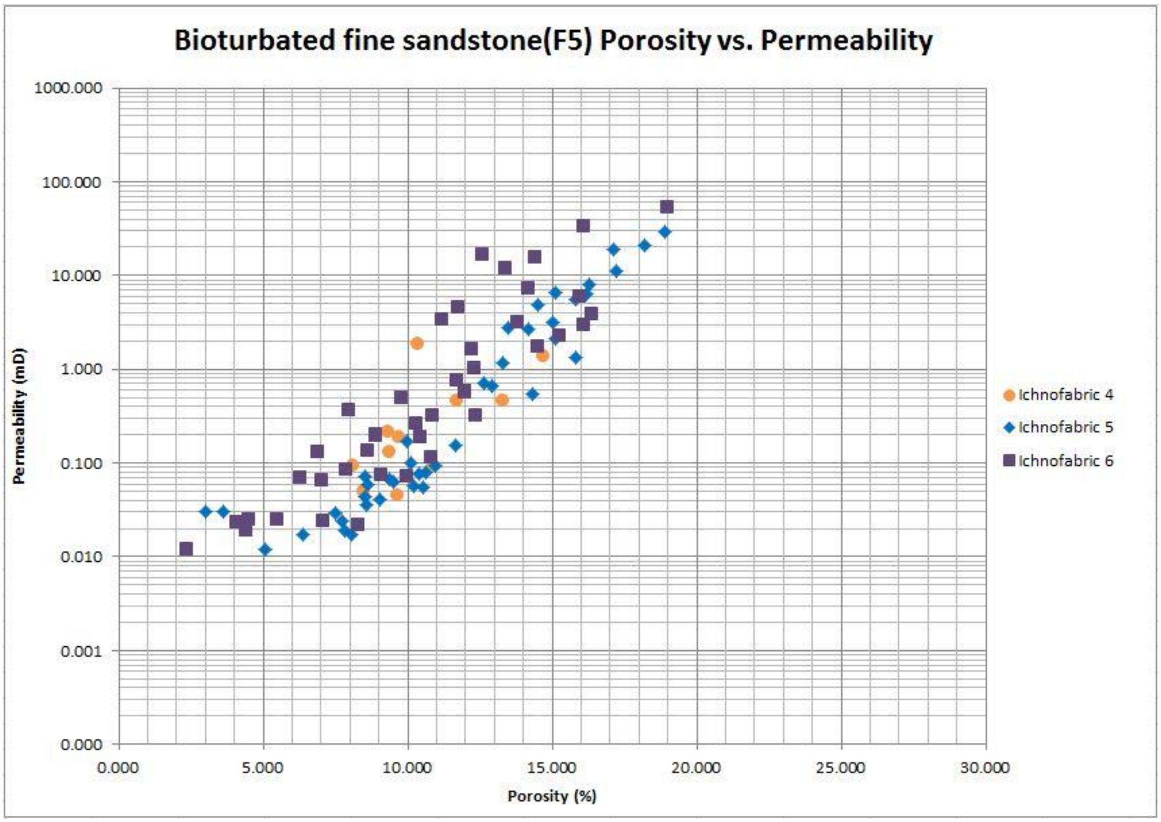

Figure 3.9. Plot of porosity and permeability values from core plugs taken from bioturbated fine sandstones (Facies 5), with the data separated by ichnofabric. Note that no data exists for Ichnofabric 7 in Facies 5.

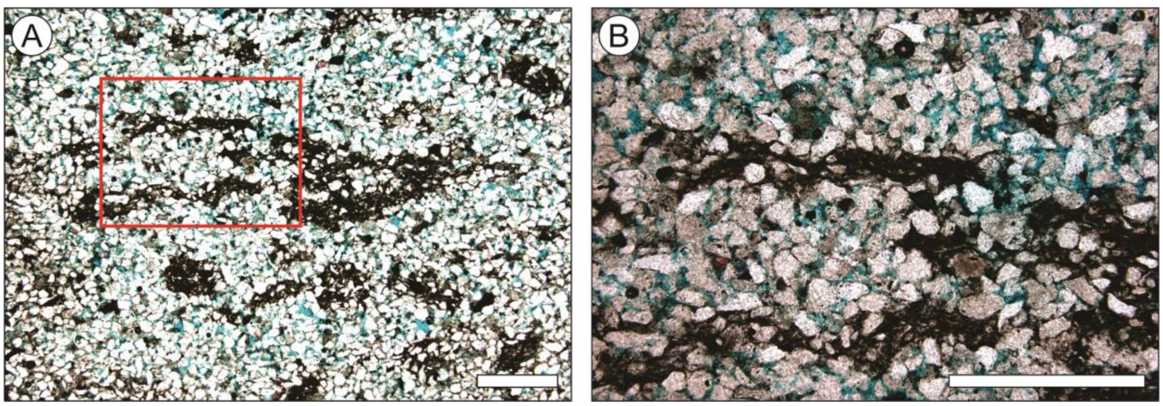

Figure 3.10. Microscope thin section from the Hebron M-04 core, 3015.25 m, showing *Phycosiphon* burrows and blue dye impregnation of pore space. Scale bars are 500 µm.

Bromley, 1994; Bednarz and McIlroy, 2012). Burrow connectivity has been shown to be quite high in *Phycosiphon*-dominated ichnofabrics displaying high bioturbation intensity (Bednarz and McIlroy, 2012).

8. Minipermeametry of slabbed core sections

Five samples were selected from the West Bonne Bay F-12 core for minipermeametry analyses. Sample 1 was taken from cross-bedded medium- to coarse-grained sandstone (Facies 10) and contains one vertical *Ophiomorpha* burrow and several horizontal burrows (Figure 3.11). The sample is 21 cm long by 9 cm wide and a total of 91 grid points were measured. Samples 2-5 were taken from various positions within a single storm bed 1.34 m in thickness (Figure 3.12). Sample 2 was taken from lower section of the fine-grained sandstone bed and is cryptobioturbated (Figure 3.13). Sample 3 was taken from the middle of the sandstone bed where no bioturbation was evident and distinct mudstone laminae were visible (Figure 3.14). Sample 4 was taken from the upper section of the storm bed where a lower degree of bioturbation was visible in the laminated sandstone facies (corresponding to Ichnofabric 6; Figure 3.15). Sample 5 was taken immediately above sample 4 at the top of the storm bed were the highest degree of bioturbation was observed (Figure 3.16).

In Sample 1, the *Ophiomorpha* burrows display a marked decrease in permeability relative to the surrounding sediment (Figure 3.11). In the vertical *Ophiomorpha*, the thick, muddy burrow wall creates a local baffle to fluid flow. The horizontal *Ophiomorpha* galleries in the upper and lower right side of the sample are partially dolomite cemented,

	P3	P6	P9	P12	P15	P18
S1	50.63	202.08	212.51	181.81	75.37	2.47
S2	7.97	193.34	194.18	216.66	51.34	8.97
S3	80.55	65.24	73.04	95.03	41.70	14.73
S4	177.12	29.20	87.62	80.49	32.31	50.11
S5	120.66	2.08	97.23	36.06	44.09	13.59
S6	136.03	2.41	31.05	23.54	14.15	84.95
S7	108.34	2.58	60.90	120.81	64.66	122.03
S8	36.38	59.88	6.62	148.82	98.32	100.93
S9	126.19	256.54	2.81	60.08	97.29	106.11
S10	130.72	315.43	43.77	173.29	94.56	77.77
S11	254.66	83.93	66.89	48.68	82.27	1.79
S12	142.13	90.63	45.67	7.81	51.69	10.66
S13	86.05	124.61	63.19	16.98	5.89	3.99
S14	227.88	162.43	49.20	4.15	3.25	8.52
S15	54.97				106.30	8.56
S16						198.71
S17						175.17
S18						188.25
S19						87.65

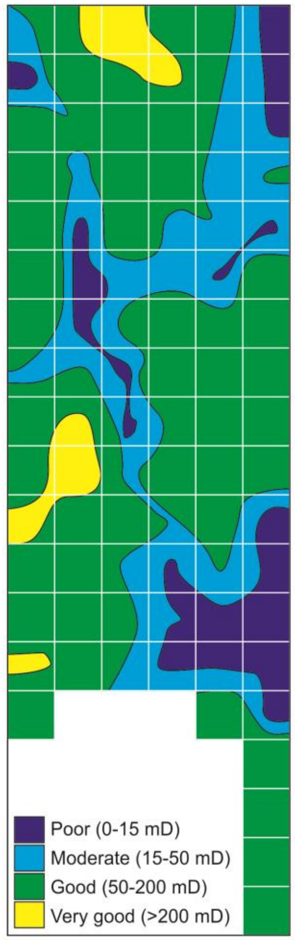

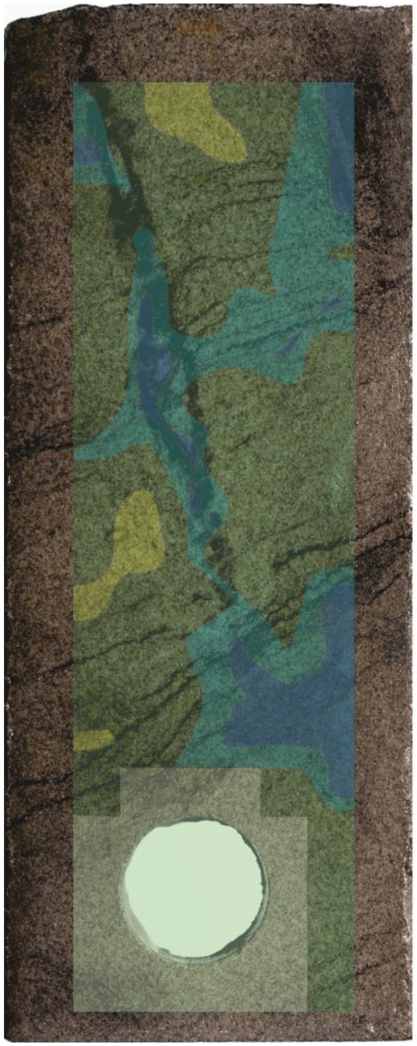

Figure 3.11. Minipermeametry of a slabbed core section from a cross-bedded medium- to coarse-grained sandstone (Facies 10) containing vertical and horizontal components of *Ophiomorpha* burrows. Left, colour contour map overlay on core section. Right, numerical distribution of permeability values on grid. Grid squares are 1 cm2.

which is the likely cause of the low permeability in these areas. Burrow fills of *Ophiomorpha* have been found to display higher permeabilities than the surrounding host rock (see Baniak et al., 2014), though the opposite is also possible (Tonkin et al., 2010). The reason for the dolomite cementation in these *Ophiomorpha* burrows is not well understood, but it is possible that the burrows were more permeable during an earlier stage of diagenesis when mineral-rich pore waters were able to permeate the burrows (cf. Gingras et al., 2004a).

The remaining samples were taken from a single storm bed to assess potential differences in permeability as a result of burrowing activity. The studied storm bed corresponds to the parallel laminated sandstone facies (Facies 6), which display some of the highest porosity and permeability core plug values of all the analyzed lithofacies (see Figure 3.6). It was found that there is a decrease in permeability towards the top of the bed as bioturbation intensity increases (Figure 3.12).

Sample 2 contains fuzzy, broken mudstone laminae produced by cryptobioturbation (Figure 3.13). This sample displays the highest permeability values measured by minipermeameter for the storm bed, and ranks average when compared to the core plug values for Facies 6, Ichnofabric 8 (see Figure 3.7). When compared to the unbioturbated Sample 3, Sample 2 has a vertical trend in the distribution of permeability values (Figure 3.13 and 3.14) in contrast to permeability distributions from Sample 3 that are oriented in horizontal bands. This is hypothesized to be the result of intact mudstone laminae in Sample 3 preventing vertical connectivity of pore space between layers (cf. Gingras et al., 2009).

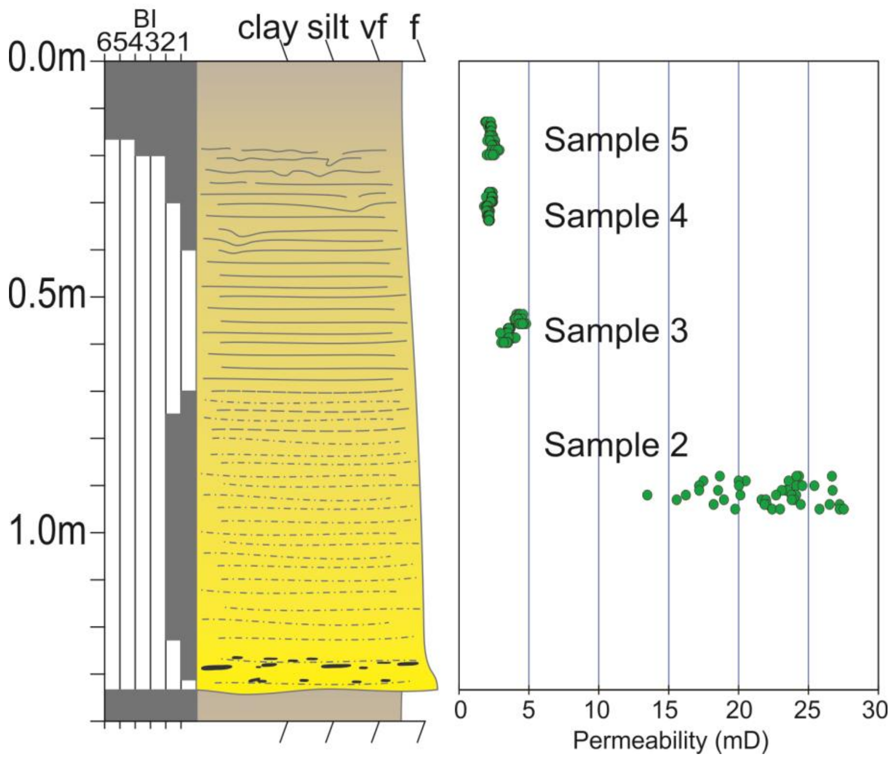

Figure 3.12. Location of Samples 2-5 in a storm bed. Permeability values from minipermeametry of each sample are graphed at a level that corresponds to their location in the bed. Bioturbation index is graphed on the left side of the storm bed.

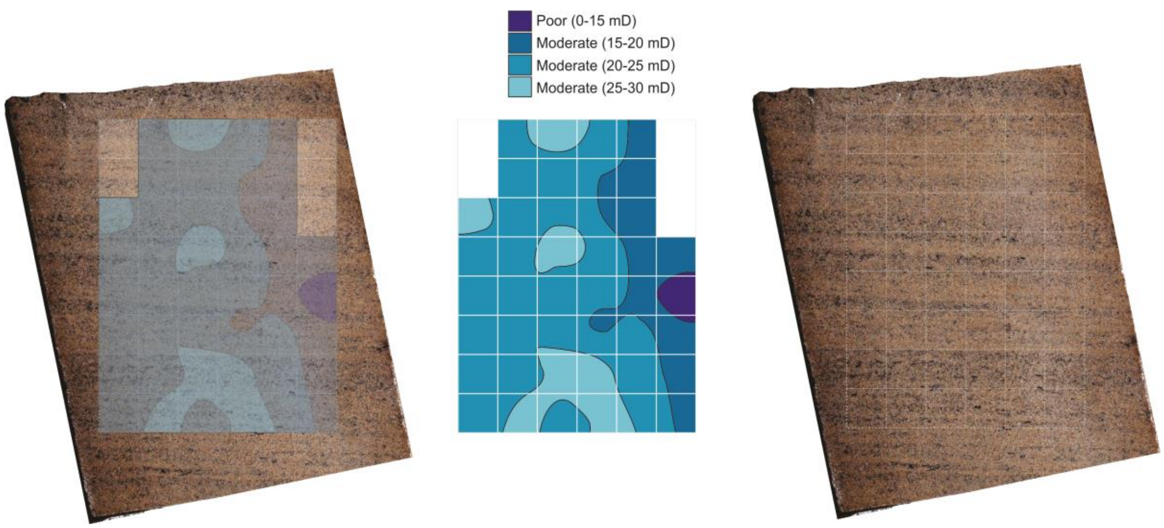

Figure 3.13. Colour contour map of permeability data from minipermeametry analysis of the cryptobioturbated Sample 2. Grid squares are 1 cm2.

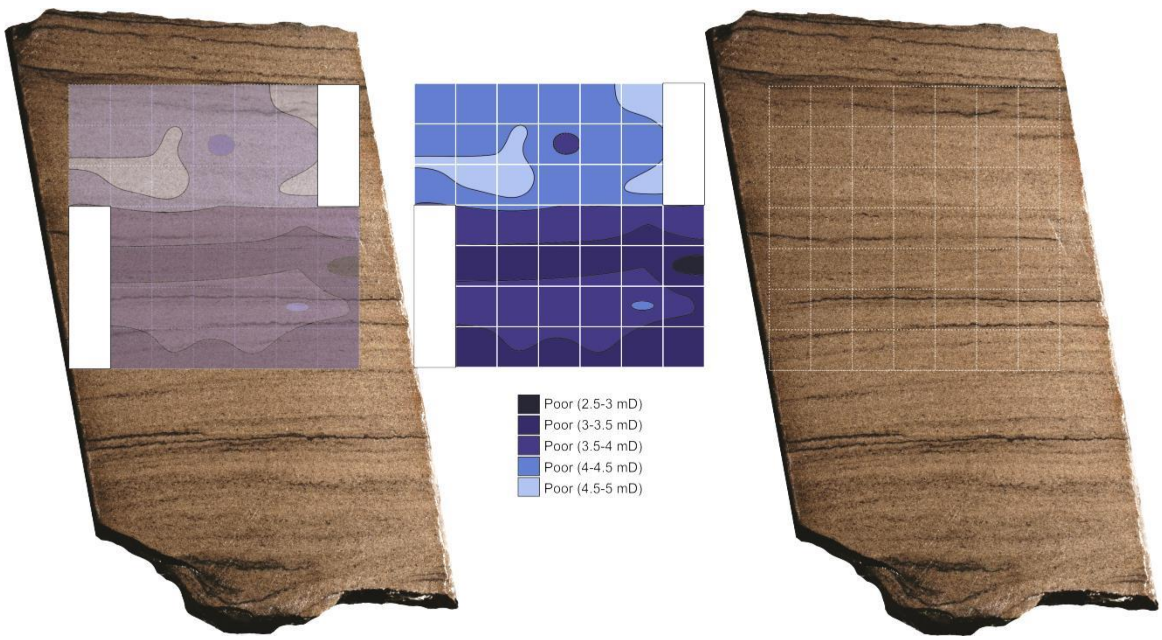

Figure 3.14. Colour contour map of permeability data from minipermeametry analysis of laminated sandstone showing horizontal trends in permeability distribution from Sample 3. Grid squares are 1 cm2.

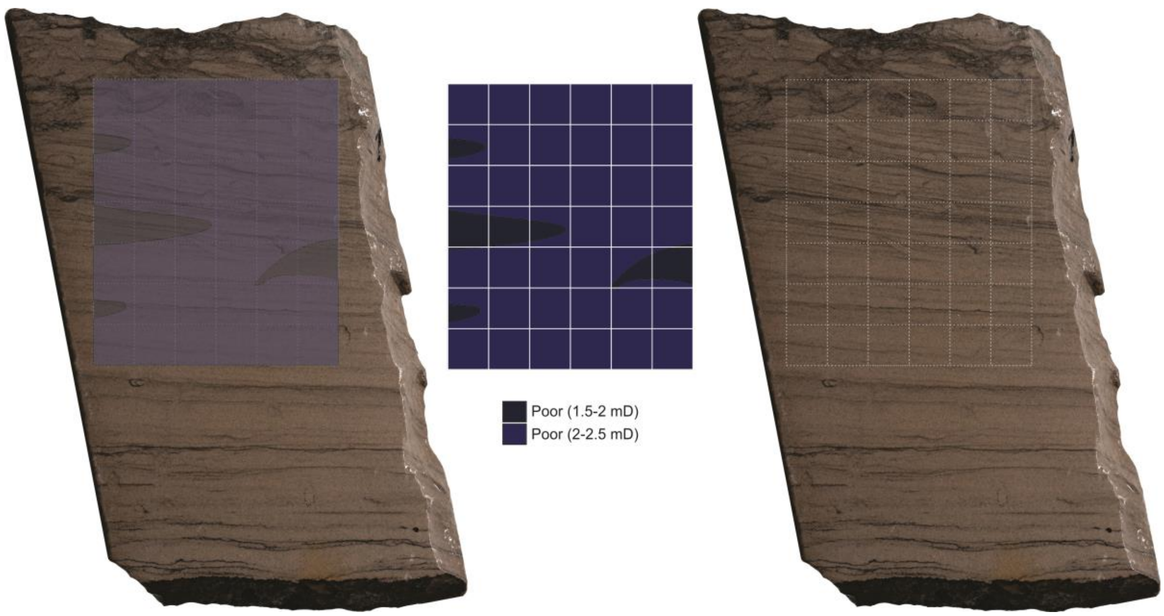

Figure 3.15. Colour contour map of permeability data from minipermeametry analysis of Sample 4 displaying low bioturbation. Grid squares are 1 cm2.

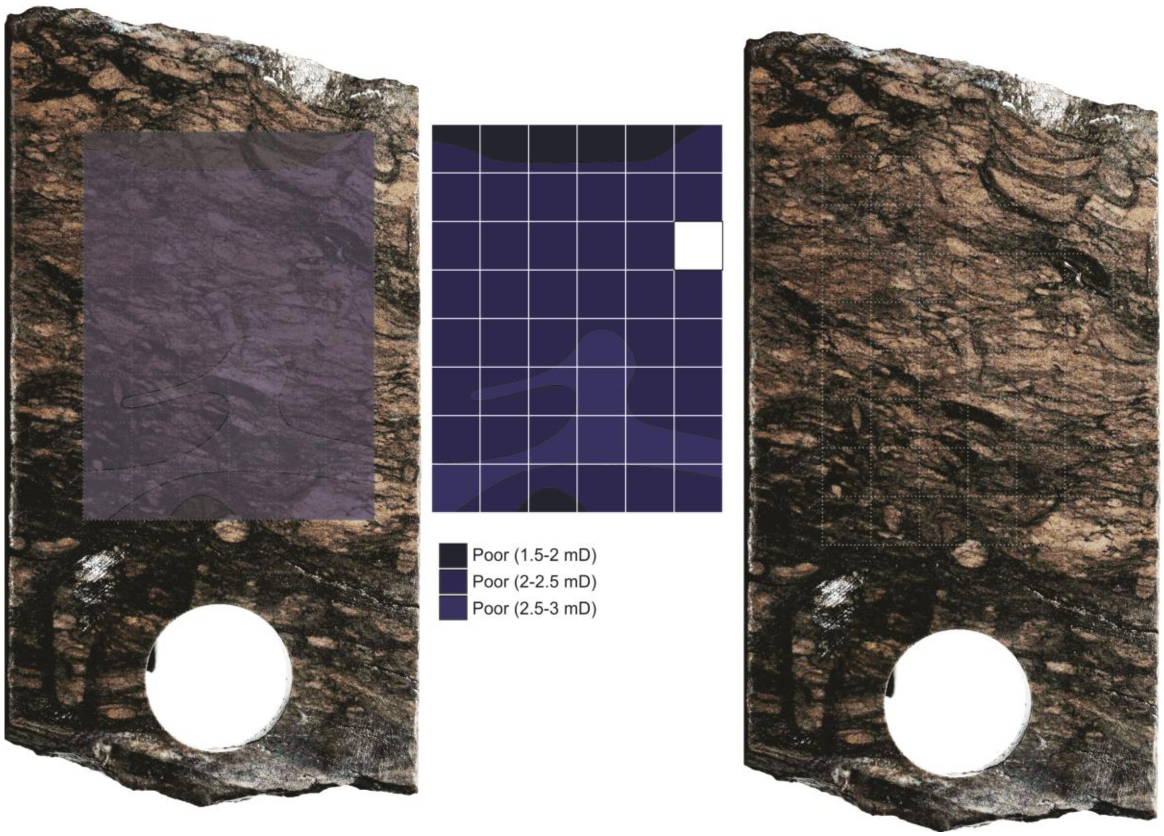

Figure 3.16. Colour contour map of permeability data from minipermeametry analysis of highly bioturbated Sample 5. Grid squares are 1 cm2.

Samples 4 and 5 display very similar ranges in permeability (Figures 3.12, 3.15, and 3.16). Given that Sample 4 displays more visual similarities with Sample 3, it was expected that the two would also share a similar range in permeability values (Figures 3.14 and 3.15). However, the permeability transition from Sample 3 up to Sample 5 is likely a function of the increased clay content in the bed, and the increase in the intensity of bioturbation altering the grain sorting of the sedimentary fabric. The similar permeabilities observed in Samples 4 and 5 may suggest that the overall ratio of sand grains to clay-grade material is unchanged between the two samples despite the apparent differences in grain distribution (Figures 3.15 and 3.16).

9. Discussion

Porosity and permeability of sandstones are affected by grain sorting, compaction, cementation, and the ratio of sand to clay-grade material (Bjørlykke, 2010). Well-sorted sediments commonly exhibit higher porosity characteristics than poorly sorted sediments (Bjørlykke, 2010). Compaction and cementation further decrease porosity and limit flow pathways thereby also decreasing permeability (Bjørlykke, 2010). The effects of bioturbation on porosity and permeability characteristics, and how they relate to reservoir quality and recovery, are now well documented (e.g. Gingras et al., 2004a, 2004b, 2009; Pemberton and Gingras, 2005; Tonkin et al., 2010; Bednarz and McIlroy, 2012; La Croix et al., 2012, 2013; Baniak et al., 2014). The greatest effects on porosity and permeability result from changes in the distribution of sand and clay-grade material as a result of burrowing activity (Gingras et al., 2009).

In the highly permeable cross-bedded sandstones of Facies 10, *Ophiomorpha* burrows tend to act as baffles to fluid flow due to the presence of a mud-lined burrow wall, and decrease the reservoir volume. The *Ophiomorpha* producers actively remove clay and fine-grained material from the system and concentrate it in the burrow wall (Leaman & McIlroy 2015), thereby actively changing the distribution of grain sizes. The density and distribution of *Ophiomorpha* is therefore a concern for reservoir quality and hydrocarbon recoverability regardless of facies.

The cryptobioturbated parallel-laminated storm beds (Facies 6) display breaks in the muddy laminations separating sandstone layers resulting in an increase in the vertical connectivity of the bed. However, distinguishing cryptobioturbated beds from unbioturbated equivalents is a difficult task using porosity and permeability data alone (see Figure 3.7). Visual references are required to accurately identify these beds. This is an important distinction since higher vertical connectivity improves hydrocarbon recovery in reservoir facies (Pemberton and Gingras, 2005; Gingras et al., 2009).

The highly bioturbated storm bed top (Sample 5, Figure 3.16) can be shown to have the same permeability as the underlying, less bioturbated, laminated sandstones (Sample 4, Figure 3.15). It is possible that the ratio of sand to clay material is similar between the two, or that the higher degree of bioturbation has changed the way in which the sediment was compacted after burial (i.e. the laminated sandstone is more easily compacted than the more heterogeneous bioturbated fabric). The low permeability of the storm bed top reduces communication between stacked storm beds in a reservoir setting. Vertical communication between storm beds could however be achieved if: 1) the bed top was deeply eroded by the subsequent storm deposit; or 2) deep tier, open burrows where to extend down to the more permeable sandstones (i.e. Facies 6), overprinting the bed top ichnofabric, and become filled with the overlying storm sands (cf. Bromley, 1975). Modelling of bathymetric location and storm frequency would be required to determine where in the basin communication between beds due to erosion would be most likely to occur.

Perhaps the most impressive alteration to the sedimentary fabric by burrowing activity is that of *Phycosiphon* in the muddy siltstone facies (Facies 2). The abundance and size of pore spaces in the *Phycosiphon* halo are higher than that of the surrounding host rock. The *Phycosiphon* ichnofabric is distributed throughout the muddy siltstone facies, which is commonly interbedded with parallel laminated storm beds (Facies 6) and very fine-grained laminated storm beds (Facies 3). From a reservoir standpoint, the presence of *Phycosiphon* burrows is likely to encourage hydrocarbon flow and connectivity between storm beds. Additionally, *Phycosiphon* ichnofabrics have been shown to increase fracturability and thus hydrocarbon recovery in shale reservoirs (Bednarz and McIlroy, 2012).

10. Conclusions

The objective of this study was to examine the porosity and permeability characteristics of lithofacies from the Hebron Member, Upper Hibernia Zone and to determine what effects bioturbation had on these data. Core plug analyses show that facies with better grain sorting have higher porosity and permeability values. While thoroughly bioturbated sandstone facies display a decrease in permeability range, porosity values are wide ranging. It is inferred that the decrease in permeability is the result of an introduction of clay material by burrowing activity and a disruption of the primary sedimentary grain sorting. Muddy siltstone facies display a wide range in porosity values, which is likely the direct result of the density and distribution of *Phycosiphon*-dominated ichnofabric (Ichnofabric 2). *Phycosiphon* burrows are noted in thin section to display enhanced porosity in the burrow halo.

From minipermeametry of slabbed core sections, a more detailed look at the effects of bioturbation was achieved. Mud-lined *Ophiomorpha* burrows significantly decrease permeability values in otherwise highly permeable cross-bedded sandstone. If present in a great enough density, *Ophiomorpha* burrows would act as baffles to hydrocarbon flow, and decrease reservoir volumes, thereby reducing connectivity, and recovery rate.

Through minipermeametry analysis of a parallel laminated storm bed, which normally displays good permeability and porosity values from core plug analysis, a notable decrease in permeability towards the top of the bed was documented. Minipermeametry of the cryptobioturbated section of the storm bed showed a vertical trend in permeability values relative to the unbioturbated equivalent. Cryptobioturbation therefore is found to increase vertical connectivity a single bed, and therefore has the potential to improve hydrocarbon recovery.

The main factors influencing the porosity and permeability characteristics in the studied facies is grain sorting and the ratio of sand grains to clay material. Specialized burrowing behaviours that change the distribution of sand and clay are the most effective at modifying porosity and permeability characteristics (i.e. mud-lined *Ophiomorpha* burrows decrease sandstone permeability, whereas *Phycosiphon* increases the porosity of muddy siltstones), though all burrowing behaviours causes change to some degree. It is important that these effects be understood in their facies context to make predictions that will maximize the efficiency of hydrocarbon recovery.

11. Acknowledgements

Thank you to Husky Energy and the School of Graduate Studies, Memorial University of Newfoundland, for providing funding for this research.

12. References

BANIAK, G.M., LA CROIX, A.D., POLO, C.A., PLAYTER, T.L., PEMBERTON, S.G., GINGRAS, M.K. 2014. Associating x-ray microtomography with permeability contrasts in bioturbated media. *Ichnos*, v. 21, p. 234-250.

BEDNARZ, M. and MCILROY, D. 2012. Effect of phycosiphoniform burrows on shale hydrocarbon reservoir quality. *AAPG Bulletin*, v. 96, p. 1957-1980.

BJØRLYKKE, K. 2010. Petroleum Geoscience: From Sedimentary Environments to Rock Physics. Springer, New York, 508 p.

BROMLEY, R.G. 1975. Trace fossils at omission surfaces. *In*: R.W. Frey (ed.), The Study of Trace Fossils. Springer-Verlag, New York, p. 399-428.

BROMLEY, R.G. 1996. Trace Fossils: biology, taphonomy and applications. London, Chapman and Hall, 361 p.

BROMLEY, R.G. and EKDALE, A.A. 1986. Composite ichnofabrics and tiering of burrows. *Geological Magazine*, v. 123, p. 59-65.

EKDALE, A.A. and BROMLEY, R.G. 1983. Trace fossils and ichnofabric in the Kjølby Gaard Marl, uppermost Cretaceous, Denmark. *Bulletin of the Geological Society of Denmark*, v. 31, p. 107-119.

GINGRAS, M.K. and ZONNEVELD, J. 2015. Tubular Tidalites: a biogenic sedimentary structure indicative of tidally influenced sedimentation. Journal of Sedimentary Research, v.85, p. 845-854.

GINGRAS, M.K., MENDOZA, C.A., and PEMBERTON, S.G. 2004a. Fossilized worm burrows influence the resource quality of porous media. *AAPG Bulletin*, v. 88, p. 875-883.

GINGRAS, M.K., PEMBERTON, S.G., HENK, F., MACEACHERN, J.A., MENDOZA, C.A., ROSTRON, B., O'HARE, R., SPILA, M., and KONHAUSER, K. 2009. Application of ichnology to fluid and gas production in hydrocarbon reservoirs. *SEPM*, v. 52, p. 131-145.

GINGRAS, M.K., PEMBERTON, S.G., MUELENBACHS, K., and MACHEL, H. 2004b. Conceptual models for burrow-related, selective dolomitization with textural and isotopic evidence from the Tyndal Stone, Canada. *Geobiology*, v. 2, p. 21-30.

GOLDRING, R., POLLARD, J.E., and TAYLOR, A.M. 1991. *Anconichnus horizontalis*: a pervasive ichnofabric-forming trace fossil in post-Palaeozoic offshore siliciclastic facies. *Palaios*, v. 6, p. 250-263.

LA CROIX, A.D., GINGRAS, M.K., DASHTGARD, S.E., and PEMBERTON, S.G. 2012. Computer modeling bioturbation: the creation of porous and permeable fluid-flow pathways. *AAPG Bulletin*, v. 96, p. 545-556.

LA CROIX, A.D., GINGRAS, M.K., PEMBERTON, S.G., MENDOZA, C.A., MACEACHERN, J.A., and LEMISKI, R.T. 2013. Biogenically enhanced reservoir properties in the Medicine Hat gas field, Alberta, Canada. *Marine and Petroleum Geology*, v. 43, p. 464-477.

LEAMAN, M. and MCILROY, D. 2015. Petrophysical properties of *Ophiomorpha irregulaire* ichnofabrics from BN L-55 of Hebron Field, offshore Newfoundland. *In*: D. McIlroy (ed.), Ichnology: Papers from ICHNIA III. Geological Association of Canada, Miscellaneous Publication, v. 9, p. 127-139.

MCILROY, D. 2004. Some ichnological concepts, methodologies, applications and frontiers. *In*: D.McIlroy (ed.), The Application of Ichnology to Palaeoenvironmental and Stratigraphic Analysis. Geological Society Special Publication, v. 228, p. 3-27.

MCILROY, D. 2008. Ichnological analysis: the common ground between ichnofacies workers and ichnofabric analysts. *Palaeogeography, Palaeoclimatology, Palaeoecology*, v. 270, p. 332-338.

PERMBERTON, S.G. and GINGRAS, M.K. 2005. Classification and characterizations of biogenically enhanced permeability. *AAPG Bulletin*, v. 89, p.1493-1517.

SHEPPARD, D., MAC PHERSON, C., MACINNIS, D. 2006. Geological Report on Husky Oil et al West Bonne Bay F-12 East Coast Canada. Husky Oil Operations Limited. pp 258.

SINCLAIR, I.K., FLINT, S., STOKES, R., and BIDGOOD, M. 2005. Hibernia Formation (Cretaceous) sequences and Breathitt Group (Pennsylvanian) analogue: implications for reservoir compartmentalization and modeling, offshore Newfoundland. *In*: R.N. Hiscott and A.J. Pulham (eds.), Petroleum resources and reservoirs of the Grand Banks, eastern Canadian margin. Geological Association of Canada, Special Paper 43, p. 143-167.

TAYLOR, A. and GOLDRING, R. 1993. Description and analysis of bioturbation and ichnofabric. *Journal of the Geological Society*, v. 150, p. 141-148.

TAYLOR, A., GOLDRING, R., and GOWLAND, S. 2003. Analysis and application of ichnofabrics. *Earth Science Reviews*, v. 60, p. 227-259.

TONKIN, N.A., MCILROY, D., MEYER, R., and MOORE-TURPIN, A. 2010. Bioturbation influence on reservoir quality: a case study from the Cretaceous Ben Nevis Formation, Jeanne d'Arc Basin, offshore Newfoundland, Canada. *AAPG Bulletin*, v. 94, p. 1059-1078.

WANLESS, H.R., TEDESCO, L.P., and TYRRELL, K.M. 1988. Production of subtidal tubular and surficial tempestites by Hurricane Kate, Caicos Platform, British West Indies. *Journal of Sedimentary Petrology*, v. 58, p. 739-750.

WETZEL, A. and BROMLEY, R.G. 1994. *Phycosiphon incertum* revisited: *Anconichnus horizontalis* is its junior subjective synonym. *Journal of Paleontology*, v. 68, p. 1396-1402.

CHAPTER 4

Stratigraphic interpretation of the Hibernia Formation in the southern Jeanne d’Arc Basin, offshore Newfoundland, Canada

Elizabeth R. Schatz[1, 2], Duncan McIlroy[2],

[1] Corresponding author: elizabeth.schatz@mun.ca

[2] Department of Earth Sciences. Memorial University of Newfoundland, 300 Prince Philip Drive, St. John’s, NL, A1B 3X5, Canada. dmcilroy@mun.ca

1. Abstract

The Jeanne d’Arc Basin was formed as the result of three rifting events spanning from the Late Triassic to Early Cretaceous as a result of the opening of the Atlantic Ocean. Accommodation and stratigraphic architecture were primarily tectonically driven. Wireline logs from seven wells were integrated with detailed sedimentary logs from three core samples to determine stratigraphic correlation of the Hibernia Formation in the southern Jeanne d’Arc Basin. Three major flooding surfaces could be identified across all wells: the basal Hebron, middle Hebron, and top Hebron flooding surfaces. Analysis of facies distribution suggests that autocyclic lobe switching contributed to differences in sediment distribution between the Hebron and West Bonne Bay regions, the Hebron delta lobe being more active. Sandstone units observed in wireline logs from the West Ben Nevis B-75 and Ben Nevis I-45 wells may be the result of longshore drift from the

Hebron distributary. Further data collection from the southern Jeanne d'Arc Basin is needed.

2. Introduction

The Hibernia Formation has been an exploration target for the petroleum industry for over 30 years (Arthur et al., 1982; Tankard and Welsink, 1987; Mackay and Tankard, 1990; Sinclair et al., 1992). However, the Hibernia Formation in the southern region of the Jeanne d'Arc Basin has been little studied and the Hebron and Cape Island Members even less so (see Figure 2.2). This facies-based study of core material is used to infer paleoenvironment of deposition and to infer stratigraphic stacking and correlation of the southern expression of the Hibernia Formation with the aid of wireline log data. Because core recovery from the Hibernia Formation in this region is low, and wells are typically ~ 6 km apart, this study serves as a starting point to promote discussion and further study of the Hibernia Formation in the southern Jeanne d'Arc Basin.

3. Geological Setting

The upper section of the Hibernia Formation is divided into two informal members: the Cape Island Member and the Hebron Member (see Figure 2.2; Sinclair et al., 2005). The Cape Island Member overlies a shale interval known as the Middle Hibernia and is characterized by coarsening-upwards patterns as determined from gamma-ray log analysis. The Hebron Member lies between the Cape Island Member and the B-Marker limestone above. The B-Marker limestone is a prominent marker in well logs and is known to extend across much of the Jeanne d'Arc Basin. As such, the B-Marker limestone serves as the datum from which the wells in this study were correlated.

The Jeanne d'Arc Basin is the product of three rifting events during the formation of the Atlantic Ocean. The Hibernia Formation was deposited during the second rifting episode which occurred from the Late Jurassic to the Early Cretaceous (Sinclair et al., 1999). The lower Hibernia Formation—and much of the Cape Island Member—is considered to be Berriasian in age while the Hebron Member corresponds to the early Valanginian based on palynology and micropaleontology data (Sinclair et al., 2005; Ainsworth et al., 2006). The Jeanne d'Arc Basin was an active rift zone consisting of a complex system of north-south and east-west running faults (Figure 4.1) that--for much of its depositional history-- was subject to tectonically controlled relative sea level change and accommodation generation (Tankard and Welsink, 1987; Brown et al., 1989; Hiscott et al., 1990; Mackay and Tankard, 1990; Sinclair et al, 1992, 1999, 2005).

4. Sedimentology and stratigraphy

4.1. Core material

Three core samples have been recovered from the Hebron Member in the southern Jeanne d'Arc Basin: Hebron I-13 core 4 (17.5 m), Hebron M-04 core 3 (110 m), and West Bonne Bay F-12 core 1 (110 m). The cores from the Hebron Field are located within the same fault block and are situated approximately 20 km west of West Bonne Bay F-12

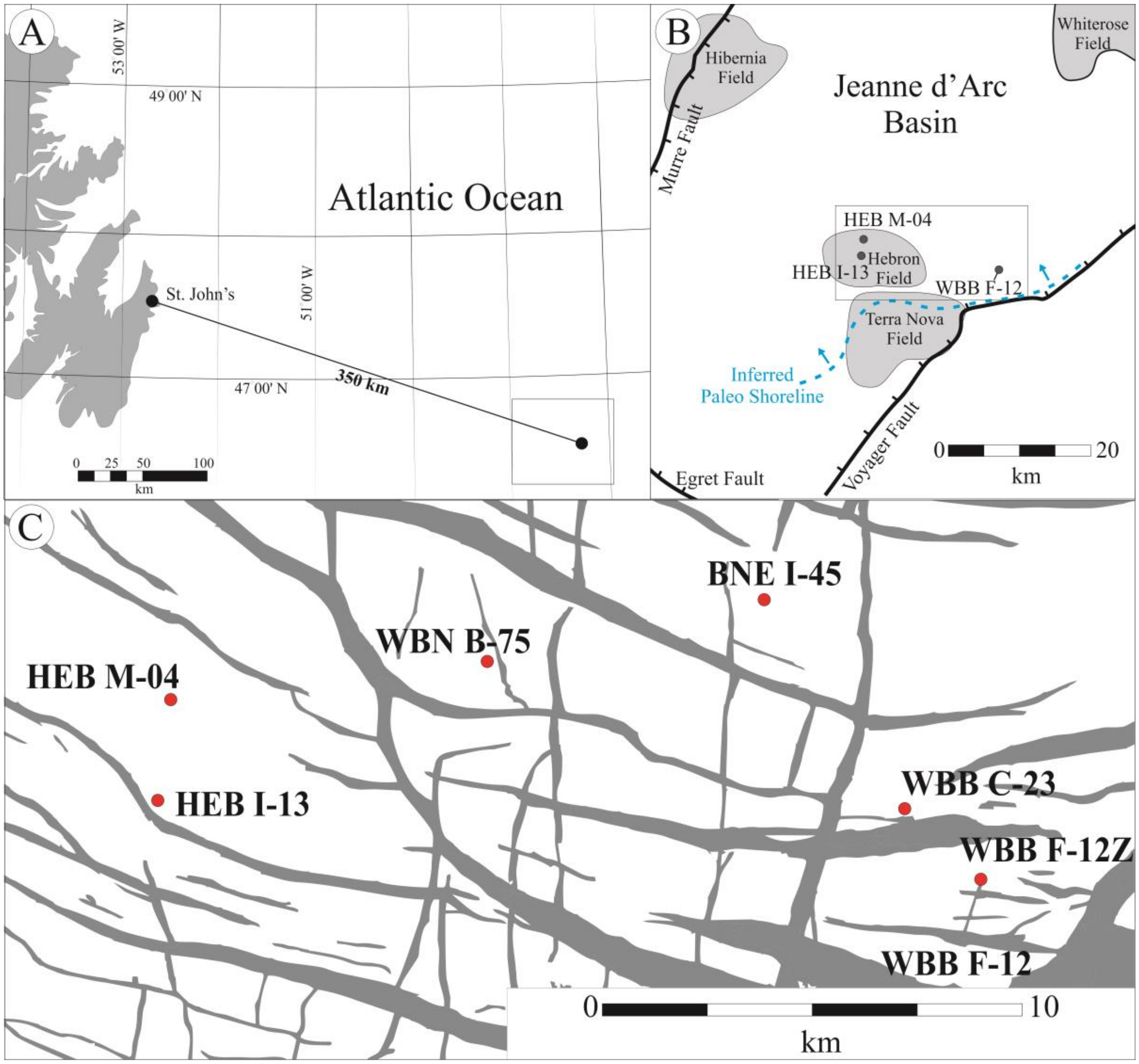

Figure 4.1. Well location map in the Jeanne d'Arc Basin displaying the location of major oil fields, faults, and inferred paleo shoreline during the deposition of the Hebron Member (A and B). Blue arrows indicate direction of increasing water depth from the shoreline. C, Detail of well locations with minor north-south and east-west trending faults.

(WBB F-12) well (Figure 4.1c). Facies analyses (see Chapter 2) suggest that the 'Hebron Member' was deposited in a wave-influenced deltaic setting. Palaeoenvironmental analysis based on facies and facies associations allow the recognition of flooding surfaces that enable the core data to be placed within a sequence stratigraphic framework. Flooding surfaces were identified on the basis of inferred increases in water depth and concomitant decreases in sediment supply (Catuneanu et al., 2009).

Interpreted depositional environment and flooding surfaces for WBB F-12 core 1 are featured in Figure 4.2. At the base of the WBB F-12 core, delta mouthbar sandstones are overlain by offshore mudstones (4030 m to 4033 m, Figure 4.2). A coarse-grained, poorly sorted sandstone interpreted as a transgressive lag separates the mudstones and sandstones. *Ophiomorpha* burrows in the delta mouthbar sandstone are filled with material from the lag deposit and feeding cone-equilibrium structures (cf. Leaman & McIlroy 2015; Leaman et al. 2015; Evans & McIlroy 2016) are present at the base of the lag suggesting an abrupt change in environmental conditions associated with the hiatus (Figure 4.3a).

Lower shoreface sandstones transition to delta front mouth bars displaying a progradational trend in the facies architecture (3994 m to 4030 m, Figure 4.2). A flooding surface at 3993.5 m marks the return to a lower shoreface setting and a change to an aggradational-retrogradational stacking pattern moving upwards in the core section to a thin offshore mudstone at approximately 3966.5 m (Figure 4.2). Carbonate-cemented coarse shell debris interbedded with parallel laminated sandstones are interpreted as high energy wave deposited during a period of low sediment input (3967 m to 3975 m, Figure

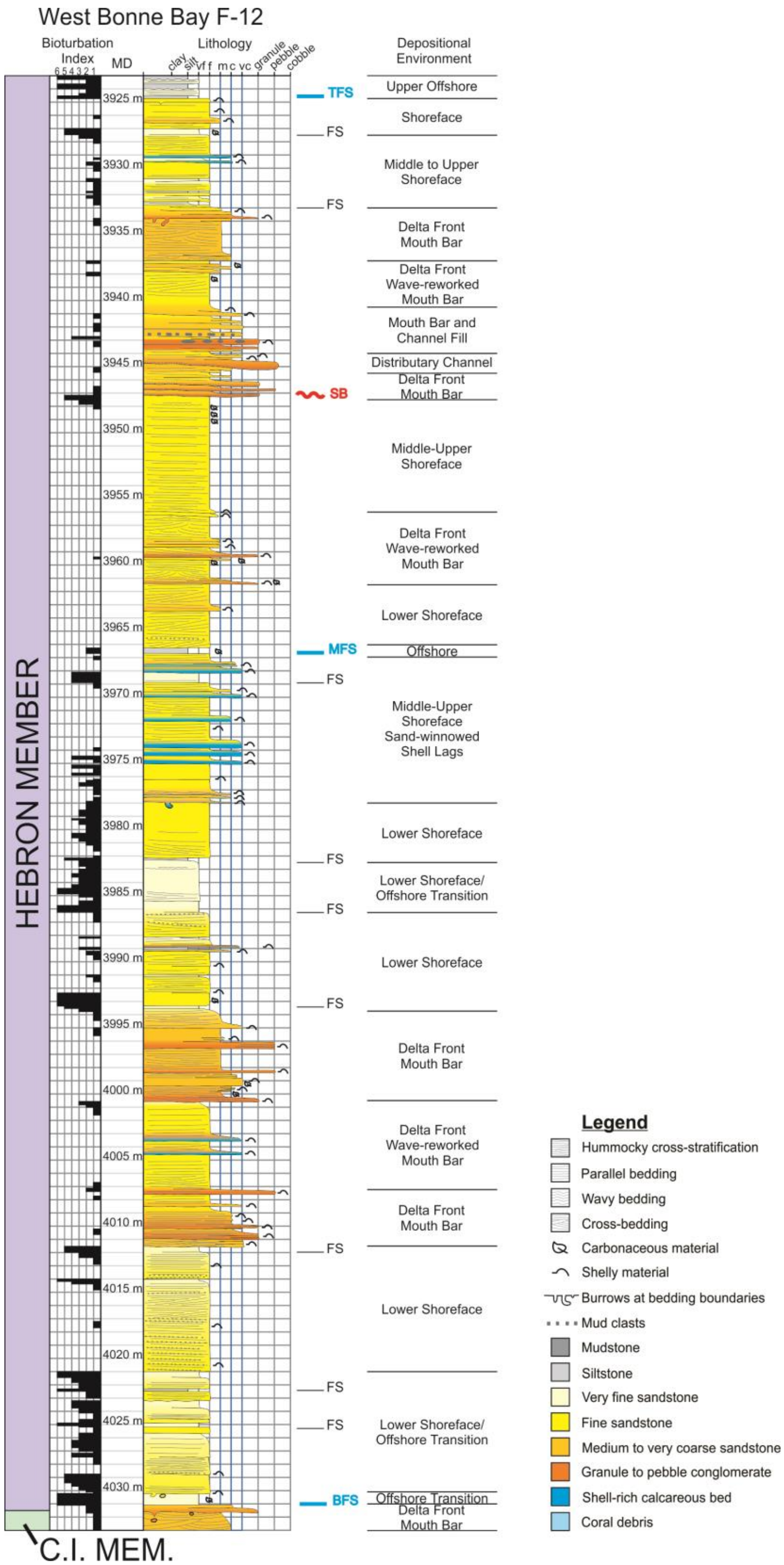
West Bonne Bay F-12
Bioturbation Index
6 5 4 3 2 1
MD
Lithology
clay
silt
vf f m c vc
granule
pebble
cobble
Depositional Environment
HEBRON MEMBER
C.I. MEM.
3925 m
3930 m
3935 m
3940 m
3945 m
3950 m
3955 m
3960 m
3965 m
3970 m
3975 m
3980 m
3985 m
3990 m
3995 m
4000 m
4005 m
4010 m
4015 m
4020 m
4025 m
4030 m
TFS
FS
FS
SB
MFS
FS
FS
FS
FS
FS
FS
FS
BFS
Upper Offshore
Shoreface
Middle to Upper Shoreface
Delta Front Mouth Bar
Delta Front Wave-reworked Mouth Bar
Mouth Bar and Channel Fill
Distributary Channel
Delta Front Mouth Bar
Middle-Upper Shoreface
Delta Front Wave-reworked Mouth Bar
Lower Shoreface
Offshore
Middle-Upper Shoreface Sand-winnowed Shell Lags
Lower Shoreface
Lower Shoreface/ Offshore Transition
Lower Shoreface
Delta Front Mouth Bar
Delta Front Wave-reworked Mouth Bar
Delta Front Mouth Bar
Lower Shoreface
Lower Shoreface/ Offshore Transition
Offshore Transition
Delta Front Mouth Bar
Legend
Hummocky cross-stratification
Parallel bedding
Wavy bedding
Cross-bedding
Carbonaceous material
Shelly material
Burrows at bedding boundaries
Mud clasts
Mudstone
Siltstone
Very fine sandstone
Fine sandstone
Medium to very coarse sandstone
Granule to pebble conglomerate
Shell-rich calcareous bed
Coral debris

Figure 4.2. West Bonne Bay F-12 core 1 sedimentological description. Stratigraphic nomenclature is displayed in the left column. Note the presence of the Cape Island Member (C.I. MEM.) at the base of the log. Interpreted depositional environment is presented on the right with surfaces of stratigraphic significance: Sequence boundary (SB), top Hebron flooding surface (TFS), middle Hebron flooding surface (MFS), basal flooding surface (BFS), and flooding surface (FS).

4.2). The offshore mudstone at 3966.5 m is inferred to represent the maximum transgression and displays a notable positive spike in the gamma ray log (Figure 4.3b).

Evidence of slicken-slide surfaces in the offshore mudstone at 3966.5 m (Figure 4.2) and the abrupt facies change to shoreface sandstones suggests the presence of minor faulting. The overlaying shoreface sandstones are erosively cut by coarse-grained sandstones and pebble conglomerates interpreted as terminal distributary channels and mouth bars (3947 m, Figures 4.2 and 4.3c). This is interpreted as a candidate sequence boundary based on a similar shallowing facies trend observed in the Hebron wells (3036 m, Figure 4.4). The channel fill and overlying sandstones convey a complex depositional history that has been interpreted as a back-barrier environment with mixed fluvial-tidal processes and considerable erosion (see Chapter 2). The thickness of the deposits is considerably less than the corresponding deposits in the Hebron M-04 core section likely due to this complex depositional setting. A transgressive lag deposit occurs at 3925 m (Figure 4.2) that has *Ophiomorpha* burrows filled with coarse-grained material and is abruptly overlain by offshore mudstones and hummocky cross-bedded siltstones and sandstones. This lag is interpreted as a transgressive surface, which precedes the basin-wide increase in sea level that resulted in the deposition of the 'B-Marker' limestone.

Unlike the WBB F-12 core, the Hebron M-04 core 3 is characterized by muddier facies and more diverse trace fossil assemblages suggesting a deeper overall bathymetric position with a dominance of marine processes. A retrogradational stacking pattern is noted in the Hebron M-04 core from 3050.5 m to 3094 m (Figure 4.4). The facies in this section of the core are interpreted as marine with minor deltaic influence. The Hebron I-

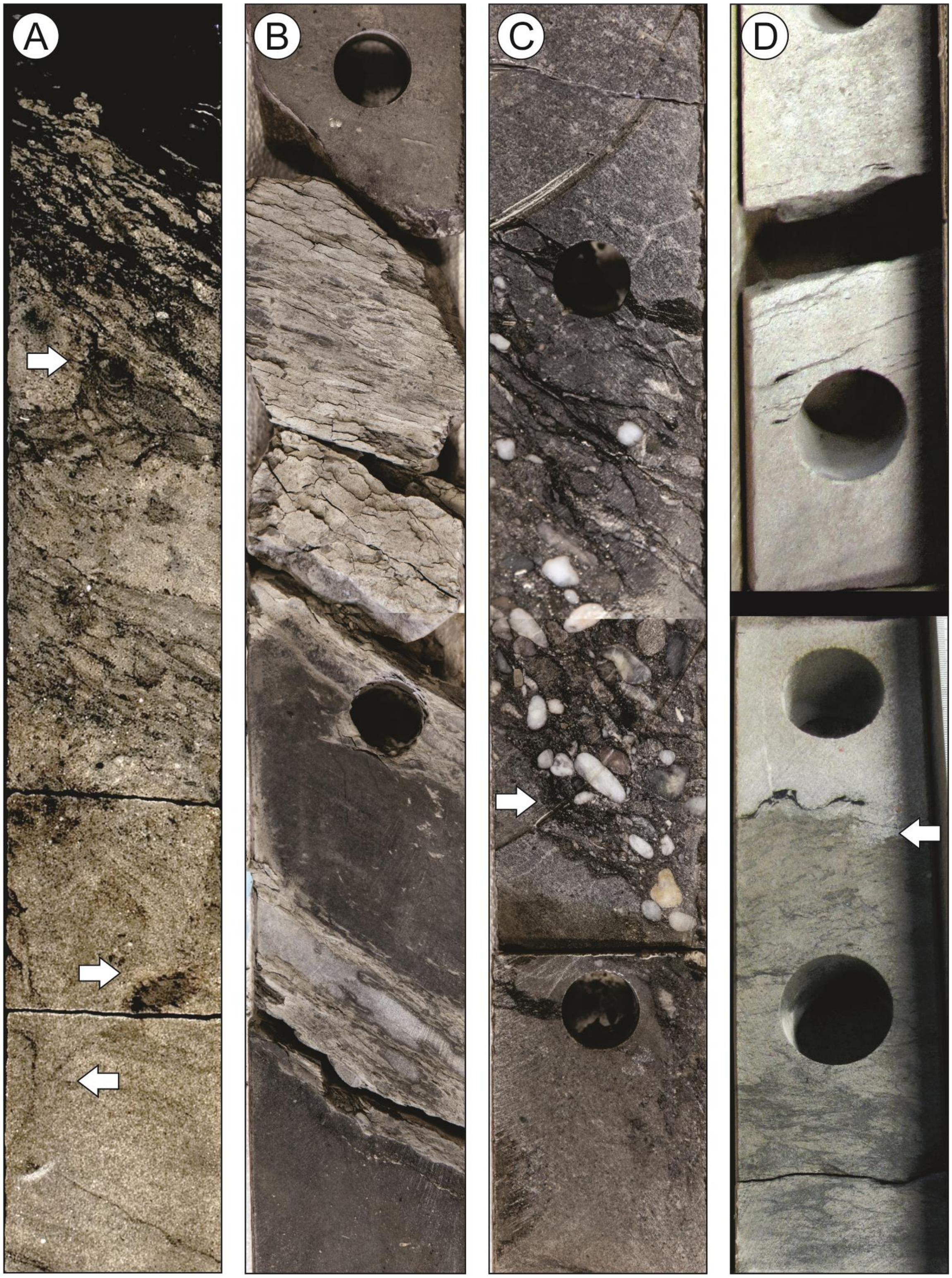
A
B
C
D

Figure 4.3. Core photos of major stratigraphic surfaces from WBB F-12 core1 and Hebron M-04 core 3. A, 4031-4031.5 m in WBB F-12 core 1. Cape Island Member cross-bedded sandstone with Ophiomorpha burrows and funnel structures (arrows) overlain by transgressive lag and dark mudstone at the top. B, 3944.6-3945.1 m in WBB F-12 core 1. Middle Hebron flooding surface mudstone with swelling clay. C, 3966.2-3966.7 m in WBB F-12 core 1. Candidate sequence boundary with poorly sorted, pebble conglomerate (arrow). D, 3035.6-3036.1 m in Hebron M-04 core 3. Candidate sequence boundary (arrow) with lower shoreface sandstones abruptly overlain by cross-bedded coarse-grained sandstone. Images are 9 cm across.

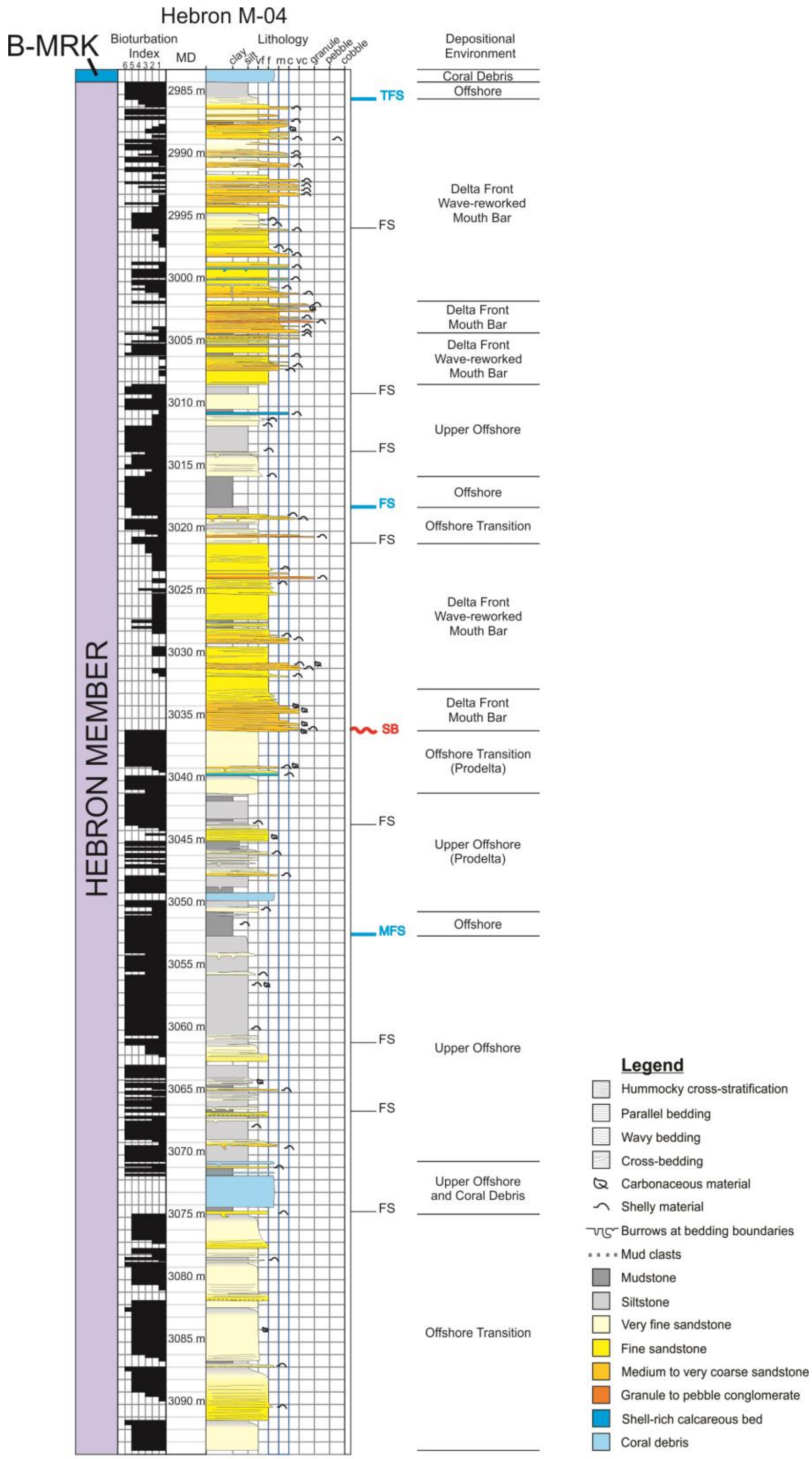
Hebron M-04
B-MRK
Bioturbation Index
6 5 4 3 2 1
MD
Lithology
clay
silt
vf
f
m
c
vc
granule
pebble
cobble
Depositional Environment
HEBRON MEMBER
2985 m
2990 m
2995 m
3000 m
3005 m
3010 m
3015 m
3020 m
3025 m
3030 m
3035 m
3040 m
3045 m
3050 m
3055 m
3060 m
3065 m
3070 m
3075 m
3080 m
3085 m
3090 m
TFS
FS
SB
MFS
Coral Debris
Offshore
Delta Front Wave-reworked Mouth Bar
Delta Front Mouth Bar
Delta Front Wave-reworked Mouth Bar
Upper Offshore
Offshore
Offshore Transition
Delta Front Wave-reworked Mouth Bar
Delta Front Mouth Bar
Offshore Transition (Prodelta)
Upper Offshore (Prodelta)
Offshore
Upper Offshore
Upper Offshore and Coral Debris
Offshore Transition
Legend
Hummocky cross-stratification
Parallel bedding
Wavy bedding
Cross-bedding
Carbonaceous material
Shelly material
Burrows at bedding boundaries
Mud clasts
Mudstone
Siltstone
Very fine sandstone
Fine sandstone
Medium to very coarse sandstone
Granule to pebble conglomerate
Shell-rich calcareous bed
Coral debris

Figure 4.4. Core descriptions for Hebron M-04 core 3. Note the presence of the B Marker limestone (B-MRK) at the top of the Hebron M-04 log. Surfaces of stratigraphic significance are displayed in the right-hand columns: Sequence boundary (SB), top Hebron flooding surface (TFS), middle Hebron flooding surface (MFS), and flooding surface (FS).

13 core 4 (Figure 4.5) correlates roughly to the section of Hebron M-04 core from 3058 m to 3038 m (Figure 4.4). Fluvial influence is more pronounced in the Hebron I-13 core section; carbonaceous material is more abundant in the wave-reworked mouth bar sandstones of the Hebron I-13 core (2948 m to 2955 m, Figure 4.5) and only faintly detectable in the corresponding parallel laminated sandstone beds of the Hebron M-04 core (3044 m to 3048 m, Figure 4.4). Both Hebron cores contain a muddy interval that is correlated to the maximum transgression observed in the WBB F-12 core section at 3966.5 m in Figure 2 (3051 m, Figure 4.4; 2955.5 m, Figure 4.5).

An erosive coarse-grained sandstone bed abruptly overlays offshore muddy sandstones at 3036 m in the Hebron M-04 core (Figures 3d and 4). This is interpreted as a candidate sequence boundary and is correlated to the delta distributary channels in the WBB F-12 core (3947 m, Figure 2). The Hebron M-04 candidate sequence boundary is overlain by 15 meters of cross-bedded and parallel laminated mouth bar sandstones (3036 m to 3012 m, Figure 4.4). These deposits likely represent a lowstand delta that is absent in the WBB F-12 core due to its proximity to the paleoshoreline. Flooding surfaces at 3021 m and 3018 m in the Hebron M-04 core mark a rise in sea level and return to offshore conditions (Figure 4.4).

A complex facies association is present from 3008 m to 2986 m in the Hebron M-04 core. Fine- to coarse-grained mouth bar sandstones are interbedded with parallel laminated sandstones and thoroughly bioturbated sandstones and siltstones. Abundant shell debris is present at bedding contacts and thin mudstone interbeds are interpreted as fluid muds. The core section is inferred to represent a series of cyclical deltaic deposits of varying

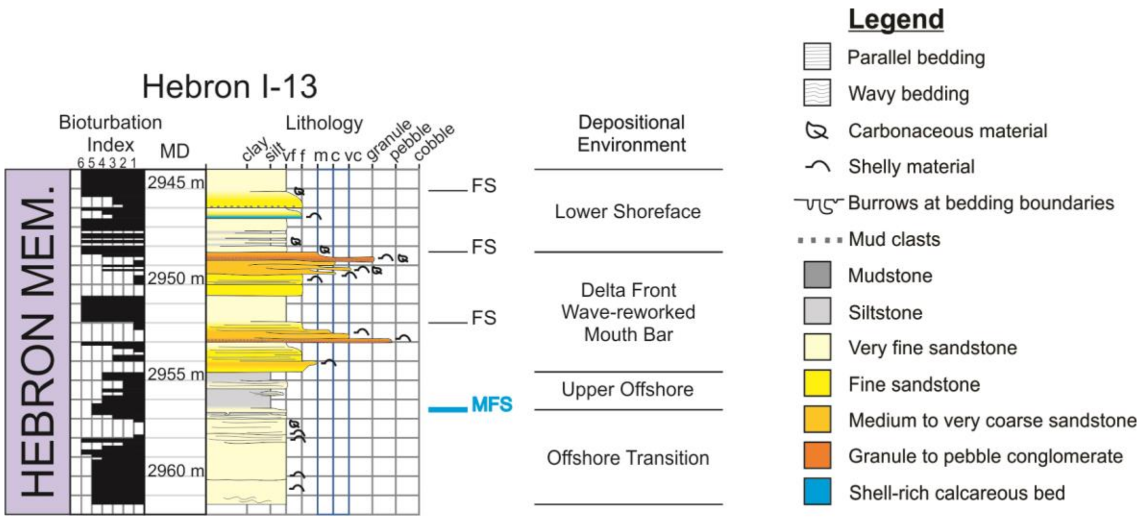

Figure 4.5. Core description for Hebron I-13 core 4. Surfaces of stratigraphic significance are displayed in the right-hand columns: Sequence boundary (SB), middle Hebron flooding surface (MFS), and flooding surface (FS).

sediment load and density reworked by wave processes in a shoreface setting. A flooding surface at 2986 m denotes a rise in relative sea level corresponding to the basin-wide flooding before deposition of the 'B-Marker' limestone (present in the top of the M-04 core section; Figure 4.4).

4.2. Wireline logs

Seven wells in the southern Jeanne d'Arc Basin were utilized; Hebron I-13, Hebron M-04, West Ben Nevis B-75, Ben Nevis I-45, West Bonne Bay C-23, West Bonne Bay F-12Z, and West Bonne Bay F-12. The core descriptions discussed in the previous section were integrated with wireline log data to aid in correlation of flooding surfaces between wells (Figure 4.6). In accordance with the confidentiality agreement between Husky Energy Inc. and Memorial University, only the gamma ray logs, depth scale, and well names are shown.

The Cape Island Member commonly exhibits a coarsening upward pattern in gamma ray logs from wells proximal to the paleo-shoreline and two coarsening upward sandstone units separated by a mixed sand-mud interval in more distal wells (e.g. Hebron M-04 well, Figure 6). The separate sandstone units in more distal wells suggest the presence of two outbuilding events. The Hebron Member typically displays a noisy gamma ray log signature due to the mixed lithology of the wave-influenced deltaic system interpreted from core section.

There are three major flooding surfaces observed from the Hebron Member that can be correlated across all the logs: the basal Hebron, the middle Hebron, and the top Hebron

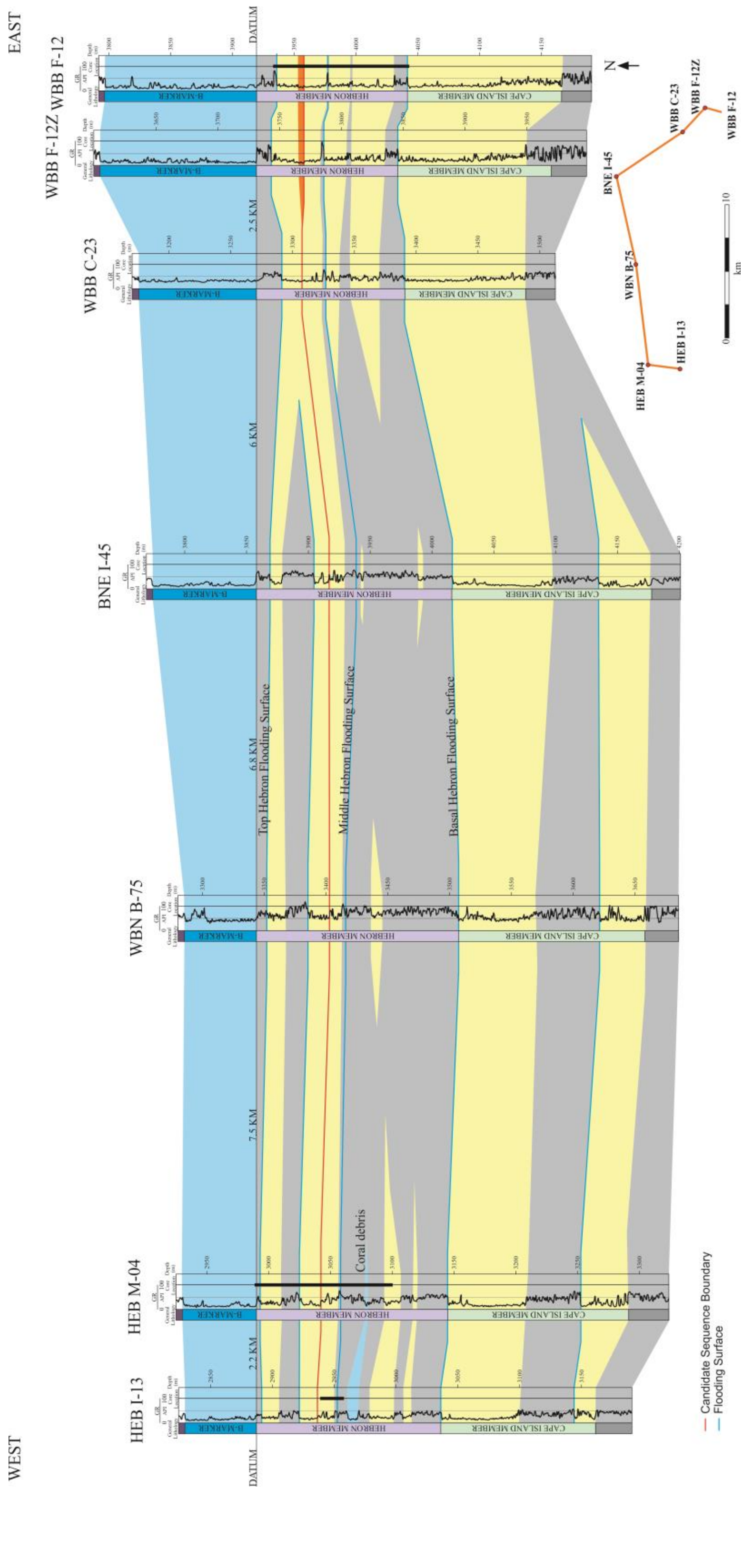

EAST
WEST
WBB F-12
WBB F-12Z
WBB C-23
BNE I-45
WBN B-75
HEB M-04
HEB I-13
DATUM
2.5 KM
6 KM
6.8 KM
7.5 KM
2.2 KM
B-MARKER
HEBRON MEMBER
CAPE ISLAND MEMBER
Top Hebron Flooding Surface
Middle Hebron Flooding Surface
Basal Hebron Flooding Surface
Coral debris
N
0
10
km
Candidate Sequence Boundary
Flooding Surface

Figure 4.6. Correlation of gamma ray logs from seven wells located west to east in the study area. The base of the B-Marker limestone (blue) is used as datum. Sandstone intervals are shaded in yellow, mudstone in grey. The location of the delta distributary channel is marked in orange across the West Bonne Bay wells. A location map with scale bar is provided in the lower right corner. Distance between wells is marked along datum. Well cross section is vertically exaggerated 25x.

flooding surfaces (Figure 4.6). The basal flooding surface separates the Cape Island Member from the Hebron Member and is observed in the base of the WBB F-12 core (Figure 4.3a). This is interpreted as a transgressive surface, as discussed in the previous section. The middle flooding surface is present as a single positive gamma spike or a series of positive gamma spikes. This is represented by offshore mudstones and siltstones in the observed core sections (Figure 4.3b). The flooding surface at the top of the Hebron Member precedes the B-Marker limestone and basin-wide flooding event.

The West Ben Nevis B-75, Ben Nevis I-45, and Hebron wells display greater thickness compared to the West Bonne Bay wells when comparing the Hebron Members. Based on observations of cored material from the WBB F-12 well, the difference in thickness is likely the result of increased erosion and low deposition rates in the more proximal, high energy wave environment of the West Bonne Bay location. The West Ben Nevis B-75 (WBN B-75) and Ben Nevis I-45 (BNE I-45) wells are considerably muddier in gamma ray logs compared to the Hebron wells. Fine-grained material from the delta is likely kept in suspension and moved offshore and eastward due to longshore drift (cf. Hiscott et al., 1990).

5. Discussion

Placement of the paleoshoreline (Valanginian) along the southern margin of the study area (see Figure 4.1b) is based on core interpretations, examination of wireline log data, and previous studies of the Jeanne d'Arc Basin (e.g. Hiscott et al., 1990; Sinclair et al., 2005). Given the thickness of sandstone in wireline log data from the Cape Island

Member (Figure 4.6), the paleoshoreline extended further north during the late Berriasian (cf. Figures 18 and 19, Sinclair et al., 2005). Interpretation of paleocurrent direction by Hiscott et al. (1990) suggests that longshore drift was west to east. It is likely that sediment transport from the Hebron distributary contributed to the development of storm-influenced sandstone beds in the West Ben Nevis (WBN) and Ben Nevis (BNE) well locations (see Hebron Member, Figure 4.6).

The sandstone interval noted at the base of the Cape Island Member in the WBN B-75, BNE I-45, and Hebron wells does not correlate to the wells in the West Bonne Bay area. Without core data, the stratigraphic significance of this sandstone interval is unclear. It can be speculated that the interval represents a delta progradation that was erosionally removed from the rock record in the West Bonne Bay area or not deposited due to autocyclic lobe switching and channel abandonment. It is also possible that the sandstone interval represents a highstand delta progradation that is better correlated to the 'Middle Hibernia' shale underlying the 'Cape Island Member'.

Observations from core analysis suggest that autocyclic lobe switching and channel abandonment contributed to many variations observed between the Hebron and West Bonne Bay area wells. Following the basal Hebron flooding surface, the Hebron area experienced deposition of hummocky cross-stratified sandstones interbedded with fully marine mudstones (see Figure 4.6). In the West Bonne Bay wells, wave-influenced lower shoreface sandstones are interbedded with coarse-grained delta front mouth bars. Isolated sandstone lenses are observed in wireline log data from the WBN B-75 and BNE I-45 wells, suggesting that the Hebron distributary system was either inactive or contributing minimal sediment to the region at this time. It is inferred from the presence of coral debris in the Hebron M-04 core and the observation of abundant oolites in drill cutting samples from the Hebron I-13 well that the absence of an active distributary allowed for the establishment of a small carbonate platform. Both distributaries were active following the middle Hebron flooding event and relative sea level drop resulting in the candidate sequence boundary. However, the core analysis of the sandstone interval preceding the top Hebron flooding surface suggests that the Hebron area distributary was more active.

5.1. Implications for hydrocarbon discovery

The Cape Island Member sandstones present in the bottom of the WBB F-12 core 1 display oil staining and excellent porosity and permeability characteristics. Previous studies by this author have found the sandstones to display porosities averaging 16.4% and permeability ranging from 184 to 962 mD (see Chapter 3). The thick sandstone packages observed in wireline logs would likely serve as good quality reservoirs if sufficient seals were in place. As noted from core samples, the offshore sediments overlaying the Cape Island Member are highly bioturbated and interbedded with hummocky cross-stratified sandstones. These facies display good porosity and permeability characteristics and would promote hydrocarbon migration into the Hebron Member above (see Chapter 3).

The B Marker limestone is regionally extensive and serves as a seal over much of the basin. Initial interest in the West Bonne Bay area was based on structural mapping and hydrocarbon shows in the WBB F-12 discovery well (West Bonne Bay F-12 EOW

Report, Sheppard et al. 2006). However, poor to moderate permeability and porosity characteristics of the Hebron Member reservoir sandstones from the West Bonne Bay area are problematic for hydrocarbon recovery even though the sandstone intervals appear to have good vertical connectivity (Chapter 3). Comparisons between permeability-porosity of the WBB F-12 core 1 and the Hebron M-04 core 3 revealed that the Hebron well averaged higher for similar facies types. This is due to a decrease in the amount of carbonate cement and carbonate nodule growth that is prevalent in the West Bonne Bay area. Given the potential for hydrocarbon migration into the Hebron Member and the presence of a regional limestone seal, further exploration along the paleo-shoreline in the Hebron area and eastward is encouraged especially in more proximal settings where shoreface sandstones are superimposed.

6. Conclusion

Some degree of uncertainty is expected in any interpretation. However, the data limitations for this study increase that uncertainty owing to the lack of significant hydrocarbon discoveries in the southern Jeanne d'Arc Basin, Hibernia interval. Prolific discoveries in the Hibernia and White Rose Fields (west and east Jeanne d'Arc Basin, respectively; see Figure 4.1) resulted in drilling of numerous closely-spaced wells and core samples being taken from multiple reservoir intervals (see Mackay and Tankard, 1990; Sinclair et al., 1992, 1999). Well placement in the southern basin is sparse, averaging 6 km, and core samples taken from the upper Hibernia Formation number only three, all of which from the Hebron Member. The small thickness of the Hebron Member also restricts the use of seismic images for stratigraphic purposes.

More data collection in the southern Jeanne d'Arc Basin is necessary to increase our understanding of the paleogeography of this area. Therefore, this study serves as a starting point to encourage discussion and further investigation into the depositional processes and controls on the stratigraphy of the Hibernia Formation.

7. Acknowledgements

Thank you to Iain Sinclair and Doug Stewart of Husky Energy Inc. for providing the well data and for many productive discussions regarding Hibernia stratigraphy. Thank you to Husky Energy and the School of Graduate Studies for funding this project.

8. References

AINSWORTH, N.R., RILEY, L.A., BRAHAM, W., and BAILEY, H.W. 2006. Well West Bonne Bay F-12, offshore eastern Canada, biostratigraphy of the interval 1410m-4612m (T.D.). Husky Energy-Norsk Hydro Report, Riley Geoscience ltd. 44 p.

ARTHUR, K.R., COLE, D.R., HENDERSON, G.G.L., and KUSHNIR, D.W. 1982. Geology of the Hibernia discovery. *In*: The Deliberate Search for the Subtle Trap, M.T. Halbouty (ed.). American Association of Petroleum Geologists, Memoir 32, p. 181-195.Brown, D.M., McAlpine, K.D. and Yole, R.W. 1989. Sedimentology and sandstone diagenesis of Hibernia Formation in Hibernia Oil Field, Grand Banks, Newfoundland. The American Association of Petroleum Geologists Bulletin, v. 73, p. 557-575.

BROWN, D.M., MCALPINE, K.D. and YOLE, R.W. 1989. Sedimentology and sandstone diagenesis of Hibernia Formation in Hibernia Oil Field, Grand Banks, Newfoundland. *The American Association of Petroleum Geologists Bulletin*, v. 73, p. 557-575.

CATUNEANU, O., ABREU, V., BHATTACHARYA, J.P., BLUM, M.D., DALRYMPLE, R.W., ERIKSSON, P.G., FIELDING, C.R., FISHER, W.L., GALLOWAY, W.E., GIBLING, M.R., GILES, K.A., HOLBROOK, J.M., JORDAN, R., KENDALL, C.G.St.C., MACURDA, B., MARTINSEN, O.J., MIALL, A.D., NEAL, J.E., NUMMEDAL, D., POMAR, L., POSAMENTIER, H.W., PRATT, B.R., SARG, J.F., SHANLEY, K.W., STEEL, R.J., STRASSER, A., TUCKER, M.E., WINKER, C. 2009. Towards the standardization of sequence stratigraphy. *Earth-Science Reviews*, v. 92, p. 1-33.

EVANS, J.N. and MCILROY, D. 2016. Ichnology and palaeobioligy of *Phoebichnus trochoides* from the Middle Jurassic of north-east England. *Papers in Palaeontology*, v. 2, p. 139-154.

HISCOTT, R.N., WILSON, R.C.L., HARDING, S.C., PUJALTE, V. and KITSON, D. 1990. Contrasts in Early Cretaceous depositional environments of marine sandbodies, Grand Banks-Iberian Corridor. *Bulletin of Canadian Petroleum Geology*, v. 38, p. 203-214.

LEAMAN, M. and MCILROY, D. 2015. Petrophysical properties of Ophiomorpha irregulaire ichnofabrics from BN L-55 of Hebron Field, offshore Newfoundland. *In*: D. McIlroy (ed.), Ichnology: Papers from ICHNIA III. Geological Association of Canada, Miscellaneous Publication, v. 9, p. 127-139.

LEAMAN, M., MCILROY, D., HERRINGSHAW, L.G., BOYD, C, and CALLOW, R.H.T. 2015. What does *Ophiomorpha irregulaire* really look like? *Palaeogeography, Palaeoclimatology, Palaeoecology*, v. 439, p. 38-49.

MACKAY, A.H. and TANKARD, A.J. 1990. Hibernia Oil Field-Canada Jeanne d'Arc Basin, Grand Banks Offshore Newfoundland. *In*: N.H. Foster and E.A. Beaumont (compilers), Structural traps: tectonic fold traps 3. The American Association of Petroleum Geologists, p. 145-175.

SHEPPARD, D., MAC PHERSON, C., MACINNIS, D. 2006. Geological Report on Husky Oil et al West Bonne Bay F-12 East Coast Canada. Husky Oil Operations Limited. pp 258.

SINCLAIR, I.K., EVANS, J.E., ALBRECHTSONS, E.A. and SYDORA, L.J. 1999. The Hibernia Oilfield-effects of episodic tectonism on structural character and reservoir compartmentalization. *In*: A.J. Fleet and S.A.R. Boldy (eds.), Petroleum Geology of Northern Europe: Proceedings of the 5th Conference. London, Geological Society, p. 517-528.

SINCLAIR, I.K., FLINT, S., STOKES, R., and BIDGOOD, M. 2005. Hibernia Formation (Cretaceous) sequences and Breathitt Group (Pennsylvanian) analogue: implications for reservoir compartmentalization and modeling, offshore Newfoundland. *In*: R.N. Hiscott and A.J. Pulham (eds.), Petroleum Resources and reservoirs of the Grand Banks, eastern Canadian margin. Geological Association of Canada, Special Paper 43, p. 143-167.

SINCLAIR, I.K., MCALPINE, K.D., SHERWIN, D.F., and MCMILLAN, N.J. 1992. Part 1: Geological framework. *In*: Petroleum resources of the Jeanne d'Arc Basin and environs, Grand Banks, Newfoundland. Minister of Supply and Services Canada, p. 1-38.

TANKARD, A.J. and WELSINK, H.J. 1987. Extensional tectonics and stratigraphy of Hibernia Oil Field, Grand Banks, Newfoundland. *The American Association of Petroleum Geologists Bulletin*, v. 71, p. 1210-1232.

CHAPTER 5

Summary

1. Review of Research Topic and Objectives

Integrated sedimentological and ichnological studies are essential to gain a thorough understanding of the depositional environment and how it has changed over time. Sedimentology provides a look at the depositional processes and ichnological analysis gives insight into the physical and chemical stress factors affecting the contemporary endobenthic community and their interaction with the substrate. Together these provide a more comprehensive view of the study area and allow for the development of a more predictive depositional model.

The Hibernia Formation in the southern Jeanne d'Arc Basin is of interest to the petroleum industry owing to the prolific hydrocarbon reservoirs in the Hibernia Field, western Jeanne d'Arc Basin. However, sparse well spacing and the complex fault morphology in the southern region of the basin have resulted in a limited data set and a lack of detailed sedimentological studies. This research provides a detailed look at the sedimentology and ichnology of the Hibernia Formation in the southern Jeanne d'Arc Basin with the following objectives:

1) To describe the sedimentology and ichnology of the Hibernia Formation though observation of core samples and to infer the depositional setting

2) To assess permeability and porosity characteristics of sedimentary facies and associated ichnofabrics and discern how these characteristics affect hydrocarbon migration and reservoir potential

3) To integrate sedimentological and ichnological data with wireline logs to infer facies distribution and sequence stratigraphic stacking patterns for the Hibernia Formation

2. Summary of Conclusions

Through detailed core analysis, it was inferred that the Hibernia Formation in the southern Jeanne d'Arc Basin was a deltaic environment which experienced considerable wave influenced. Facies analysis showed that the dominant facies was hummocky cross-stratified sandstones interbedded with thoroughly bioturbated muddy sandstones representing fair weather periods. Facies associations showed a dominance of wave processes with some fluvial input which lead to the classification of wave-influenced delta (following Bhattacharya and Giosan, 2003; Bhattacharya, 2006).

As a result of the high wave influence in the depositional setting, storm beds with good permeability and porosity characteristics were produced in a shoreface setting. Muddy siltstone facies dominated by *Phycosiphon* ichnofabric are often interbedded with hummocky cross-stratified sandstones. It was discovered that *Phycosiphon* burrow halos display increased porosity compared to the surrounding rock which have potential to promote vertical connectivity between the storm beds. In more proximal settings, amalgamation of storm beds is more common where bioturbated bed tops are deeply eroded providing more connectivity between storm beds. Comparisons between wireline logs and permeability and porosity data from core plugs showed that the Hebron area sandstones displayed higher overall permeabilities and porosities. This is likely owing to the prevalence of carbonate cements and carbonate nodule growth in the West Bonne Bay region.

Analysis of wireline log data from the southern Jeanne d'Arc Basin allowed for the correlation of three flooding surfaces and recognition of a low order candidate sequence boundary. The Cape Island Member of the Hibernia Formation displays excellent reservoir potential; however, the overlaying storm beds and *Phycosiphon*-dominated fair weather siltstones allow for hydrocarbon migration with the basin-wide B-Marker limestone serving as a top seal.

3. Suggestions for Future Research

The Cape Island Member sandstones displayed excellent permeability and porosity characteristics in wireline log data and core plug analysis. Oil staining was observed in the Cape Island Member, West Bonne Bay core 1, below the flooding surface contact at the base of the Hebron Member. Wireline logs show a thick succession of sandstone units making up the Cape Island Member which would serve as a good reservoir unit if not for the poor seal and apparent hydrocarbon migration into the Hebron Member sandstones.

Further exploration of the southern Jeanne d'Arc Basin is recommended. This study was limited by the low number of available core samples and the large distance between well locations. Perhaps in the future as hydrocarbon exploration in the Jeanne d'Arc Basin expands, more wells will be drilled thus increasing the data set and reduce uncertainty. The complex fault morphology in the basin increases the probability that a fault-trap may exist isolating the sandstones of the Cape Island Member possibly preventing migration into the Hebron Member. In addition, exploration along the paleoshoreline of the Hebron Member may reveal higher quality reservoir sandstones.

4. Bibliography and References

BHATTACHARYA, J. 2006. Deltas. *In*: Facies Models Revisited, H.W. Posamentier and R.G. Walker (eds.). SEPM Special Publication 84, p. 237-292.

BHATTACHARYA, J. and GIOSAN, L. 2003. Wave-influenced deltas: geomorphological implications for facies reconstruction. *Sedimentology*, v. 50, p. 187-21.